



THE HONG KONG
POLYTECHNIC UNIVERSITY

香港理工大學

Pao Yue-kong Library

包玉剛圖書館

Copyright Undertaking

This thesis is protected by copyright, with all rights reserved.

By reading and using the thesis, the reader understands and agrees to the following terms:

1. The reader will abide by the rules and legal ordinances governing copyright regarding the use of the thesis.
2. The reader will use the thesis for the purpose of research or private study only and not for distribution or further reproduction or any other purpose.
3. The reader agrees to indemnify and hold the University harmless from and against any loss, damage, cost, liability or expenses arising from copyright infringement or unauthorized usage.

If you have reasons to believe that any materials in this thesis are deemed not suitable to be distributed in this form, or a copyright owner having difficulty with the material being included in our database, please contact lbsys@polyu.edu.hk providing details. The Library will look into your claim and consider taking remedial action upon receipt of the written requests.



The Hong Kong Polytechnic University
Department of Electrical Engineering

ROBUST POWER SYSTEM STABILIZER
DESIGN BY EVOLUTIONARY
ALGORITHMS

WANG ZHEN

A thesis submitted in partial fulfilment of the
requirements for the Degree of Doctor of Philosophy

March 2008

CERTIFICATE OF ORIGINALITY

I hereby declare that this thesis is my own work and that, to the best of my knowledge and belief, it reproduces no material previously published or written, nor material that has been accepted for the award of any other degree or diploma, except where due acknowledgement has been made in the text.

_____ (Signed)

_____ WANG Zhen _____ (Name of student)

DEDICATION

TO MY FAMILY

SYNOPSIS

With the growth of interconnected power systems and particularly the deregulation of the industry, problems related to low frequency oscillation have been widely reported, including major incidents. As the most cost-effective damping controller, power system stabilizer (PSS) has been widely used to suppress the low frequency oscillation and enhance the system dynamic stability. Among many PSS design methods, probabilistic PSS design approach can address robust PSS design over a wide range of operating conditions. However, there are some limitations on previous studies on probabilistic PSS design and other related issues, for example, some gradient-based nonlinear optimization methods suffer from the problem of high demand on initialization and trapping in local optimum; system contingencies are not systematically considered in previous approaches; the optimal siting, i.e. minimum PSS location, is not considered by and large. To address the above mentioned problems, this thesis is devoted to the extended development of robust and coordinated PSS design in power systems.

Evolutionary algorithms (EAs) have attracted a great deal of attention recently and have been found to be robust approaches for solving non-linear, non-differentiable and multi-modal optimization problems, which can overcome the weakness of gradient-based nonlinear optimization methods. Genetic algorithm (GA), particle swarm optimization (PSO) and differential evolution (DE) are three representative EAs that will be employed to solve several PSS design problems in the thesis.

Differential evolution (DE) is a novel evolutionary algorithm characterized as simple to implement and little tuning on control parameters. Thus DE is often recommended to receive primary attention when facing new optimization problems. The PSS design model in the thesis differing from most previous models lies in that the former includes a probabilistic eigenvalue-based optimization model. The probabilistic PSS design model will therefore be primarily investigated by DE method. The performance of the

proposed DE-based PSS is demonstrated based on two test systems by probabilistic eigenvalue analysis and nonlinear simulation. The results indicate that the probabilistic PSS design by DE is more robust than a gradient-based conventional method.

Genetic algorithm (GA) has been one of the most popular EAs during the past decade because it is computationally simple and easy to implement. The BLX- α operator based GA has been previously reported to be able to achieve prominent performance in PSS design. However, the previous PSS design methods did not include a systematic way to handle the system contingencies. In the thesis, the PSS design by the BLX- α GA approach will be further extended to consider system contingencies. The number of contingencies is first significantly reduced by a three-stage critical contingency screening process. The PSS design problem is thus formulated as a multi-objective optimization model with contingencies taken into account. The BLX- α GA will be recursively used to tune PSS parameters so that the prescribed damping criteria subject to contingencies are satisfied under a wide range of operating conditions. An-eight machine system is utilized to demonstrate the effectiveness of the proposed approach and a comparison of the proposed method with a pre-contingency tuning scheme is reported.

Particle swarm optimization (PSO) is a swarm intelligence algorithm that mimics the movement of individuals (fishes, birds, or insects) within a group (school, flock, and swarm). PSO is reported to potentially have smaller population-size requirement than other population-based EAs so that PSO might converge faster when they are applied to those highly complex problems that require time-consuming simulations to determine the value of objective function. The probabilistic PSS design with system contingencies taken into account proposed in the thesis is a very complicated problem. Hence, PSO is employed to solve this optimization problem. The effectiveness of the proposed approach is discussed on an eight-machine system and a comparison study of PSO with the DE and the BLX- α GA is primarily conducted. The results also show that PSO consumes less computing time than the DE and the BLX- α GA.

To consider the optimal-siting scheme in the probabilistic PSS design, a combination optimization model with mixed discrete and continuous variables is proposed. In this

case, GA is also very powerful and flexible in handling this combination optimization problem, which is a little hard for DE or PSO. Hence, a mixed integer-binary coded GA is developed to solve this problem. A partially matched crossover (PMX) operator is introduced to cope with the integer bit conflict. The influence of the probability of crossover and mutation operator on the GA convergence performance is primarily investigated. The effectiveness of the proposed PSS is demonstrated based on two test systems by probabilistic eigenvalue analysis and nonlinear simulation. Case studies show that the proposed optimal-siting probabilistic PSS design method can achieve adequate robust stability, while using a reduced number of PSSs.

PUBLICATIONS ARISING FROM THE THESIS

Journal papers:

1. Wang Z., Chung C.Y., Wong K.P., and Tse C.T., "Robust PSS design under multioperating conditions using differential evolution", *IET Proceedings-Generation, Transmission & Distribution*, vol. 2, no. 5, pp. 690-700, Sept. 2008

Journal papers under review:

2. Wang Z., Chung C.Y., and Wong K.P., "Systematic Approach to Consider System Contingencies in PSS Design", submitted to *Electric Power Systems Research*, 2008

Conference papers:

3. Wang Z., Chung C.Y., Wong K.P., Tse C.T., and Wang K.W., "Robust PSS design under multioperating conditions using canonical particle swarm optimization", in *Proceedings of the IEEE Power System Society General Meeting*, Tampa, FL, USA, June 2007, pp. 1-7

4. Wang Z., Chung C.Y., Wong K.P., Tse C.T., Wang K.W., and Zhang J.F., "Probabilistic PSS design using differential evolution", in *Proceedings of IET International Conference on the 2006 Advances in Power System Control, Operation and Management*, Hong Kong, Oct. 2006, pp. 1-5

Journal papers under preparation:

5. Wang Z., Chung C.Y., and Wong K.P., "Robust optimal-siting PSS design considering system contingencies", to be submitted to *IEEE Transactions on Power Systems*, 2008

ACKNOWLEDGEMENTS

I would first like to express my utmost gratitude to my chief supervisor, Dr. C. Y. Chung, for his invaluable guidance and advice, his patience, support and encouragement. His unremitting pursuit in the realm of power system researches always inspires me.

I would also like to express my deep gratitude to Professor K. P. Wong and Dr. C.T. Tse, my co-supervisors, for their valuable comments and discussions on the research project. Professor K. P. Wong is very generous to share his rich experience in doing researches with us.

Sincere thanks and gratitude are extended to Professor Wen Fushuan, who was my supervisor during my graduate studies at Zhejiang University, who led me on the road of doing researches. I also thank Professor Han Zhenxiang, Professor Qiu Jiaju and Professor Gan Deqiang in Zhejiang University, for their continuous support and encouragement. I also thank Mr. Wang Kangyuan and other friends in Zhejiang University; I had a good time there.

Many thanks are devoted to the members of Computational Intelligence Applications Research Laboratory (CIARLab). The author is also grateful to Ms. Zhang Jianfen for many academic discussions and helps.

Special thanks go to my dear parents. Their unconditional love has been with me throughout my life. I owe them a debt that can never be repaid.

I offer my deepest thanks to my wife Zhang Jie, Jane. She has contributed more to this thesis than she can imagine.

The last but not the least, the financial support provided by the Research Committee of the Hong Kong Polytechnic University through the award of studentship is also appreciated.

TABLE OF CONTENTS

CERTIFICATE OF ORIGINALITY	i
DEDICATION	ii
SYNOPSIS	iii
PUBLICATIONS ARISING FROM THE THESIS	vi
ACKNOWLEDGEMENTS	viii
LIST OF FIGURES, TABLES, AND ABBREVIATIONS	xiv
CHAPTER 1 INTRODUCTION	1
1.1 Power System Stability.....	1
1.2 Small Signal Stability	4
1.3 A Literature Review	6
1.3.1 Siting of PSS and damping controller.....	6
1.3.2 Design of PSS and damping controller	7
1.4 PSS Structure.....	12
1.5 Motivation of the Thesis.....	14
1.5.1 An introduction of EAs	15
1.5.2 Application of EAs in the thesis	16
1.6 Outline of the Thesis	18

CHAPTER 2 AN INTRODUCTION TO PROBABILISTIC EIGENVALUE ANALYSIS 21

2.1	Introduction	21
2.2	Probabilistic Damping Criteria.....	22
2.3	Probabilistic Sensitivity Indices (PSIs)	24
2.4	Case Studies.....	25
2.4.1	Three-machine power system (system I)	26
2.4.2	Eight-machine power system (system II).....	29
2.4.3	PSS location and signal selection.....	33
2.5	Summary.....	34

CHAPTER 3 ROBUST PSS DESIGN UNDER MULTIOPERATING CONDITIONS USING DIFFERENTIAL EVOLUTION 35

3.1	Introduction	35
3.2	Problem Formulation of Probabilistic PSS Design	37
3.2.1	PSS structure	37
3.2.2	Parameter optimization model	38
3.3	Probabilistic PSS Design Using Differential Evolution.....	39
3.3.1	Principal components of DE	39
3.3.2	Design procedure	42
3.4	Applications.....	43
3.4.1	System I	43
3.4.2	System II	51

3.5	Summary.....	54
CHAPTER 4 POWER SYSTEM STABILIZER DESIGN CONSIDERING SYSTEM CONTINGENCIES		55
4.1	Introduction	55
4.2	Contingency-based PSS Tuning Modeling	57
4.2.1	Critical contingency screening.....	57
4.2.2	Optimization model.....	61
4.3	Solution by the BLX- α GA	64
4.3.1	Principal components of the BLX- α GA	65
4.3.2	GA steps.....	67
4.3.3	Design procedure	68
4.4	Case Studies.....	69
4.4.1	System configuration	70
4.4.2	Algorithm performance.....	73
4.4.3	The first tuning results	74
4.4.4	The second tuning results.....	76
4.4.5	Transient simulation.....	77
4.5	Summary.....	81
CHAPTER 5 PROBABILISTIC PSS DESIGN CONSIDERING SYSTEM CONTINGENCIES		82
5.1	Introduction	82
5.2	Contingency-based Probabilistic PSS Design.....	83

5.2.1	Critical contingency screening.....	83
5.2.2	Optimization model.....	84
5.3	Solution by PSO	86
5.3.1	Basic algorithm	86
5.3.2	Parameter setting.....	88
5.3.3	Design procedure	90
5.4	Numerical Experiments	92
5.4.1	Algorithm performance.....	93
5.4.2	The first tuning results	95
5.4.3	The second tuning results.....	96
5.4.4	Transient simulation.....	97
5.5	Methodology Comparison	101
5.6	Summary.....	103

CHAPTER 6 PROBABILISTIC POWER SYSTEM STABILIZER DESIGN

CONSIDERING OPTIMAL SITING 104

6.1	Introduction	104
6.2	Probabilistic PSS Design with Optimal Siting	105
6.3	Optimization by the Mix-coding GA	107
6.3.1	GA coding scheme	109
6.3.2	GA operators	111
6.3.3	Design procedure	114
6.4	Case Studies.....	116

6.4.1	System I	116
6.4.2	System II	122
6.5	Summary.....	125
CHAPTER 7 CONCLUSIONS AND FUTURE WORK		126
7.1	Summary.....	126
7.2	Recommendation for Future Work.....	129
APPENDIX A PROBABILISTIC EIGENVALUE ANALYSIS		131
A1	Power System Model.....	131
A2	Probabilistic Eigenvalue Analysis.....	133
APPENDIX B MACHINE MODELS		137
B1	Fourth-order Generator Model	137
B2	Sixth-order Generator Model	138
APPENDIX C TEST SYSTEM DATA		140
C1	Three-machine System (System I)	140
C2	Eight-machine System (System II).....	142
REFERENCES		

LIST OF FIGURES, TABLES, AND ABBREVIATIONS

List of Figures

Figure 1-1. Classification of power system stability

Figure 1-2. Structure of typical PSS

Figure 2-1. Probabilistic eigenvalue distribution

Figure 2-2. Desired eigenvalue distribution region

Figure 2-3. Single line diagram of three-machine system

Figure 2-4. Daily operating curves of load powers in system **I**

Figure 2-5. Daily operating curves of generation powers in system **I**

Figure 2-6. Single line diagram of eight-machine system

Figure 3-1. Illustration of the mechanism of DE/rand-to-best/1/bin

Figure 3-2. Convergence performance with random strategy for K

Figure 3-3. Convergence performance with $K=F$

Figure 3-4. System response at light load condition (solid lines for DE-PPSS and dotted lines for GPSS)

Figure 3-5. System response at medium load condition (solid lines for DE-PPSS and dotted lines for GPSS)

Figure 3-6. System response at heavy load condition (solid lines for DE-PPSS and dotted lines for GPSS)

Figure 3-7. Convergence performance of system **II**

Figure 3-8. Transient responses of generator G1, G2, G3, G5, G6 and G7 (solid lines for DE-PPSS and dotted lines for GPSS)

Figure 4-1. Flow chart for critical contingency screening

Figure 4-2. The BLX- α operation of the real-coded GA

Figure 4-3. Flow chart for contingency-based PSS design

Figure 4-4. Post-contingency modes of the open-loop system **II** under 480 operating conditions

Figure 4-5. Objective function evolution in the first GA round

Figure 4-6. Objective function evolution in the second GA round

Figure 4-7. Post-contingency modes of the closed-loop system **II** after the first GA round

Figure 4-8. Post-contingency modes of the closed-loop system **II** after the second GA round

Figure 4-9. Transient simulation curves in different cases

Figure 5-1. Flow chart of the contingency-based probabilistic PSS design

Figure 5-2. Objective function evolution in the first PSO round

Figure 5-3. Objective function evolution in the second PSO round

Figure 5-4. Histogram of convergence performance statistics

Figure 6-1. Flow chart of the recursive GA

Figure 6-2. Cases of the PMX operation with $K_{PSS}=4$ and $N_{PSS}=7$

Figure 6-3. PMX operation of integer-coded GA strings

Figure 6-4. Swap mutation on the integer bits

Figure 6-5. The influence of p_c on the recursive GA

Figure 6-6. The influence of p_{mr} on the recursive GA

Figure 6-7. The influence of p_{ms} on the recursive GA

Figure 6-8. Transient responses of system **I** under typical load conditions

Figure 6-9. Transient responses of G8 of system **II** under typical operating conditions

Figure A-1. Two types of elementary transfer blocks

Figure B-1. GMT/PMT representation of the fourth-order generator model

Figure B-2. Block diagram of sixth-order generator model

Figure B-3. GMT/PMT representation of the sixth-order generator model

Figure C-1. Block diagram of static exciters in system **I**

Figure C-2. Block diagram of IEEE-Type I exciters in system **II**

Figure C-3. Block diagram of speed-governor in system **II**

List of Tables

- Table 2-1. Electromechanical modes of the open-loop system **I**
- Table 2-2. PSIs corresponding to residue in system **I**
- Table 2-3. PSIs corresponding to participation factor in system **I**
- Table 2-4. Electromechanical modes of the open-loop system **II**
- Table 2-5. PSIs corresponding to participation factors in system **II** (Speed Signal)
- Table 2-6. PSIs corresponding to residues in system **II** ($\times 0.01$) (Speed Signal)
- Table 2-7. PSIs corresponding to residues in system **II** (Power Signal)
- Table 3-1. Pseudo-code of the DE-based probabilistic PSS design
- Table 3-2. Final PSS parameters for system **I**
- Table 3-3. Electromechanical modes of the closed-loop system **I**
- Table 3-4. The parameters of GPSS for system **I**
- Table 3-5. Performance indices of system **I**
- Table 3-6. PSS parameters for system **II**
- Table 3-7. Electromechanical modes of the closed-loop system **II**
- Table 3-8. The parameters of GPSS for system **II**
- Table 3-9. Performance indices of system **II**
- Table 4-1. The BLX- α GA parameter configuration
- Table 4-2. Post-contingency profiles of the open-loop system **II**
- Table 4-3. The top 5 least-damping contingencies

Table 4-4. PSS parameters after the first GA round

Table 4-5. Post-contingency modes after the first GA round

Table 4-6. PSS parameters after the second GA round

Table 4-7. Post-contingency modes after the second tuning

Table 4-8. Test cases for transient stability simulation

Table 4-9. Performance indices of the test cases

Table 5-1. PSO algorithm parameters

Table 5-2. Post-contingency modes of the open-loop system

Table 5-3. PSS parameters after the first PSO round

Table 5-4. Post-contingency modes after the first PSO round

Table 5-5. PSS parameters after the second PSO round

Table 5-6. Post-contingency modes after the second PSO round

Table 5-7. Test cases for transient stability simulation

Table 5-8. Performance indices of the test cases

Table 5-9. Parameter configuration of three methods

Table 5-10. Computing time of three methods

Table 6-1. The pre-specified parameters

Table 6-2. The results of GA parameter experiments in system **I**

Table 6-3. Final PSS parameters for system **I**

Table 6-4. Electromechanical modes of the closed-loop system **I**

Table 6-5. Performance indices of system **I**

Table 6-6. PSS parameters for system **II**

Table 6-7. Electromechanical modes of the closed-loop system **II**

Table 6-8. Performance indices of system **II**

Table C-1. Bus data of system **I**

Table C-2. Line data of system **I**

Table C-3. Generator parameters of system **I**

Table C-4. Exciter parameters of system **I**

Table C-5. Bus data of system **II**

Table C-6. Shunt capacitor of system **II**

Table C-7. Line data of system **II**

Table C-8. Generator parameters of system **II**

Table C-9. Exciter parameters of system **II**

Table C-10. Governor/turbine parameters of system **II**

Table C-11. Typical daily operation curves

List of Abbreviations

ATV	Averaged total variation
AVR	Automatic voltage regulator
CI	Computational intelligence
CPSS	Conventional power system stabilizer
DE	Differential evolution
EA	Evolutionary algorithm
ES	Evolution strategies
FACTS	Flexible AC transmission system
GA	Genetic algorithm
GEP	The exciter, generator and power system
MIMO	Multi-input multi-output
ODE	Ordinary differential equation
PMX	Partially matched crossover
PSI	Probabilistic sensitivity index
PSO	Particle swarm optimization
PSS	Power system stabilizer
RGA	Relative gain array
SGA	Simple genetic algorithm
SVD	Singular value decomposition

SSSA	Small signal stability analysis
TSA	Transient stability analysis
VSA	Voltage stability analysis
WAMS	Wide area measurement system

1 INTRODUCTION

1.1 Power System Stability

Power system stability is defined as the ability of an electric power system, for a given initial operating condition, to regain a state of operating equilibrium after being subjected to a physical disturbance, with all system variables bounded so that the system integrity is preserved [72]. In history, almost all power system blackout incidents were concerned with some power system stability problems, from early 1965 grid blackout of northeast US and Canada Ontario power system [143] to the latest 2003 major grid blackouts in north America and Europe [9], which often resulted in huge economic losses, life threat and inconvenience to people. These blackout incidents have attracted attention of the public and of regulatory agencies, utilities as well as engineers, to the problem of stability and importance of power system reliability.

Nowadays, power systems are being operated under increasingly stressed conditions due to the prevailing trend to make the most use of existing facilities. Increased competition, open transmission access, construction, environmental constraints, etc. are shaping the operation of electric power systems in new ways that present greater challenges for secure system operation. Moreover, the fast rise of electricity consumption in those countries with fast economic growth has driven some transmission corridors to run very close to their operating limits [155, 169]. These facts

are abundantly clear from the increasing number of major power grid blackouts that have been experienced in recent years [85].

Planning and operation of today's power systems require a careful consideration of all forms of system instability. This motivated the publishing of a report by a joint IEEE/CIGRE Task Force on *Power System Stability Terms, Classification, and Definitions* [72].

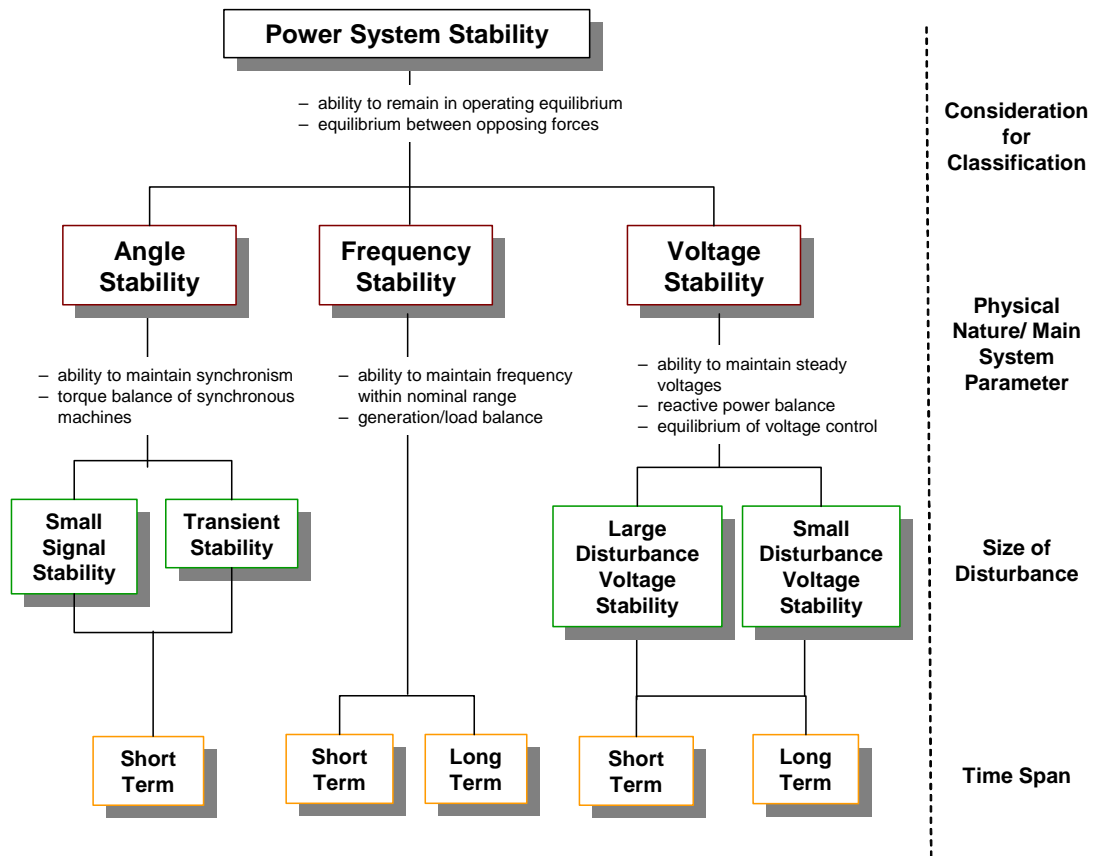


Figure 1-1. Classification of power system stability [85]

The core classification of power system stability in the report is illustrated in Figure 1-1, which is based on the following considerations [72, 84, 85, 87]:

- The physical nature of the resulting instability related to the main system parameter in which instability can be observed;

- The size of the disturbance considered indicates the most appropriate method of calculation and prediction of stability;
- The devices, processes, and time span that must be taken into consideration in order to determine stability.

The scope of this thesis is mainly concerned with the problem of angle stability, in particular, the small signal stability problem. *Rotor angle stability* is concerned with the ability of interconnected synchronous machines of a power system to remain in synchronism under normal operating conditions and after being subjected to a disturbance. It depends on the ability to maintain/restore equilibrium between electromagnetic torque and mechanical torque of each synchronous machine in the system. Instability that may result occurs mainly in the form of increasing angular swings of some generators leading to their loss of synchronism with other generators. On the stability performance evaluation, the concern is the behavior of the power system when subjected to a transient disturbance. A *disturbance* is a sudden change or a sequence of changes in one or more of the parameters of the system, or in one or more of the operating quantities. The disturbance may be small or large. Small disturbances in the form of load changes take place continually, and the system adjusts itself to the changing conditions. Sometimes, power systems also undergo large disturbances of a severe nature, initiated by a short circuit on a transmission line or loss of a large generator.

1.2 Small Signal Stability

Under small disturbances, the ability of a system to maintain synchronism is the *small signal stability*. The disturbances are considered to be sufficiently small so that linearization of system equations is permissible for purposes of analysis. Such disturbances are continually encountered in normal system operation, such as small changes in load. Small signal stability analysis (SSSA) is based on linearization of a group of ordinary differential equations (ODE) that characterize the power system dynamics. Often, it includes eigenanalysis and/or modal analysis that can provide valuable information about the inherent dynamic characteristics of the power system [85, 128].

Since the 1960s, the problem of low frequency oscillations in power systems has gradually emerged around the world with the advent of bulk interconnection of power systems [35], resulting in some major incidents [83]. The main reasons for the appearance of these low frequency oscillations were [115]:

1. The introduction of high-gain, low-time constant automatic voltage regulators (AVR), which mainly serves three purposes: the high-gain AVR keeps the terminal voltage within close control; it improves steady state stability limit; it improves the transient stability limit. But on the other hand, large-gain AVR amplifies the negative damping produced by the AVR [85].
2. The efforts to transmit bulk power over long distances. Deregulation of power systems has been giving a remarkable impetus to this trend during the past ten years. Power systems are undergoing an increase of unplanned power exchanges

due to competition among utilities. As a consequence, unacceptable inter-area oscillations have become one limiting factor for large amount of power transmission over interconnected power systems [35].

In essence, small signal stability is largely a problem of insufficient damping of oscillations. With the interconnection of large systems, several types of oscillation modes are involved. *Local modes* are oscillations associated with generators in one area swinging with respect to the rest of the system. The frequencies of these oscillations are typically in the range of 1 to 2 Hz [35, 82]. *Inter-area modes* are associated with the swing of a group of machines in one part of the system against groups of machines in other parts, and have frequencies typically in the range of 0.1 to 1 Hz. *Control modes* are associated with generating units and other controls, and *torsional modes* are associated with the turbine-generator shaft system rotational components.

To enhance system oscillation damping, various types of damping controllers have been developed. For instance, *power system stabilizer* (PSS) is designed to introduce a damping torque by using supplementary signal(s) acting on the generator excitation system [85]. As the most cost-effective damping controller, PSS has been extensively used to enhance power system oscillation damping. The Western Systems Coordinating Council (WSCC) in USA has set guidelines that all machines above 75MVA are mandated to be equipped with a PSS [11, 85]. Damping controllers are also equipped on some FACTS devices to enhance system stability [90, 108, Pourbeik P.].

1.3 A Literature Review

To improve damping in a power system, a supplemental damping controller can be applied to the primary regulator of one of those transmission devices or to generator controls [35]. The supplemental control action should modulate the output of a device in such a way that damping is added to the power system swing modes of concern. The damping controller siting (or sites locating, location identification) and parameters tuning are the two main topics in damping controller design studies.

1.3.1 Siting of PSS and damping controller

Siting plays an important role in the ability of a device to stabilize a swing mode [90, 104, 120]. Many approaches or indices based on open-loop system model have been proposed and successfully used to guide damping controller placement. Participation factor analysis aids in the identification of which state variables significantly participate in the selected modes so that the related generators are the most suitable for PSSs implementation [69, 119]. Residue method is derived from the modal control theory of linear time-invariant systems, which can give an indication of the controllability and/or observability of a device so as to select effective location [84, 90, 104, 160]. Sensitivity analysis attempts to calculate the sensitivity of an electromechanical mode with respect to the stabilizer parameters to find which generator is most effective for damping enhancement with a PSS [52, 140, 170]. The damping torque analysis method is based on a physical understanding of the electromechanical oscillations of power systems [59, 120, 146]. A comparative study was presented in [146] and the most reliable techniques

and indices for PSS location were identified as the residue method and the damping torque analysis. Some studies also showed that there existed inherent correlation among participation factor, residue and sensitivity of a feedback controller under special conditions [114, 145]. The method based on modal analysis can identify the shape of participating machines in oscillation modes and thus the machine equipped with PSS [140]. A method to decide coherent generators is another similar siting method [65]. In Reference [29], the root-locus approach was adopted to design damping controller of the multi-input multi-output (MIMO) system with multiple input signals. The root-locus approach was also used for checking the effectiveness of PSSs [138, 140]. Reference [98] proposed an optimum control location scheme based on a L2-norm of feedback gain matrix. Recently, the methods using relative gain array (RGA) and singular value decomposition (SVD) indices, which have capability to handle MIMO control design, has been successfully applied to damping controller siting studies [62, 77, 164]. The higher order term modal analysis, such as normal form method, has been applied to the PSS siting research so that complex interaction between modes and some nonlinear behavior under stressed conditions are able to be captured [96, 127].

It is noted that other factors such as device cost, social welfare, security criterion, land price and environmental regulations, etc. also are important driving forces in the selection damping controller locations in a new competitive environment [35, 57, 157].

1.3.2 Design of PSS and damping controller

The aim of damping controller design is to adjust the controller parameters so that desirable damping criteria in a power system are well satisfied. There are two important

aspects to be carefully considered in damping controller design, the robustness and the coordination [35, 36]. The coordination requires that all damping controllers work together to enhance the system damping effect and to avoid improving damping of one group of oscillation, being accompanied with decreasing damping of other modes. It requires that those adverse interactions among various damping controllers be reduced to a minimum. The robustness is essential for damping of oscillations and increasing of stability margins. It requires that each damping controller scheme should provide satisfactory performance for a large variety of operating conditions. Moreover, a robust design is a satisfactory controller tuning even when some of power system elements are uncertain.

The basic concepts and characteristics of PSS function was explained and discussed in [42, 91] based on a Heffron-Phillips model. A conventional PSS (CPSS) with lead/lag structures and fixed parameters, as will be discussed in Section 1.4, has been widely used in power systems [12, 58, 101, 103, 116]. Several approaches have been proposed for CPSS parameter adjustment and damping controller design, such as damping torque approach [59, 141], sensitivity analysis [41, 48, 140, 158], etc. The method using phase compensation in the frequency domain and root locus [88, 91, 113] is an easy-to-fulfill method in power industry. Reference [88] conducted a comprehensive analysis of the effects of the different CPSS parameters on the overall dynamic performance of the power system. It was shown that appropriate selection of CPSS parameters would result in satisfactory performance during system upsets.

Further studies on the PVr's invariance characteristics over a wide range of operating conditions also confirmed the robustness of CPSS [60].

A Coordinated design issue

Some of above PSS design methods are sequential methods, which only consider the damping enhancement of just one critical electromechanical mode at a time. To overcome this shortcoming, pole placement methods [23, 28, 94, 163] were developed so that PSS parameters can be directly calculated from the reduced system. Some modern control theories have been applied for coordinated damping controller design, such as optimal control method [109, 132], etc. In Reference [121], a two-stage method based on the induced torque coefficients was developed to simultaneously tune the gains of PSS and FACTS.

A number of approaches to coordinated tuning of PSS and/or FACTS broadly based on parameter optimization models have been proposed, such as damping maximization model [19, 63, 105, 106], modal performance model [76, 80], transient performance model [92, 162], and closed-loop residues model [166], etc. In these publications, several gradient-based nonlinear optimization methods were employed to solve the problems. These methods are computationally fast but have difficulties in obtaining overall optimum and handling initialization [4, 80, 168]. During the past ten years, some soft computing methods have been applied to overcome the weakness of conventional optimization methods, including: heuristic methods, such as simulated annealing [3], and tabu search [2], etc; evolutionary algorithms (EAs), such as genetic algorithms (GA) [1, 14], evolutionary programming (EP) [5], and particle swarm

optimization (PSO) [4], etc. These methods are very robust for solving those non-linear, non-differentiable and multi-modal (i.e. there exists more than one local optimum) optimization problems.

To properly consider both the inter-area oscillation and local modes, Reference [6] proposed using tie-line active power and speed differences as the PSS input signals, and a two-level design scheme to coordinate the oscillation modes. A decentralized/hierarchical approach was proposed to design a global-signal PSS based on a wide area measurement system (WAMS) to enhance system damping [75]. The advantage of the WAMS-based damping controller is that global signals can convey knowledge related to the overall network dynamics. On the other hand, the signal delay effect in WAMS needs to be carefully evaluated when the remote control signal is introduced [22, 99, 156].

B Robust design issue

In many cases, PSSs are designed under particular system operating conditions. Since the system condition varies continuously with load changes and other random disturbances, it is desired to have a good dynamic performance PSS over a wide range of system operation.

A number of modern robust control techniques have been applied to power system damping controller design. For example, H_∞ optimization can take into account not only performance and robustness requirements, but also other constraints such as limitation of control input signal, noise sensitivity reduction [30, 55, 81, 137, 159]. The μ -synthesis control design technique is based on a relative gain array (RGA) matrix that

can capture the bifurcation subsystem structure [164, 165]. Both of H_∞ optimization and μ -synthesis have the advantage of handling model uncertainties. However, the selection of weighting functions in H_∞ optimization and μ -synthesis becomes an inevitable challenge [55]. Besides, both of them require modal order reduction for practical application [81]. In Reference [126], a variable structure control theory was applied to PSS design to deal with the nonlinearities associated with the system operating conditions.

The robustness issue also motivates some on-line tuning techniques to be applied to damping controller design in power systems. An adaptive damping controller can self-tune its parameters to generate the desired supplementary stabilizing signal for its local oscillation mode, and the stability of overall power system could be improved under the concept of decentralized control [8, 24, 100]. A rule-based stabilizing control scheme is proposed in Reference [66], in which six simple rules were prepared for each generator in the system. To consider more complex system operating conditions, fuzzy-based PSSs were developed to solve the stability problem by using fuzzy sets, fuzzy relation matrix and fuzzy operations [49, 67]. In References [20, 21, 130], neural network based PSS can accommodate the nonlinearities and time dependencies through the learning of history data. Despite much progress achieved in applying modern control and on-line tuning technologies to PSS design, power utilities still prefer the fixed-structure and fixed-parameter conventional PSS due to limited confidence in these tuning schemes [55, 56, 159].

To consider a wide range of operating conditions, conventional eigenanalysis has been extended to probabilistic environment and probabilistic damping controller design is developed for the conventional PSS and FACTS [13, 147]. Probabilistic sensitivity indices (PSIs) are proposed to facilitate “robust” PSS siting [33, 149]. A coordinated synthesis model of PSS parameters is developed and a quasi-Newton nonlinear programming is used to solve the probabilistic PSS problem [32, 142]. However, the optimization methods in these publications still have difficulties to obtain a global optimum.

1.4 PSS Structure

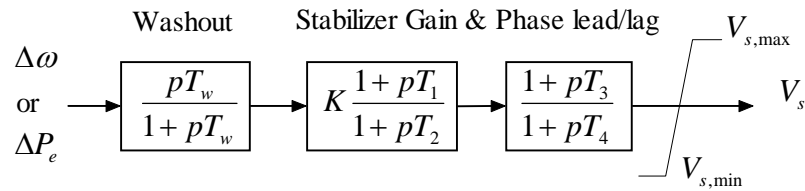


Figure 1-2. Structure of typical PSS

This thesis will focus on the robust and coordinated design of conventional structure PSS. The block diagram of a simple conventional PSS throughout this thesis is shown in Figure 1-2 [11, 73, 74]. The washout block is designed as a high-pass filter to reset the steady-state offset of the terminal voltage. The phase compensation block provides the desired phase-lead characteristic to compensate for the phase lag from the exciter, generator and power system, denoted as GEP(s), with two or more lead/lag blocks in general. The output signal is fed as a supplementary input signal, V_s , to the regulator of

the excitation system. The limiter is included to prevent the output signal of the PSS from driving the excitation system into heavy saturation.

The effectiveness of PSS in achieving the desired objectives depends on the hardware design, method of deriving the input signal, selection of control parameters, commissioning procedures and field verification. Shaft speed, accelerating power, and terminal frequency are among the commonly used input signals to PSS. Conceptually, speed is the basic variable from which oscillations can be seen, and most early PSSs are based on speed signal input. But the speed signal PSS has noise and torsional problems and it is necessary to use torsional filters, which complicate its design and restrict its effectiveness [86, 88]. The frequency signal PSS can provide greater damping contributions to inter-area modes of oscillation than the speed input signal. Because the frequency signals measured at the terminals of thermal units contain torsional components, it is necessary to filter torsional modes when used with steam turbine units. The major advantages of an accelerating power signal stabilizer is that there is no need for a torsional filter. For simplicity, many a research works also regard the negative power signal as the accelerating power signal, assuming that the mechanical power output from turbine/governor system does not vary in the short term time scale [32, 33, 147-149]. PSS parameters should be chosen, along with the other control parameters of the excitation system, so as to enhance the overall performance of power systems.

1.5 Motivation of the Thesis

The probabilistic approach for power system dynamic studies has been successfully applied under multiple operating conditions in References [32, 33, 147-149] with the following contributions:

- With nodal voltages regarded as basic random variables and determined by probabilistic load flow calculation, the probabilistic distribution of each eigenvalue is obtained from the probabilistic attributes of nodal voltages, and described by its expectation and variance under the assumption of normal distribution;
- The first and second order eigenvalue sensitivities with respect to arbitrary system parameters can be systematically determined;
- The probabilistic eigenvalue sensitivity analysis is developed for robust PSS siting under multiple operating conditions;
- The probabilistic eigenvalue analysis has been applied for the robust PSS design, either by a sensitivity approach, or by a gradient-based nonlinear optimization approach.

Despite of a number of previously published works, there still exist spaces for improvement of the probabilistic eigenvalue analysis and other related studies. On the one hand, optimization and coordination of damping controllers is a multimodal optimization problem (i.e. there exists more than one local optimum) [80, 105], so the existing coordination approaches using local optimization techniques are suffering from the high sensitivity problem of the initial conditions and unable to obtain a solution that can satisfy the prescribed damping criteria under some very stressed operating

conditions [80]. On the other hand, the existing probabilistic PSS design methods only consider the variation of operating conditions with constant system parameters; system contingencies are not systematically included. In addition, the PSIs developed for robust PSS siting is performed on open-loop power systems, which cannot provide an optimal siting scheme, i.e., the minimum number of PSS locations [52].

This thesis is therefore devoted to the extended development of robust and coordinated PSS design in power systems. In summary, the following research topics associated with robust and coordinated PSS design will be studied:

- 1) The probabilistic PSS design using evolutionary algorithms will be investigated.
- 2) Robust PSS design that can systematically incorporate contingencies will be proposed.
- 3) Probabilistic PSS design considering optimal siting will be developed.

1.5.1 An introduction of EAs

In computer science, computational intelligence (CI) is a successor of artificial intelligence. Computational intelligence is a methodology involving computing that exhibits an ability to learn and/or to deal with new situations, such that the system is perceived to possess one or more attributes of reason, such as generalization, discovery, association and abstraction [43, 54]. CI systems usually comprise hybrids of paradigms such as artificial neural networks, fuzzy systems, and evolutionary algorithms, augmented with knowledge elements, and are often designed to mimic one or more aspects of biological intelligence.

Evolutionary algorithm (EA) or evolutionary computation is an important subfield of computational intelligence that rather relies on heuristic algorithms. EAs have attracted a great deal of attention recently and have been found to be a robust approach for solving non-linear, non-differentiable and multi-modal optimization problems, which can overcome the weakness of some gradient-based nonlinear optimization methods. The history of EAs can be traced as early as forty years ago [111]. The algorithms in this category include genetic algorithm (GA), evolutionary programming (EP) and evolution strategies (ES) [10], and the recently popular particle swarm optimization (PSO) [78] and differential evolution (DE) [123]. Some of the advantages of EAs include [64]:

- Do not require derivative information
- Can simultaneously search from a wide sampling of the cost surface
- Can deal with a large number of variables
- Are well suited for parallel computers
- Can optimize variables with extremely complex cost surfaces
- Can provide a list of optimum variables, not just a single solution

1.5.2 Application of EAs in the thesis

Genetic algorithm (GA), particle swarm optimization (PSO) and differential evolution (DE) are three representative EAs that will be applied to several PSS design problem in the thesis. They are all evoked by an analogy with biology, in which a group or population of solutions evolves generation by generation through some biological mechanisms. Despite many successful applications of EAs in other areas, this thesis is

not intended to convey the impression that the PSS designs using GA, PSO, DE or other related techniques are better than other PSS designs. It is believed that each method has its own merits and shortcomings. Using a limited number of study examples does not guarantee, in any way, that an evolutionary algorithm that performs well on them will necessarily be competitive in a different set of problems [153]. The focus of this thesis is, therefore, on systematically considering the in-depth study of robust and coordinated PSS design, such as robustness of probabilistic PSS design, synthesis of system contingencies, optimal siting topics; and on exploring their potentials and values.

Differential evolution (DE) is a novel evolutionary algorithm characterized as simple to implement and little tuning on control parameters. Thus DE is often recommended to receive primary attention when facing new optimization problems [93]. The probabilistic PSS design model in the thesis differs from most previous models in that the former includes the probabilistic eigenvalue analysis. The robustness of the new model will therefore be primarily investigated by DE method.

Genetic algorithm (GA) has been one of the most popular EAs during the past decade because of its computationally simple and easy to implement. In Reference [1], the BLX- α operator based GA has been reported to be able to achieve prominent performance in PSS design. However, the PSS design model in Reference [1] did not include a systematic way to handle the system contingencies. Thus, the PSS design by the BLX- α GA approach will be extended to consider the system contingencies in the thesis.

Particle swarm optimization (PSO) is reported to potentially have smaller population-size requirement than other population-based EAs so that PSO might converge faster when they are applied to those highly complex problems that require time-consuming simulations to determine the value of objective function [45]. The probabilistic PSS design with system contingencies taken into account is a very complicated model that might require a large amount of computing time for calculation, and thus PSO will be tentatively employed to solve this problem.

As mentioned before, GA is computationally simple and easy to implement, besides it is very powerful and flexible in handling those optimization problems with mixed discrete-continuous variables. When the probabilistic PSS design considers the optimal siting issue, it can be described as an optimization problem with mixed discrete-continuous variables. Hence, a mixed integer-binary coded GA will be applied to the optimal-siting probabilistic PSS design in the thesis.

1.6 Outline of the Thesis

The remaining chapters of the thesis are organized as follows:

Chapter 2: The probabilistic eigenvalue analysis is briefly reviewed. Two PSIs are introduced, which could be regarded as probabilistic participation factor and residue, respectively. As a simple application, they are applied to determine robust PSS siting under multiple operating conditions.

Chapter 3: A robust PSS design method is introduced to enhance the damping of multiple electromechanical modes in a multi-machine system over a large

and pre-specified set of operating conditions, in which a probabilistic eigenvalue-based optimization model is formulated. The DE technique is applied for solving the highly nonlinear optimization problem. Different strategies for control parameter settings of DE will be studied.

Chapter 4: A systematic approach that can incorporate system contingencies into PSS design is proposed. In the proposed method, the number of contingencies is significantly reduced by a critical contingency screening process. The PSS design problem is formulated as a multi-objective optimization model with contingencies taken into account. A recursive GA is then presented to tune PSS parameters so that the dynamic security criteria subject to contingencies are satisfied under a wide range of operating conditions.

Chapter 5: A systematic approach that can extend the existing probabilistic PSS design by synthesizing system contingencies is developed. A critical contingency screening is conducted by a ranking of contingencies according to a probabilistic small signal stability index. A multi-objective optimization model is formulated to seek satisfactory system damping performance with contingencies taken into account. A recursive PSO technique is then used to solve the optimization model.

Chapter 6: The probabilistic PSS design that considers the optimal-siting is addressed. In the proposed method, a combination optimization model is developed and a recursive GA based on a mixed integer-binary coding and a partially matched crossover operator is developed to solve the problem. The influence

of the probability of crossover and mutation operator on the GA performance is primarily investigated.

Chapter 7: The main findings and contributions of this PhD thesis are summarized.

Some directions for future research work related to damping controller design are pointed out.

2 AN INTRODUCTION TO PROBABILISTIC EIGENVALUE ANALYSIS

2.1 Introduction

The concept of probability for power system dynamic stability studies was first introduced in Reference [17] with normal distribution assumed. From the known statistic nature of system stochastic parameters, the probabilistic density of the real part of eigenvalues was then determined. The stability probability of entire system was computed from the joint normal distribution. This approach was extended in Reference [18], where random variables could be arbitrary distributions. The random variables were described by their statistic moments, and the system stability probability was determined by Gram series. Another paper [97], using second order statistics, showed that fluctuations in loads and transmission reactances (modeled by stationary random processes) could induce a stable system to become unstable if a generator is weakly connected to it. In most of above cases, some simplifications were adopted, such as assuming normal distribution [16, 17, 134], presuming the statistical independence between variables [44, 152].

In 2000, a pioneer work [147-149] was proposed to apply probabilistic method to PSS design. In this work, multi-operating conditions were considered as uncertainty source, and linearized power flow equation was adopted for obtaining generator state and nodal

voltages in probabilistic environment. Under the assumption of normal distribution, by using a standardized eigenvalue expectation, the robust stability of a system could be directly evaluated, and the probabilistic eigenvalue sensitivity analysis was first applied to tune the PSS. The probabilistic eigenvalue analysis developed in References [147-149] laid the foundation of most research works in the thesis. In this chapter, the primary principle of the probabilistic eigenvalue analysis will be first presented. Two probabilistic sensitivity indices (PSIs) of an eigenvalue will be introduced. As a simple application, they are applied to determine robust PSS siting on two test systems.

2.2 Probabilistic Damping Criteria

Under the multioperating conditions of a power system, all nodal injections, nodal voltages and eigenvalues are regarded as random variables. Statistical attributes of nodal injections are determined from system operating samples. The statistical nature of an eigenvalue can be described by its expectation and variance. For a particular eigenvalue $\lambda_k = \alpha_k + j\beta_k$, having an expectation $\bar{\alpha}_k$ and standard deviation σ_{α_k} , the distribution within $\{-\infty, \bar{\alpha}_k + \kappa\sigma_{\alpha_k}\}$ with a distribution constant κ over [3.5, 4] has a probability from 0.99977 to 0.99997, which is very close to unity.

To ensure the stability of α_k , this distribution range should be located on the left-hand side in the complex plane as illustrated by the curves of probability density function (pdf) in Figure 2-1.

Thus, the upper limit of this distribution range α'_k in equation (2-1) can be regarded as an extended damping coefficient from which the robust stability of multioperating

conditions can be estimated. Correspondingly, the damping ratio $\xi_k = -\alpha_k / \sqrt{\alpha_k^2 + \beta_k^2}$ with expectation $\bar{\xi}_k$ and standard deviation σ_{ξ_k} has an extended value ξ_k' in equation (2-2). A brief derivation of $\bar{\alpha}_k$, σ_{α_k} , $\bar{\xi}_k$ and σ_{ξ_k} can be found in Appendix A.

$$\alpha_k' = \bar{\alpha}_k + \kappa\sigma_{\alpha_k} \quad (2-1)$$

$$\xi_k' = \bar{\xi}_k - \kappa\sigma_{\xi_k} \quad (2-2)$$

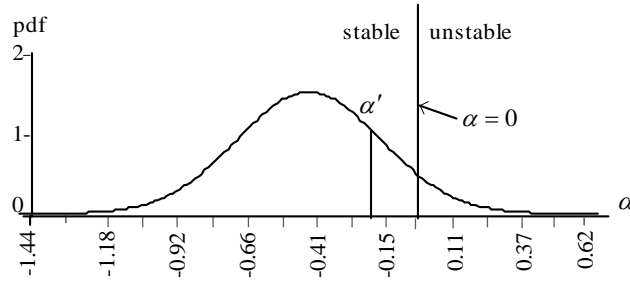


Figure 2-1. Probabilistic eigenvalue distribution

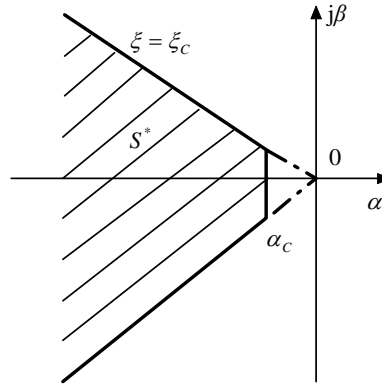


Figure 2-2. Desired eigenvalue distribution region

To ensure the system dynamic performance, all the eigenvalues need to satisfy the requirement of damping constant and damping ratio in equation (2-3) and (2-4)

respectively. In other words, all the eigenvalues should be located in the shadowed D-shape region S^* in Figure 2-2.

$$\alpha_k' \leq \alpha_C \quad (2-3)$$

$$\xi_k' \geq \xi_C \quad (2-4)$$

where α_C and ξ_C are acceptable limits for damping constant and damping ratio, respectively.

Further, it is more convenient to introduce the standardized expectations of the damping constant and damping ratio α_k^* and ξ_k^* , derived from equations (2-1), (2-2) and termed as $\kappa\sigma$ criteria, being defined as:

$$\alpha_k^* = -(\bar{\alpha}_k - \alpha_C) / \sigma_{\alpha_k} \geq \kappa \quad (2-5)$$

$$\xi_k^* = (\bar{\xi}_k - \xi_C) / \sigma_{\xi_k} \geq \kappa \quad (2-6)$$

After the standardization in (2-5) and (2-6), α_k^* and ξ_k^* are per-unit variables and can be directly compared.

2.3 Probabilistic Sensitivity Indices (PSIs)

The eigenvalue sensitivities in [114] for the problems of PSSs siting and tuning are basically developed under single operating condition. As an extension of conventional sensitivity concept, the Probabilistic Sensitivity Indices (PSIs) is proposed in [33, 149] and defined as the sensitivity of damping ratio ξ' and/or damping constant α' with respect to system parameters x under multioperating conditions.

$$S'_{\alpha_{k,x}} = \frac{\partial \alpha'_k}{\partial x} = \frac{\partial \bar{\alpha}_k}{\partial x} + \kappa \frac{\partial \sigma_{\alpha_k}}{\partial x} \quad (2-7)$$

$$S'_{\xi_{k,x}} = \frac{\partial \xi'_k}{\partial x} = \frac{\partial \bar{\xi}_k}{\partial x} - \kappa \frac{\partial \sigma_{\xi_k}}{\partial x} \quad (2-8)$$

where the sensitivities of $\bar{\alpha}_k$, $\bar{\xi}_k$, σ_{α_k} and σ_{ξ_k} are derived in Appendix A.

The PSI can be regarded as the participation factor of the sensitivity of α' with respect to a diagonal element of the state matrix A , or the damping ratio ξ' with respect to PSS gain K_m at zero gain value, which could be regarded as a PSI residue index.

$$S'_{\alpha_{k,K_m}} \Big|_{K_m=0} = \frac{\partial \alpha'_k}{\partial K_m} \Big|_{K_m=0} \quad (2-9)$$

$$S'_{\xi_{k,K_m}} \Big|_{K_m=0} = \frac{\partial \xi'_k}{\partial K_m} \Big|_{K_m=0} \quad (2-10)$$

As a simple application, PSIs could be used to identify the proper locations of PSSs under multiple operating conditions. This PSS siting strategy will be adopted throughout Chapters 3-5.

2.4 Case Studies

In this section, two test systems will be employed to demonstrate a simple application of two PSIs. One is a three-machine nine-bus power system; another is a three-area system that is composed of 8 machines and 24 buses. The criteria for the damping ratio and damping constant are chosen as $\xi_c = 0.1$ and $\alpha_c = 0$ for both systems. The distribution constants κ for the two systems are set to 4.0 and 3.5, respectively.

2.4.1 Three-machine power system (system I)

The three-machine nine-bus system shown in Figure 2-3 is modified from [128], where G3 equivalent lumped interconnection system and is regarded as the slack bus generator. All machines are represented as fourth-order models and equipped with fast-acting static exciter. System loads are represented by constant impedance models. Normal operation values of nodal powers and PV bus voltages shown in Figure 2-3 are regarded as their expectations. All network parameters, nodal powers, generator parameters and control system parameters are listed in Appendix C1. The generator model and control system models are given in the Appendix B1 and Appendix C1, respectively.

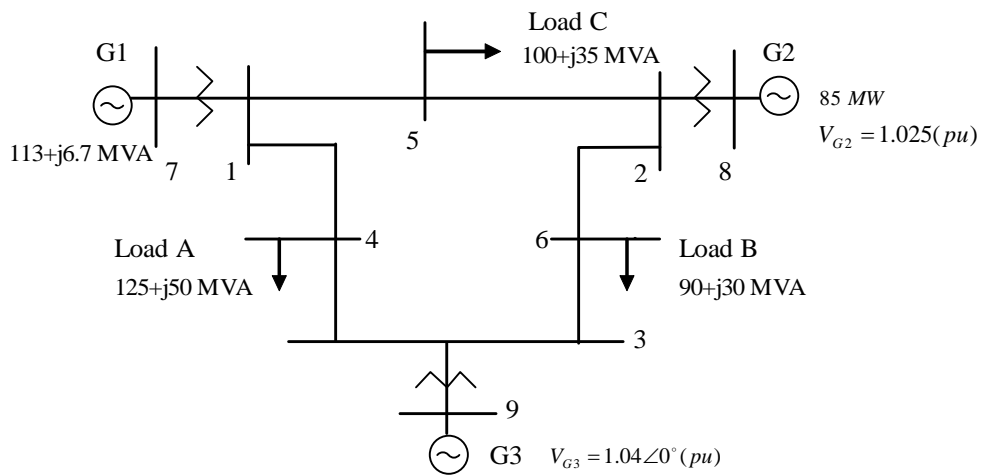


Figure 2-3. Single line diagram of three-machine system

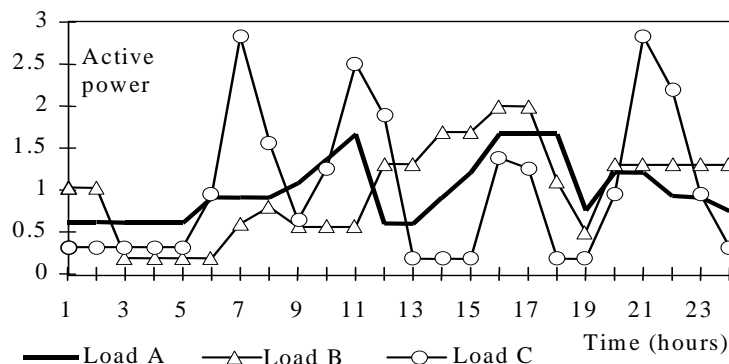


Figure 2-4. Daily operating curves of load powers in system I

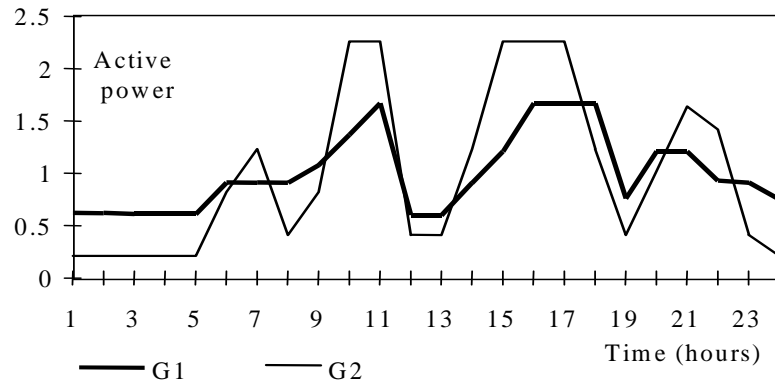


Figure 2-5. Daily operating curves of generation powers in system I

Standardized daily operating curves listed in Table C-11 of Appendix C2 are used to create the power and PV-voltage samples. Power curves are also shown in Figures 2-4 and 2-5 for this system. From these curves, 480 operating samples are created in time sequence. The sample size should be large enough so that the stochastic characteristic of these curves can be reserved. For 24-hour operating curves, 480 points corresponds to those operating points of every 3 minutes, which satisfy this requirement. Then expectations and covariances of nodal injections are determined and the statistical characteristics can be captured by the probabilistic eigenvalue analysis. The three-machine system shown in Figure 2-3 has 17 eigenvalues (7 real and 10 complex). 480 system operating samples are created and the worst scenario is very marginally stable with $\xi < 0.005$. The probabilistic eigenvalue analysis is performed and the worst damped modes are listed in Table 2-1. As discussed in Section 2.2, if the standardized expectations of both α_k^* and ξ_k^* are larger than $\kappa (= 4)$, the corresponding mode is regarded as adequate for robust stability, otherwise inadequate. In this case, two eigenvalues of the system in Table 2-1 are “inadequate” and highlighted in bold, with α_1^* , α_2^* , ξ_1^* and ξ_2^* equal to 2.88, 1.67, 0.36 and 0.38, respectively.

Table 2-1. Electromechanical modes of the open-loop system **I**

No.	$\bar{\alpha}$	$\bar{\beta}$	σ_{α}	α^*	P_{α}	$\bar{\xi}$	σ_{ξ}	ξ^*	P_{ξ}	Dominant States
1	-0.910	7.895	0.3161	2.88	0.998	0.1145	0.0402	0.36	0.641	δ_1, ω_1
2	-1.298	9.905	0.7779	1.67	0.952	0.1299	0.0783	0.38	0.649	δ_2, ω_2

Expectations: $\bar{\lambda} = \bar{\alpha} \pm j\bar{\beta}$ and $\bar{\xi}$; Standard deviation: σ

Standardized expectation: $\alpha^* = -\bar{\alpha} / \sigma_{\alpha}$ and $\xi^* = (\bar{\xi} - 0.1) / \sigma_{\xi}$

Distribution probabilities: $P_{\alpha} = P\{\alpha < 0\}$ and $P_{\xi} = P\{\xi > 0.1\}$

For PSS location selection, PSIs are calculated and adopted for the two critical eigenvalues in Table 2-1 and the results are shown in Table 2-2 and Table 2-3. PSIs values in Table 2-2 are the sensitivities with respect to PSS gains at zero value, which are corresponding to the probabilistic residues. PSIs values listed in Tables 2-3 are the sensitivities with respect to the diagonal elements of system matrix **A**, which are corresponding to the probabilistic participation factor. The prominent sensitivity values are highlighted in the tables. The probabilistic damping ratio ξ' and damping constant α' in Tables 2-2 and 2-3 are corresponding to the PSIs of the two open-loop electromechanical modes in Table 2-1.

Table 2-2. PSIs corresponding to residue in system **I**

	$\Delta\omega_1$	$\Delta\omega_2$	$\Delta\omega_3$	ΔP_{e1}	ΔP_{e2}	ΔP_{e3}
α'_1	-0.10243	-0.03379	0.04105	3.3830	1.0362	1.5850
ξ'_1	0.07236	0.02022	0.02707	-0.4314	-0.1328	-0.1592
α'_2	0.00405	-0.00350	0.01282	0.5746	9.0202	0.1342
ξ'_2	0.09452	0.15435	0.00089	-0.0677	-0.8962	-0.0013

Table 2-3. PSIs corresponding to participation factor in system I

	$\Delta\omega_1$	$\Delta\omega_2$	$\Delta\omega_3$
α'_1	0.30823	0.03243	0.17907
α'_2	0.08567	0.32503	0.02216

To increase system damping, it requires decreasing α' and increasing ξ' . It is desirable that the corresponding PSIs of the selected signal for α' and ξ' of an electro-mechanical mode have opposite sign. For example, in mode 1 the PSI value of ξ' with respect to ΔP_{e1} in Table 2-2 is 3.3830, which is of opposite sign to the PSI value of α' with respect to ΔP_{e1} (-0.4314). On the other hand, it is also desirable to have the same sign for α' and ξ' of different modes, e.g. 3.3830 and 9.0202 for α'_1 and α'_2 , and likewise -0.4314 and -0.8962 for ξ'_1 and ξ'_2 . The probabilistic participation factors in Table 2-3 also support this decision as G1 has prominent participation in mode 1 and G2 in mode 2.

2.4.2 Eight-machine power system (system II)

The system in Figure 2-6 is a three-area system consisting of 8 machines and 24 buses, which is modified from the 36-bus test system in 'Power system analysis software package (PSASP)' [47] by omitting the DC links. Buses numbered from 1 to 16 are load buses, 17 to 24 generator buses. G8 represents equivalent lumped interconnection system and is regarded as the slack bus generator. All generators are represented as sixth-order models and equipped with IEEE-Type I exciters and speed governors. System loads are represented by constant impedance models. All network parameters,

nodal powers, generator parameters and control system parameters are listed in Appendix C2. The generator model and control system models are given in the Appendices B2 and C2, respectively.

In Figure 2-6, different daily curves are assigned for nodal powers S_{L1} to S_{L9} , P_{G1} to P_{G7} , and Q_{G3} , Q_{G6} respectively, which can be referred to in Appendix C2. The reference voltage at slack bus 24 also varies according to a curve as shown in Table C-11 of Appendix C2. Similarly, the statistical characteristics of the system can be captured by the probabilistic eigenvalue analysis based on sampled 480 operating conditions.

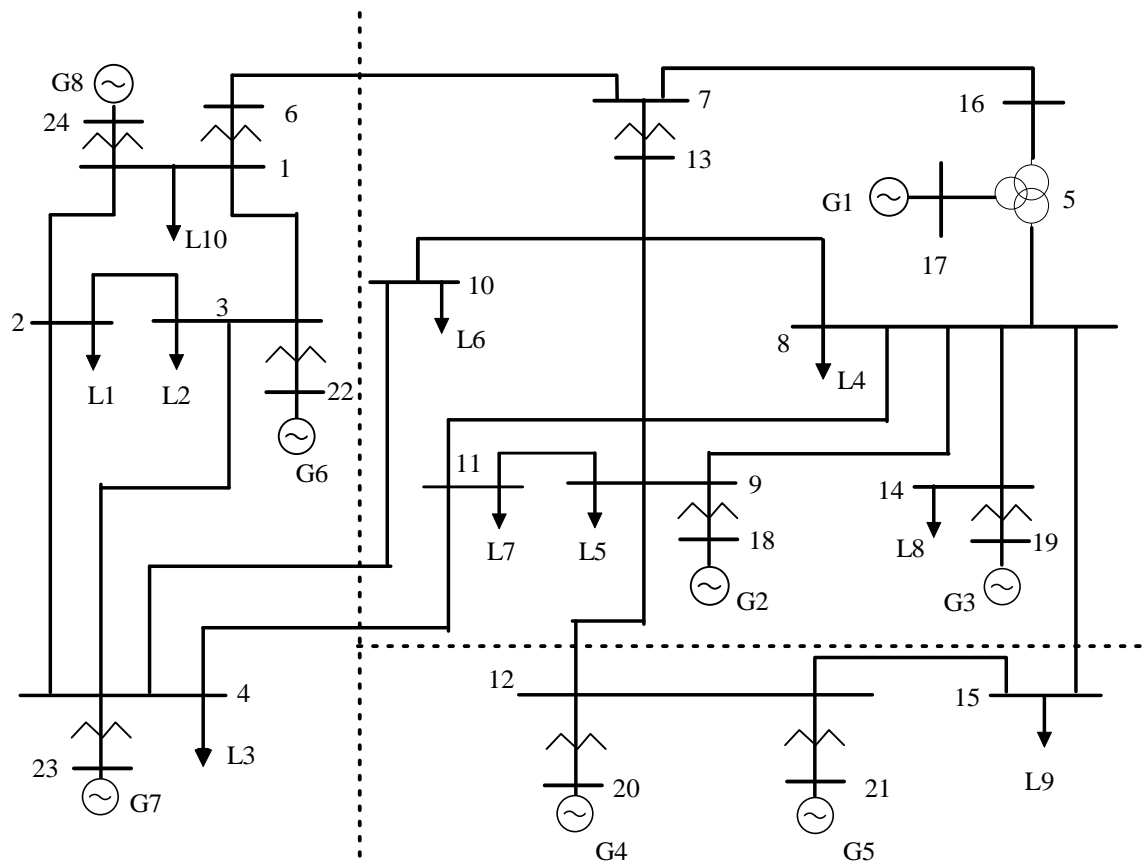


Figure 2-6. Single line diagram of eight-machine system

The eight-machine system shown in Figure 2-6 has 94 eigenvalues (50 real and 44 complex). Probabilistic eigenvalue analysis results for the 7 electromechanical modes are shown in Table 2-4 (other eigenvalues with adequate stability probabilities are not shown for simplicity). From Table 2-4, all the 7 modes are not robust stable, with mode 1 slightly inadequate and mode 7 very inadequate. The mode 7 is an inter-area mode with machines in different areas involved.

Similar PSIs analysis was performed and the results are given in Tables 2-5, 2-6, and 2-7, which correspond to the PSIs of the seven open-loop electro- mechanical modes in Table 2-4. The results of PSIs in Tables 2-5, 2-6 and 2-7 are well consistent with the results of mode analysis in Table 2-4, for example, the mode 1 is a local mode and related to G1; correspondingly, those PSIs values for G1 ($\Delta\omega_1$ or ΔP_{e1}) related to mode 1 are much larger than others; the mode 7 is an inter-area mode with G5, G7 and G8 involved, which can be observed in these tables.

Table 2-4. Electromechanical modes of the open-loop system **II**

No.	$\bar{\alpha}$	$\bar{\beta}$	σ_α	α^*	P_α	$\bar{\xi}$	σ_ξ	ξ^*	P_ξ	Dominant States
1	-1.925	15.400	0.0795	24.21	1.00	0.1240	0.0071	3.40	0.9997	δ_1, ω_1
2	-0.773	10.754	0.0700	11.03	1.00	0.0717	0.0062	-4.59	0.00	δ_2, ω_2
3	-0.590	9.705	0.0392	15.05	1.00	0.0607	0.0031	-12.65	0.00	δ_6, ω_6
4	-0.604	7.888	0.0242	24.93	1.00	0.0763	0.0044	-5.42	0.00	δ_4, ω_4
5	-0.600	7.381	0.0834	7.20	1.00	0.0810	0.0098	-1.93	0.0268	δ_3, ω_3
6	-0.365	6.420	0.0462	7.88	1.00	0.0567	0.0072	-6.05	0.00	δ_5, ω_5
7	-0.033	3.854	0.0069	4.77	1.00	0.0085	0.0018	-49.55	0.00	$\delta_7, \delta_5 \omega_8$

Table 2-5. PSIs corresponding to participation factors in system **II** (Speed Signal)

	$\Delta\omega_1$	$\Delta\omega_2$	$\Delta\omega_3$	$\Delta\omega_4$	$\Delta\omega_5$	$\Delta\omega_6$	$\Delta\omega_7$	$\Delta\omega_8$
α_1	0.5161	0.0044	0.0051	0.0010	0.0013	0.0017	0.0010	0.0000
α_2	0.0004	0.4073	0.0022	0.0039	0.0043	0.1079	-0.0017	0.0000
α_3	0.0003	0.0061	-0.0018	0.0036	0.0038	0.4266	0.0710	0.0058
α_4	0.0000	0.0000	-0.0014	0.2954	0.2214	0.0000	0.0000	0.0000
α_5	0.0000	-0.0015	0.4306	0.0471	0.0397	-0.0005	-0.0014	-0.0004
α_6	0.0003	0.0001	0.0086	0.0849	0.1321	0.0135	0.2695	0.0000
α_7	0.0003	0.0046	0.0130	0.0141	0.0197	0.0032	0.0350	0.4060

Table 2-6. PSIs corresponding to residues in system **II** ($\times 0.01$) (Speed Signal)

	$\Delta\omega_1$	$\Delta\omega_2$	$\Delta\omega_3$	$\Delta\omega_4$	$\Delta\omega_5$	$\Delta\omega_6$	$\Delta\omega_7$	$\Delta\omega_8$
ξ_1	-0.1235	-0.0004	0.0001	0.0000	0.0001	-0.0001	0.0001	0.0000
ξ_2	-0.0012	-0.1596	0.0006	0.0002	0.0006	-0.0260	0.0001	0.0000
ξ_3	-0.0012	-0.0047	0.0010	-0.0012	-0.0008	-0.1519	0.0027	-0.0003
ξ_4	0.0000	0.0000	0.0010	-0.1099	-0.0813	0.0000	0.0000	0.0000
ξ_5	-0.0019	0.0007	-0.1757	-0.0250	-0.0246	0.0005	0.0014	0.0000
ξ_6	-0.0039	-0.0005	-0.0161	-0.0053	-0.0201	-0.0055	-0.0161	0.0000
ξ_7	0.0005	-0.0073	-0.0028	0.0206	0.0250	-0.0118	-0.0156	0.0018

Table 2-7. PSIs corresponding to residues in system **II** (Power Signal)

	ΔP_{e1}	ΔP_{e2}	ΔP_{e3}	ΔP_{e4}	ΔP_{e5}	ΔP_{e6}	ΔP_{e7}	ΔP_{e8}
ξ_1	0.0890	0.0003	-0.0007	-0.0003	-0.0005	0.0004	-0.0001	0.0000
ξ_2	0.0003	-0.0725	-0.0011	-0.0012	-0.0011	0.0372	0.0022	0.0000
ξ_3	0.0004	0.0047	-0.0005	-0.0011	-0.0017	-0.0862	0.0055	-0.0047
ξ_4	0.0000	0.0000	-0.0019	-0.3511	-0.3448	0.0000	0.0002	0.0000
ξ_5	-0.0010	0.0006	-0.4827	-0.0618	-0.0845	-0.0001	-0.0016	-0.0001
ξ_6	-0.0002	0.0001	-0.0037	-0.1783	-0.3837	-0.0115	-0.1193	-0.0009
ξ_7	0.0023	-0.0087	-0.0391	-0.0522	-0.1053	-0.0167	-0.0766	0.0189

2.4.3 PSS location and signal selection

A System I

The larger is the absolute value of PSIs, the more improvement can be achieved by installing PSS there. This is the basic principle of applying PSIs for PSS siting. From Tables 2-2 and 2-3, it is obvious that these ‘desirables’ can be achieved by all the power signals ΔP_e as well as speed signals $\Delta \omega$, despite that the effect of power-signal PSS could be better than speed-signal PSS. But in the thesis, two speed-signal PSSs in G1 and G2 would be tentatively applied in system **I** for demonstration purpose and will be used in Chapters 3-5.

B System II

The PSIs results in Table 2-6 and Table 2-7 shows that system oscillation modes are much more sensitive to PSS with electrical power input than with speed signal input, which is obvious from the relationship between electrical power signal and speed signal [91]. The power-signal PSSs will be used in the system **II**. From Tables 2-5, 2-6 and 2-7, it can be observed that the modes 1, 2, 3, and 5 are most sensitive to G1, G2, G3 and G6 and can be improved by installing PSSs on those sites; the other three modes are most sensitive to G4 & G5, G5 & G7, which can be improved by PSS on G5 (G4), G7. A scheme of installing PSSs at G1, G2, G3, G5, G6, and G7 with power signal is tentatively developed and will be used in Chapters 3-5.

2.5 Summary

This chapter introduces the probabilistic analysis approach for determining the robust PSS siting and signal selection. Under the assumption of normal distribution, two probabilistic sensitivity indices are derived and calculated based on the system multi-operating conditions. In case studies, the proposed probabilistic sensitivity index is used on two test systems to select the PSS locations. In next chapter, an evolutionary algorithm will be applied to the probabilistic PSS design so that the parameters of PSS can be determined to satisfy the robust stability criteria.

3 ROBUST PSS DESIGN UNDER MULTIOPERATING CONDITIONS USING DIFFERENTIAL EVOLUTION

3.1 Introduction

Parameter optimization models for coordinated PSS design has been comprehensively developed in previous studies [19, 63, 92, 105, 106]. The model proposed in References [105, 106] aims to shift those critical eigenvalues to the left of some threshold value or into some stability region. To deal with more eigenvalues simultaneously, the objective described in References [4, 5, 19, 105, 106] is a square sum of the desired movements of real parts and/or damping ratios of all unsatisfactory eigenvalues. In Reference [92], the controller parameters are optimized by minimizing a transient performance index after system disturbances, which is calculated based on a series of time domain simulation. In References [105, 106], the steepest descent approaches is used (i.e. in the negative gradient direction) for solution; a gradient-based nonlinear approach is employed in References [19, 92].

References [32, 33, 142, 147] have extended the probabilistic eigenvalue analysis to PSS design in multimachine systems for the purpose of including a wide range of system load conditions. In References [32, 142, 147], a quasi-Newton approach is adopted to solve the probabilistic PSS design; while a sensitivity approach is applied in Reference [33]. However this optimization problem of the probabilistic PSS design is

highly nonlinear and the solution is difficult to be obtained based on the conventional optimization technique.

Evolutionary algorithms (EAs) have attracted a great deal of attention recently and have been found to be a robust approach for solving non-linear, non-differentiable and multi-modal optimization problems. EAs are evoked by an analogy with biology, in which a group or population of solutions evolves generation by generation through natural selection. In their implementations, a population of candidate solutions, referred to as the chromosomes, evolves to an optimum solution through the operation of genetic operators such as reproduction, crossover, and mutation. In recent years, some evolutionary methods such as genetic algorithm (GA) [1, 14] and particle swarm optimization (PSO) [4] have been applied to the problem of PSS design. Unlike the conventional methods, these methods can finally reach the optimal solution regardless of the initial PSS settings.

As a new branch of EAs, differential evolution (DE) has the ability to overcome some drawbacks of classic GA, such as non-isomorphic search strategies and susceptibility to coordinate rotation [124, 136]. Though simple, DE is endowed with the features of self-adaptation and rotational invariance, which are crucial for an efficient EA scheme and were pursued in the evolution strategies (ES) community with complicated designs [123]. Thus DE is often recommended to receive primary attention when facing new optimization problems. In Chapter 2, the probabilistic eigenvalue analysis is used to evaluate the system electromechanical modes and robust PSS location is determined by PSIs. In this chapter, the probabilistic PSS design problem will be first formulated as a

probabilistic eigenvalue based optimization model. Then, a novel DE-based approach to probabilistic PSS design will be developed. Finally, the effectiveness of the proposed probabilistic PSS design scheme is demonstrated on two test systems by DE robustness testing, eigenvalue analysis and nonlinear simulation.

3.2 Problem Formulation of Probabilistic PSS Design

3.2.1 PSS structure

In this thesis, a typical PSS transfer function $F(s)$ based on speed/power input signal with two lead/lag stages is used, which correspond to the PSS structure depicted in Section 1.4.

$$F_i(s) = K_i \cdot \frac{pT_w}{1 + pT_w} \cdot \frac{1 + pT_{1i}}{1 + pT_{2i}} \cdot \frac{1 + pT_{3i}}{1 + pT_{4i}} \quad (3-1)$$

where $i \in \{1, \dots, N_{\text{PSS}}\}$ and N_{PSS} is the total number of PSS to be tuned; K_i is PSS gain constant with positive value for speed input signal and negative value for power input signal; T_w is washout time constant; T_{1i}/T_{2i} and T_{3i}/T_{4i} are lead/lag time constants. It should be noted that the time constants T_{2i} and T_{4i} should not be less than 0.04s to avoid excessive amplification of input signal noise. In this thesis, T_w is fixed as 10s and 5s for speed and power input signals respectively. The ranges of the PSS parameters are set as follows: [0.1p.u., 20p.u.] for K_i of PSS with speed input signal and [-20p.u., -0.1p.u.] with power input signal, [0.06s-2.0s] for T_{1i} and T_{3i} , [0.04s-0.2s] for T_{2i} and T_{4i} [51, 125, 128].

3.2.2 Parameter optimization model

It is mentioned in Chapter 2 that all the eigenvalues should be located in the shadowed D-shape region S^* in Figure 2-2 of Chapter 2 to ensure an adequate system dynamic performance. Thus, an optimization problem is formulated in model (3-2) and only those “weak” eigenvalues ($\alpha_k^* < \kappa$ or $\xi_k^* < \kappa$) are included so that those unstable or poorly damped electromechanical oscillation modes are relocated to a more stable region. If problem (3-2) is solvable (i.e. a feasible solution exists), all the eigenvalues should be located in the D-shape region S^* in Figure 2-2 and the value of the objective function will be equal to zero; otherwise, it will be greater than zero.

$$\text{Minimize } f(\mathbf{P}) = \sum_{\alpha_k^* < \kappa} (\alpha_k^* - \kappa)^2 + \sum_{\xi_k^* < \kappa} (\xi_k^* - \kappa)^2 \quad (3-2)$$

s.t.

$$K_{i,\min} \leq K_i \leq K_{i,\max}$$

$$T_{1,\min} \leq T_{1i} \leq T_{1,\max}$$

$$T_{2,\min} \leq T_{2i} \leq T_{2,\max}$$

$$T_{3,\min} \leq T_{3i} \leq T_{3,\max}$$

$$T_{4,\min} \leq T_{4i} \leq T_{4,\max}$$

where \mathbf{P} stands for the PSS parameter vector; $K_{i,\min}, T_{1i,\min}, T_{2i,\min}, T_{3i,\min}$ and $T_{4i,\min}$ are the minimum limits of PSS parameters; $K_{i,\max}, T_{1i,\max}, T_{2i,\max}, T_{3i,\max}$ and $T_{4i,\max}$ are the maximum limits of PSS parameters.

3.3 Probabilistic PSS Design Using Differential Evolution

Differential evolution (DE) has been widely studied on a large variety of benchmark problems and practical problems, and its excellent performance is shown in these studies [89, 122-124, 135, 136]. Similar to other EAs, in DE's implementation, a population of randomly generated and real-encoding candidate solutions evolves to an optimal solution through the reproduction operation and selection. This section describes the principal components of DE and its application in solving the problem of probabilistic PSS design in (3-2). The pseudo-code of DE method is given in Table 3-1.

3.3.1 Principal components of DE

The principal components of the DE algorithm are introduced as follows:

A Chromosomes

A chromosome can be taken as an array holding a candidate group of PSS parameters. The parameters are encoded using floating-point numbers and are set as elements in the chromosomes.

B Population initialization

For convenient explanation, $X_i = [x_{i,1}, x_{i,2}, \dots, x_{i,D}]$ represents a real-coded chromosome that has a unique mapping with a group of domain variables; D is the total number of PSS parameters to be determined in problem (3-2). The initial DE population with NP (population size) candidate solutions or individuals is generated at random from the parameter domains according to:

$$x_{i,j}^{(0)} = p_j^{\min} + r \cdot (p_j^{\max} - p_j^{\min}) \quad (3-3)$$

where $i \in \{1, \dots, NP\}$; $j \in \{1, \dots, D\}$; $x_{i,j}^{(g)}$ denotes the value of the j -th PSS parameter of the i -th individual at the g -th generation, i.e. $g = 0$ for the first generation; p_j^{\max} and p_j^{\min} denote the upper and lower bounds of parameter j ; and r is a uniformly distributed random value over the range of $[0, 1]$.

Table 3-1. Pseudo-code of the DE-based probabilistic PSS design

```

Set the iteration or generation counter  $g$  to 0;
Initialize population of chromosomes  $P(g)$  at generation  $g$ ;
Evaluate the objective function values of chromosomes in  $P(g)$ ;
While (not terminate) {
    Generate the child population  $C(g)$  from the parent population  $P(g)$ 
    by reproduction operation;
    Evaluate the objective function values of  $C(g)$ ;
    Perform the one-to-one selection and reproduce the  $P(g+1)$ ;
     $g = g + 1$ ;
}

```

C Reproduction operation

The classical DE operator and its derivative operators could provide tailored candidate schemes for solving different domain problems, in which a tradeoff between the convergence speed and the population diversity could be achieved [124]. Each parent X_i will produce one offspring U_i in every generation. The reproduction operator used in this study called DE/rand-to-best/1/bin, which is designed to be easy to

understand and simple to use and with no sacrifice to effectiveness [135], is given in equation (3-4) and illustrated in Figure 3-1,

$$U_i^{(g)} = X_i^{(g)} + K(X_{best} - X_i^{(g)}) + F(X_{r_1}^{(g)} - X_{r_2}^{(g)}) \quad (3-4)$$

where $r_1, r_2 \in \{1, \dots, NP\}$ are randomly selected number with $r_1 \neq r_2 \neq i$; X_{best} is the up-to-date best individual; K and F are scale coefficients of crossover and mutation, respectively; $K(X_{best} - X_i^{(g)})$ and $F(X_{r_1}^{(g)} - X_{r_2}^{(g)})$ play a role of crossover and mutation operation, respectively. The impact of the scale coefficients K and F on the performance of DE in the probabilistic PSS design will be investigated in Section 3.4.1. DE's reproduction strategy by equation (3-4) can be viewed as a "greedy" reproduction since it exploits the information of the best individual to guide the search. This can speed up the convergence because the way the best individual is utilized here is a kind of "population acceleration" [154], whilst the diversity of the whole population can be held by the diffuse effect of mutation item. Unlike other EAs that rely on a predefined probability distribution function, the reproduction of DE is driven by the difference between randomly sampled pair of individuals in the current population. This reproduction scheme, though simple, endows DE with the features of self-tuning and rotational invariance, which are crucial for an efficient EA scheme and have long been pursued in the EA community. In ES, they are realized by complicated approaches using strategy vectors and matrices [123].

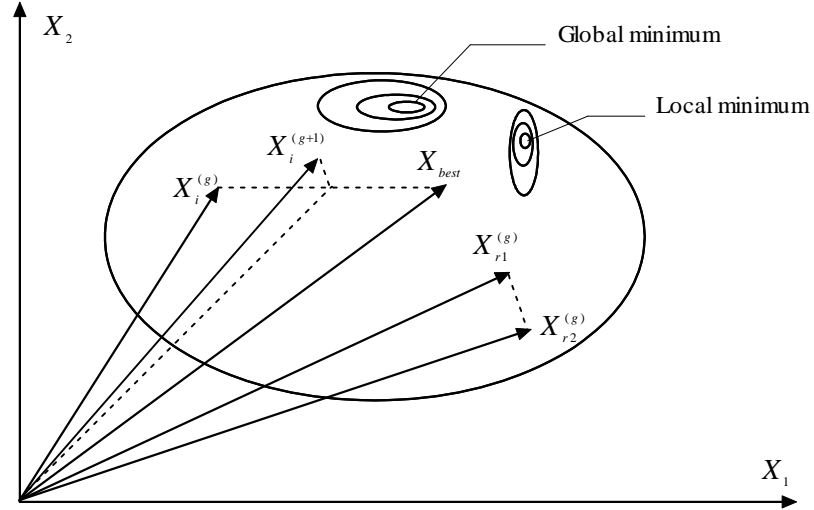


Figure 3-1. Illustration of the mechanism of DE/rand-to-best/1/bin

D Selection strategy

A one-to-one replacement strategy is employed for the DE' selection as follows:

$$X_i^{(g+1)} = \begin{cases} U_i^{(g)} & \text{if } f(U_i^{(g)}) < f(X_i^{(g)}) \\ X_i^{(g)} & \text{otherwise} \end{cases} \quad (3-5)$$

It is an elitist strategy because the current best vector of the population can only be replaced by a better vector.

3.3.2 Design procedure

With the principal components described above, the probabilistic PSS design problem can be solved by the following procedure:

Step 1 Initialization: initialize NP individuals/chromosomes in the population according to equation (3-3), which act as the initial parent population. By decoding each chromosome into a group of PSS parameters, the objective function value of each individual in the initial population is evaluated according to model (3-2) and thus the best individual $x_{best}^{(0)}$ is obtained.

Step 2 Reproduction: for each parent chromosome, a child chromosome is generated by performing the reproduction operation in equation (3-4) so that a NP -size children population is prepared. A midway fine-tuning strategy [123] will be applied if the boundary limit is violated. The objective function value of the child chromosome will be evaluated in succession. Repeat the reproduction step until NP child chromosomes are formed.

Step 3 Selection: each child will compete with its corresponding parent according to equation (3-5) and all the survivors will constitute the parent population of next generation.

Step 4 Repeat Steps 2 and 3 until the objective function becomes zero or the specified maximum number of generations is reached.

3.4 Applications

In this section, the same two test systems in Chapter 2 will be employed to demonstrate the effectiveness of the proposed method. In the studies, the same system configuration and dynamic stability criteria will be used as well.

3.4.1 System I

Following the result of probabilistic sensitivity analysis in Chapter 2, two speed-based PSSs are installed at G1 and G2 of Figure 2-3; and in total 10 parameters of PSSs need to be decided. The population size (NP) and the maximum generation for DE in this study are set to be 100 and 50 respectively.

A *DE robustness*

Studies on the selection of DE control parameters and its robustness are first conducted. It has been revealed in equation (3-4) that K controls the strength of the contractive pressure of the population, while F controls the strength of the diffuse pressure of the population. The larger the value of K or F , the stronger the contractive or diffuse pressure is. High ratio of K to F may lead to premature convergence, while low ratio of K to F may make the convergence too slow. So, K and F must be coordinately set in order to achieve the best performance. One strategy recommended by K. V. Price [123] is choosing K randomly from the range of $[0, 1]$ for every individual at each generation, which is found to be frequently very effective, while setting the F to be some fixed value within $[0, 1]$. Another simpler strategy of setting $K=F$ has been validated to be widely effective and applied to aerodynamic optimization, digital filters design, etc [135]. The influence of these two parameter setting strategies on the performance of the proposed method will be investigated thoroughly in two experiments: (1) Setting K randomly for every individual of each generation; and then increasing the F from 0.1 to 0.9; (2) Setting $K=F$ and then increasing them from 0.1 to 0.9. Based on 50 trial simulations, the average convergence curves of two cases are presented in Figures 3-2 and 3-3. From Figure 3-2, it is shown that the algorithm is nearly insensitive to F control parameter over the ranges $[0.5, 0.9]$ when K is randomly determined. Figure 3-3 shows that keeping $K=F$ has the similar characteristics; however, setting $K=F$ between 0.5 and 0.9 performs prominently. These observations indicate that DE is not remarkably sensitive to its control parameters over specified ranges. Thus,

their values are relatively easy to choose, which is consistent with the experimental conclusions in [123]. Hence the setting $K=F=0.85$ will be kept for DE in the remaining studies.

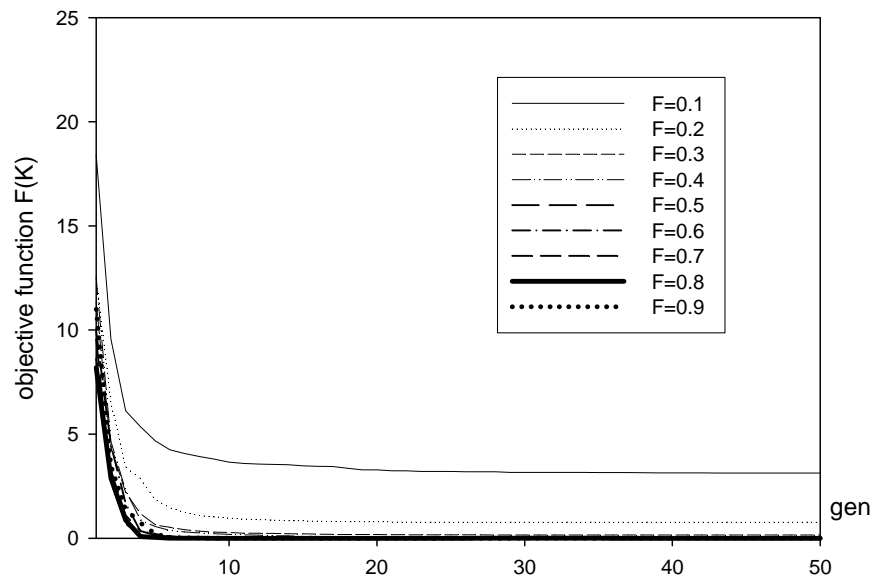


Figure 3-2. Convergence performance with random strategy for K

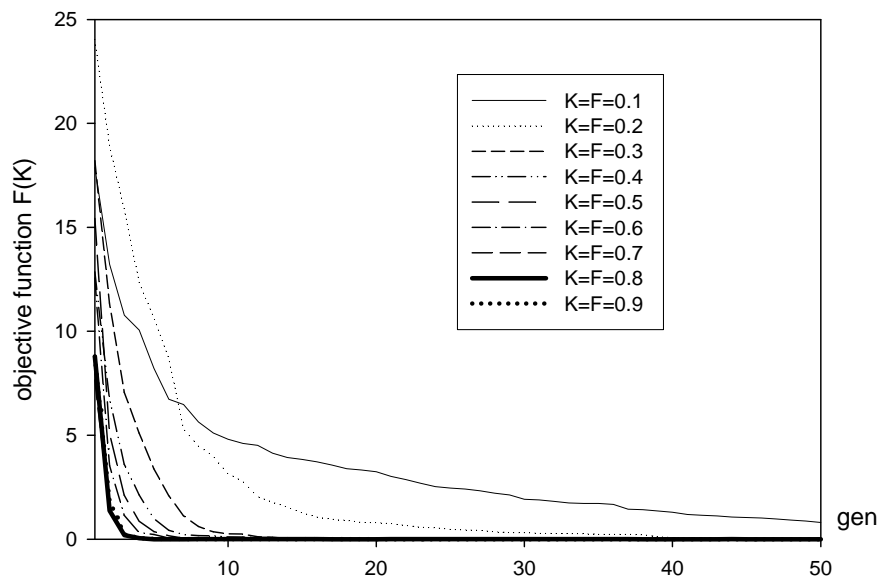


Figure 3-3. Convergence performance with $K=F$

B Tuning results

Based on the proposed method in Section 3.2, the final PSS settings are determined in Table 3-2, and all eigenvalues as shown in Table 3-3 are adequate for robust stability. When compared with the original values in Table 2-1, the system stability is much improved.

Table 3-2. Final PSS parameters for system **I**

	K_{PSS}	T_1	T_2	T_3	T_4
PSS1	1.732	0.186	0.098	0.692	0.127
PSS2	2.931	0.226	0.045	0.406	0.158

Table 3-3. Electromechanical modes of the closed-loop system **I**

No.	$\bar{\alpha}$	$\bar{\beta}$	σ_α	α^*	P_α	$\bar{\xi}$	σ_ξ	ξ^*	P_ξ
1	-1.886	7.175	0.155	12.14	1.00	0.2542	0.0148	10.40	1.00
2	-4.912	5.801	0.186	26.44	1.00	0.6462	0.0228	23.92	1.00

C Effectiveness validation

The performance of the proposed PSS design approach is evaluated and compared with that of the gradient-based PSS (GPSS) [32, 105, 142], which is designed under the worst scenario of the 480 operating conditions by pushing all the eigenvalues into the stability region. In addition, the same damping criteria and constraints are used in the conventional design for fair comparison. The GPSS parameters for system **I** are given in Table 3-4 for comparison purpose.

Table 3-4. The parameters of GPSS for system I

	K_{PSS}	T_1	T_2	T_3	T_4
PSS1	0.655	1.00	0.08	1.10	0.08
PSS2	0.272	1.00	0.08	1.10	0.08

To simulate a large disturbance imposed on the system, a six-cycle three-phase-to-earth fault is applied near to bus 6 at $t = 0.2$ s as shown in Figure 2-3. The fault is then cleared by line isolation without reclosure. The study system with the large disturbance impulsion will be tested under 480 sampled operation conditions with DE-PPSS (probabilistic PSS design with DE) and GPSS independently installed. A nonlinear time domain simulation will be conducted for each case by a Matlab-based simulation tool, PST [27]. The output limits of field voltage are set to ± 5 p.u. respectively. The output limits of PSSs are set to ± 0.1 p.u. Investigation on the following physical variables is performed:

- (i) Rotor angle of G1, G2 (relative to G3) in degree
- (ii) Field voltage of G1, G2 and G3 in p.u.
- (iii) Terminal voltage of G1, G2 and G3 in p.u.

The criteria employed in automatic control process to assess the quality of transient response, such as the settling time and overshoots, can quantitatively be estimated by its deviation characteristics and therefore this idea is now adopted in evaluating the transient stability performance of the obtained PSSs under wide operation conditions. Two performance indices on the basis of multi-operating conditions are defined here in this thesis to measure the averaged total variation (ATV) of signal [133],

$$J_1 = \frac{1}{N} \sum_{n=1}^N \int_{t=0}^{t=t_{sim}} |\Delta \varepsilon(t)| dt \quad (3-6)$$

$$J_2 = \frac{1}{N} \sum_{n=1}^N \int_{t=0}^{t=t_{sim}} t \cdot \Delta^2 \varepsilon(t) dt \quad (3-7)$$

where $\varepsilon(t)$ represents all the time response of the selected physical variables and $\Delta \varepsilon(t) = \varepsilon(t) - \varepsilon(t-1)$; N is the total number of samples; and t_{sim} is the total simulation time. It is obvious that the lower the values of these indices, the smaller deviation of the signal will present in response to disturbance.

The ATV values for GPSS (denoted as M1) and DE-PPSS (denoted as M2) are listed in Table 3-5. Most of ATV values of DE-PPSS are less than those of GPSS. Indeed, it is well expected that DE-PPSS outperforms GPSS because the proposed DE-PPSS method is derived from probabilistic eigenvalue analysis; and multi-operating conditions and certain nonlinear characteristic of the system have been taken into account in the PSS design. However, GPSS is designed based only on a linearized model under a stressed operating condition and its performance may be unsatisfactory when the operating environment varies significantly due to large disturbances.

The typical transient response curves at light, medium and heavy load conditions of the daily operating curve are shown in Figure 3-4, Figure 3-5 and Figure 3-6 respectively. Although GPSS stabilizes the system, DE-PPSS exhibits better damping properties generally and this result is consistent with the performance index analysis.

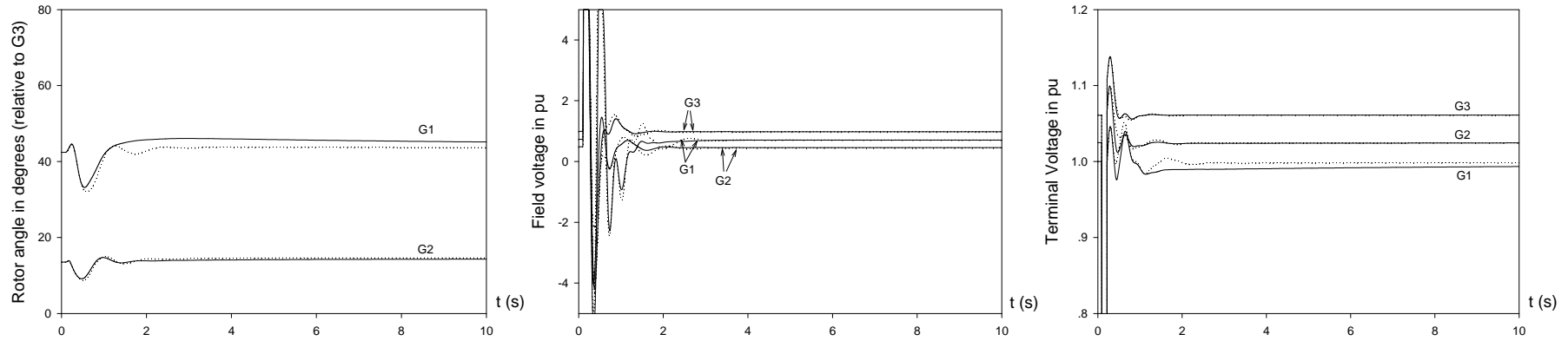


Figure 3-4. System response at light load condition (solid lines for DE-PPSS and dotted lines for GPSS)

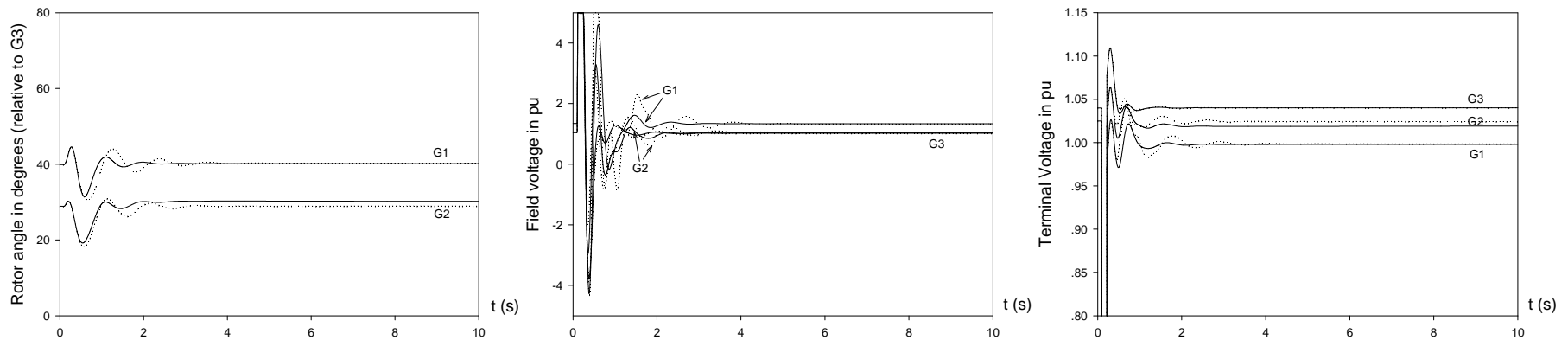


Figure 3-5. System response at medium load condition (solid lines for DE-PPSS and dotted lines for GPSS)

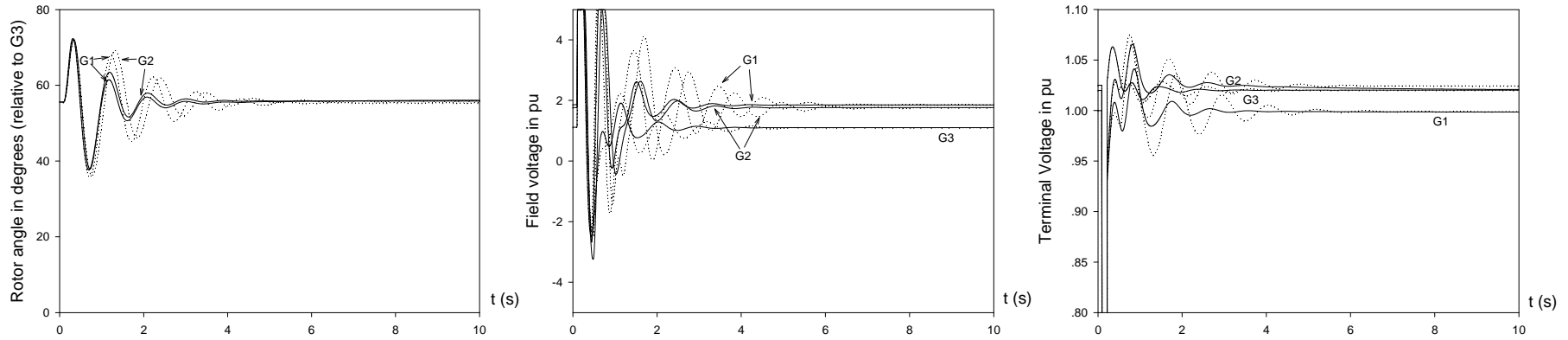


Figure 3-6. System response at heavy load condition (solid lines for DE-PPSS and dotted lines for GPSS)

Table 3-5. Performance indices of system I

		δ_1	δ_2	v_{f1}	v_{f2}	v_{f3}	v_{t1}	v_{t2}	v_{t3}
J_1	M1	0.1226	0.1235	0.0565	0.0421	0.0253	0.0024	0.0032	0.0033
	M2	0.0492	0.0586	0.0390	0.0291	0.0206	0.0022	0.0030	0.0033
J_2	M1	0.0202	0.0231	0.0024	0.00164	0.00059	0.00005	0.00012	0.00016
	M2	0.0018	0.0032	0.0014	0.00069	0.00045	0.00005	0.00012	0.00016

3.4.2 System II

Following the result of probabilistic sensitivity analysis in Chapter 2, a scheme of power-signal PSSs at G1, G2, G3, G5, G6, and G7 of Figure 2-6 is tentatively applied. Total of 30 PSS parameters need to be determined. The population size and the maximum generation for DE in this case are set to be 200 and 100 respectively. With the proposed DE-PPSS approach, the resulting PSS parameters and electro-mechanical modes are listed in Tables 3-6 and 3-7, with the system damping effectively enhanced.

Table 3-6. PSS parameters for system II

	K_{PSS}	T_1	T_2	T_3	T_4
PSS1	-0.086	0.107	0.192	0.194	0.199
PSS2	-0.014	1.276	0.044	1.420	0.144
PSS3	-0.824	0.169	0.121	0.135	0.054
PSS5	-0.030	1.273	0.049	0.106	0.185
PSS6	-0.019	0.951	0.064	0.612	0.110
PSS7	-0.739	0.286	0.141	0.061	0.162

Table 3-7. Electromechanical modes of the closed-loop system II

No.	$\bar{\alpha}$	$\bar{\beta}$	σ_α	α^*	P_α	$\bar{\xi}$	σ_ξ	ξ^*	P_ξ
1	-2.020	15.07	0.094	21.61	1.00	0.133	0.007	4.44	1.00
2	-1.682	12.81	0.120	14.06	1.00	0.130	0.008	3.97	1.00
3	-1.546	11.31	0.073	21.09	1.00	0.135	0.003	11.06	1.00
4	-0.846	7.495	0.019	45.49	1.00	0.112	0.003	4.02	1.00
5	-4.498	4.931	0.252	17.87	1.00	0.674	0.023	25.08	1.00
6	-1.600	3.939	0.285	5.62	1.00	0.376	0.059	4.71	1.00
7	-0.853	3.028	0.153	5.56	1.00	0.271	0.038	4.57	1.00

The convergence rate of system **II** is given Figure 3-7, which shows the proposed method converges quickly.

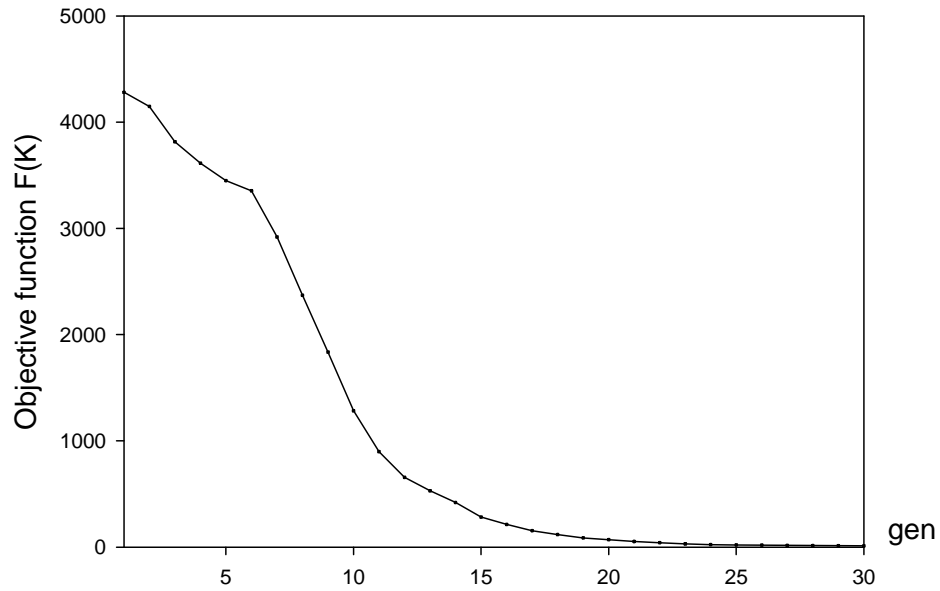


Figure 3-7. Convergence performance of system **II**

For transient performance checking, a six-cycle three-phase fault is applied to the tie-line 8-15 near bus 15 at $t = 0.2$ s as shown in Figure 2-6. The fault is then cleared by line isolation without reclosure, making the tie-line out of operation. The system responses are simulated under typical wide operating conditions, which are composed of 24 operating conditions of each hour in the operating curve. The output limits of voltage regulator are set to ± 10 p.u. respectively. The GPSS parameters for system **II** are listed in Table 3-8 for comparison purpose. The transient response of generators' electrical power in p.u. are investigated and the performance indices are presented in Table 3-9; and the electrical power responses of generators with PSS under different operating conditions are plotted in Figure 3-8. Again, DE-PPSS is superior to GPSS in terms of damping ability under a wide range of operating conditions.

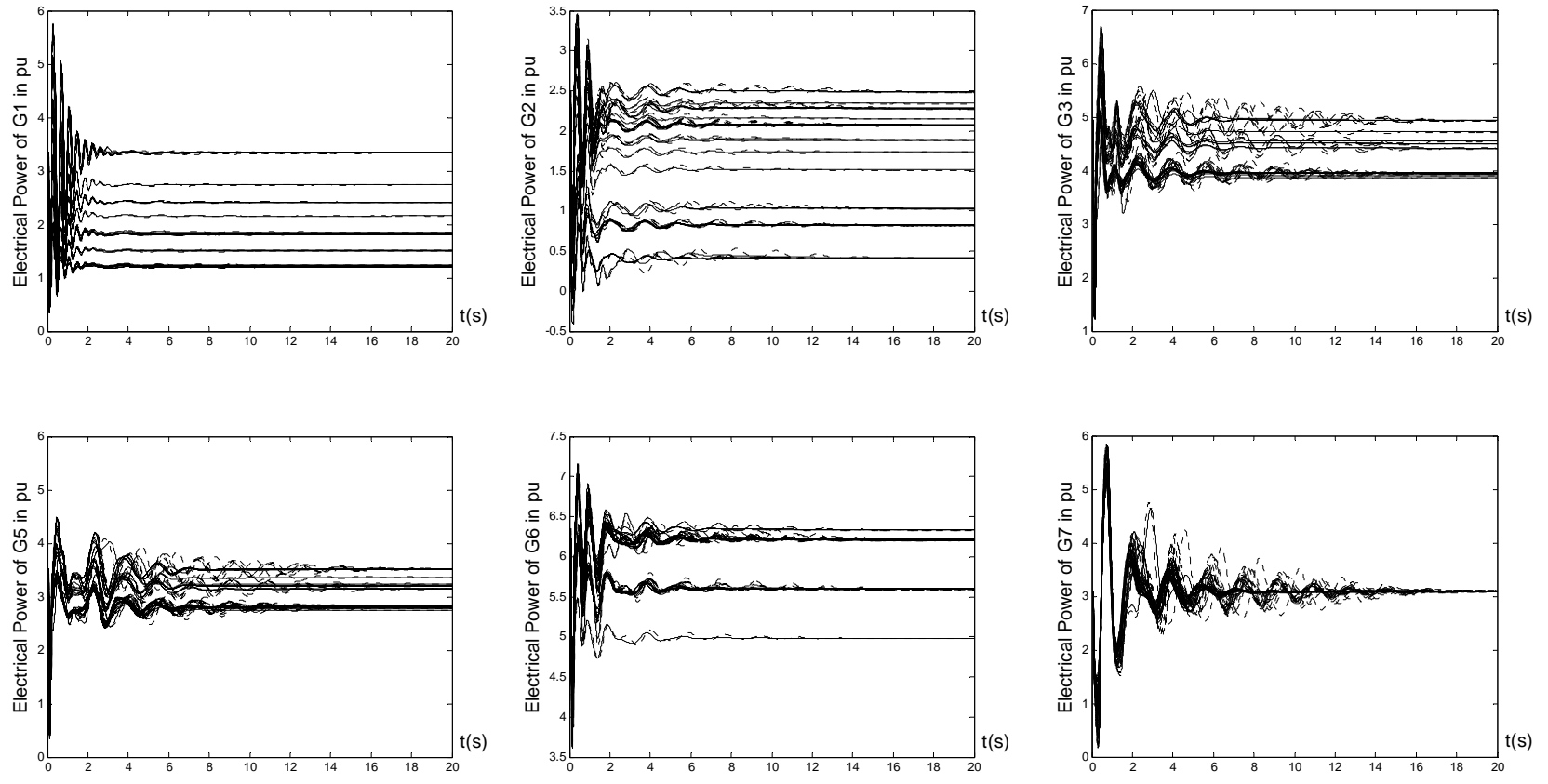


Figure 3-8. Transient responses of generator G1, G2, G3, G5, G6 and G7 (solid lines for DE-PPSS and dotted lines for GPSS)

Table 3-8. The parameters of GPSS for system II

	K_{PSS}	T_1	T_2	T_3	T_4
PSS1	-0.063	0.091	0.165	1.621	0.041
PSS2	-0.195	1.492	0.194	0.293	0.077
PSS3	-0.064	1.827	0.066	1.132	0.192
PSS5	-0.099	1.560	0.042	0.117	0.200
PSS6	-0.226	0.593	0.044	0.624	0.087
PSS7	-1.346	1.773	0.153	0.074	0.167

Table 3-9. Performance indices of system II

		P_{e1}	P_{e2}	P_{e3}	P_{e4}	P_{e5}	P_{e6}	P_{e7}	P_{e8}
J_1	M1	0.0770	0.0571	0.1414	0.0845	0.1208	0.0678	0.2051	0.4106
	M2	0.0759	0.0428	0.0765	0.0607	0.0777	0.0519	0.1087	0.1385
J_2	M1	0.0066	0.0023	0.0146	0.0058	0.0124	0.0033	0.0175	0.1069
	M2	0.0068	0.0020	0.0096	0.0047	0.0093	0.0029	0.0051	0.0121

3.5 Summary

A probabilistic PSS design for multi-machine system under multi-operating conditions using DE is proposed in this chapter. A comprehensive comparison between the probabilistic PSS and a gradient-based conventional PSS (GPSS) is conducted on two test systems and the results have indicated that the probabilistic PSS is more robust than the GPSS, which is partly because the probabilistic PSS design has considered a wide range of operation conditions in the design process and the DE is able to tune the PSS parameters in a coordinated way. The studies have also showed that DE is not remarkably sensitive to its control parameters over specified ranges. This makes it easy to select its parameters for the probabilistic PSS design problem.

4 POWER SYSTEM STABILIZER DESIGN CONSIDERING SYSTEM CONTINGENCIES

4.1 Introduction

Most of conventional sequential methods as well as modern heuristic optimization methods [1, 14, 19, 60, 88, 91, 92, 105, 144] perform PSS tuning under some stressed load conditions and then verify the performance of the tuned PSS via time domain simulation at a given set of credible contingencies. From the perspective of system operation, however, the design of damping controllers under heavy load and strong transmission operation may not always be sufficient; some contingencies may have significant impact on system oscillation modes. The system dynamic behavior may be greatly changed due to those contingencies, and the corresponding post-contingency conditions may become an important element for PSS design. PSS designed under normal condition may not consistently damp out post-contingency system oscillations and overall satisfactory system performance cannot be guaranteed.

Some of previous publications [1, 14, 92, 162] have considered contingent elements into PSS design. References [1, 14] regarded several contingencies as tuning conditions in the PSS tuning models. References [92, 162] emphasized on achieving the optimal PSS parameters by means of a series of time domain simulation subject to some prescribed contingencies. However, a method to consider the contingencies

systematically is lacking of in these previous works. The aim of this chapter is to propose a method that can systematically incorporate contingent elements into PSS design in an effective way.

The genetic algorithm (GA) is one of the most popular EAs during the past decade because of its computationally simple and easy to implement. GA is inspired by biological evolution mechanisms: reproduction, mutation, recombination/crossover, natural selection and survival of the fittest [61, 68]. GA was formally introduced in the United States in the 1970s by John Holland at University of Michigan. GA in particular became popular through the work of John Holland in the early 1970s, and particularly his book *Adaptation in Natural and Artificial Systems* [68]. His work originated with studies of cellular automata, conducted by Holland and his students at the University of Michigan. David Goldberg's book *Genetic Algorithms in Search, Optimization, and Machine Learning* has made further important contribution to the understanding and design of scalable genetic algorithms [61]. One drawback of GA is that it has possibility to converge prematurely to a suboptimum [4, 5, 54]. To assure global optimum, great care should be taken in selecting algorithm parameters, such as probability of crossover and mutation operation. Repeated runs should be made with several sets of randomly chosen initial values.

In Reference [1], the BLX- α operator based GA has been reported to be able to achieve prominent performance in PSS design. However, the PSS design model in Reference [1] did not include a systematic way to handle the system contingencies.

Thus, the PSS design by the BLX- α GA approach will be extended to consider the system contingencies in this chapter.

Given this background, the objective of this chapter is to propose a method that can systematically incorporate contingent elements into PSS design in a feasible way. Specifically, the number of contingencies is first reduced significantly by a critical contingency screening process. The PSS design problem is then formulated as an eigenvalue-based multi-objective optimization mode to pursue satisfactory system damping performance under both pre-contingency and post-contingency situations. A recursive GA-based algorithm is presented to solve this optimization problem so that the resulting PSSs can enhance all post-contingency damping under a wide range of operating conditions. Finally, the effectiveness of the developed PSS design scheme is demonstrated on the eight-machine system under a wide range of system contingencies.

4.2 Contingency-based PSS Tuning Modeling

4.2.1 Critical contingency screening

There are several kinds of contingency screening criteria in power industry, such as those used in transient stability analysis (TSA) [15], voltage stability analysis (VSA) [46] and small signal stability analysis (SSSA) [34, 151]. Screening of critical contingencies is usually achieved by ranking contingencies according to a severity index defined in these fields. In this chapter, contingency screening is only concerned with SSSA and related stability criteria will be employed. This screening process is

usually capable of selecting a small set of potentially harmful contingencies from the entire set of credible contingencies. Because of some distinct characteristics in SSSA, special consideration must be given to the selection of credible contingencies and screening of critical contingencies. Studies have shown that different contingencies have different impacts on different types of modes. For example, loss of tie-lines usually has a significant impact on inter-area modes, while circuits connecting generators with the grid are more likely to interfere with local modes only. Therefore, the objectives of the analysis should be considered when selecting proper contingencies.

The purpose of critical contingency screening proposed in this chapter is to identify those potentially harmful contingencies, more definitely, those that require special attention for robust PSS design. Usually, it could not be confirmed that those contingencies that happened under more stressed load conditions have less damping ratio. The on-going power industry deregulation introduces a great deal of changes to the ways power system operates and thus it is necessary to investigate the power system damping over a wide range of operating conditions.

In SSSA, the small-signal stability index ξ , used to measure system damping performance, is defined as the damping ratio of the least stable rotor angle mode in the system. The system under certain operating condition is small-signal secure if $\xi \geq \xi_T$, where ξ_T is normally system dependent and its value is based on operating experience [35]. In this chapter, the stability index is employed to screen contingencies because its value can reflect the performance of post-contingency system conditions [34, 151]. The

lower the stability index is, the weaker damping effect the power system will have, and hence the system is more prone to the small signal stability problem.

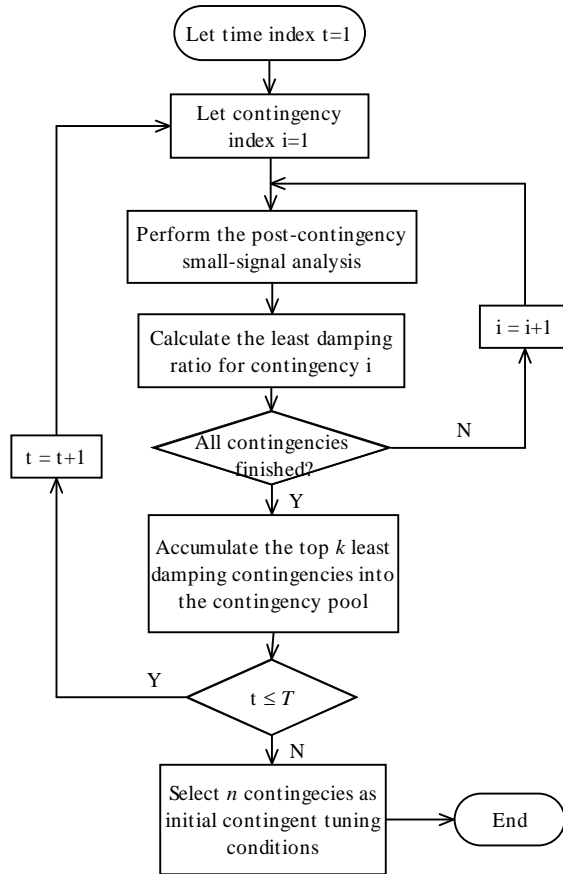


Figure 4-1. Flow chart for critical contingency screening

The contingency screening procedure is described by the flow chart in Figure 4-1. Although the overall procedure is general and can be extended to the multi-contingency case, the procedure in Figure 4-1 is confined to the case of N-1 line outage only. In the procedure, it is assumed that no contingency will break the power network into isolated islands. In addition, it is also taken that unvaried load level of a power system even in a small time period represents an operating condition. As shown in Figure 4-1, for a total of T number of time periods and I number of credible contingencies to be investigated, there are three stages in the selection process. In the first stage, shown by

the inner loop of the flow chart, the stability indices for all post-contingency cases are calculated one by one for one time period t . The contingency cases with $\xi < \xi_T$ will not be all recorded, but the top k (usually 3-5) most severe contingencies will be selected as the critical contingencies for the operating condition in time period t . The process will continue until all the operating conditions in the total time period T are checked. In the second stage shown by the outer loop of the flow chart in Figure 4-1, all the selected critical contingencies found in the first stage are accumulated into a contingency pool and ranked according to their stability index ξ . The size of contingency pool is given by $k \times T$. In the third stage shown by the bottom rectangular block in Figure 4-1, n out of the $k \times T$ contingencies are selected as the initial contingent tuning conditions to be met according to the averaged least damping ratio $\bar{\xi}$ and the percentage of a contingency listed in the $k \times T$ size contingency pool. These two statistic data can measure the degree of severity of a contingency in the contingency pool. The lower value of $\bar{\xi}$ and/or higher percentage of a contingency indicate it is more prominent in the contingency pool. The number n is normally system dependent, which may result in the increase of number of GA computation (i.e. the number of outer loop in Figure 4-2) if it is too small and the increment of the computation burden of the objective function if it is too large. There are several reasons for the above selection strategies: (1) Experience shows that damping ratios of remaining contingencies will be smoothly satisfied when the PSSs are tuned in a coordinated way; (2) If a power system has certain weakness related to transmission corridors, resulting in a decrease of system damping after its removal. It is unnecessary to consider this contingency over all operating conditions; (3) Physical

reality tells us that contingencies in a power system have some degree of coherence due to geographical linkage; (4) Handling in this way is able to lighten the overall computational burden.

4.2.2 Optimization model

As shown in References [1, 19, 105, 144], the goal of PSS tuning is to make all eigenvalues satisfy some criteria, for example, all eigenvalues should be within the shadowed D-shape region S^* in Figure 2-2 described by the following equations:

$$\alpha_j \leq \alpha_c \quad (4-1)$$

$$\xi_j \geq \xi_c \quad (4-2)$$

where α_c and ξ_c are acceptable limits for damping constant and damping ratio, respectively.

The basic idea of the proposed method differs from conventional methods in that the damping criteria are expected to be satisfied under pre-contingency condition with the first priority, the most severe contingency with the second priority, the second most severe contingency with third priority and so on and so forth. To simultaneously determine the PSS parameters with all above requirements satisfied, the PSS tuning problem is formulated as the following multi-objective problem:

$$\text{Minimize } [F_0(\mathbf{K}), F_1(\mathbf{K}), \dots, F_n(\mathbf{K})] \quad (4-3)$$

s.t.

$$K_{\min} \leq K_i \leq K_{\max}$$

$$T_{1,\min} \leq T_{1i} \leq T_{1,\max}, \quad T_{2,\min} \leq T_{2i} \leq T_{2,\max}$$

$$T_{3,\min} \leq T_{3i} \leq T_{3,\max}, \quad T_{4,\min} \leq T_{4i} \leq T_{4,\max}$$

where the parameters $K_i, T_{1i}/T_{2i}$ and T_{3i}/T_{4i} has the same meaning as those in problem (3-2) of Chapter 3. The objective function set are listed as follows:

$$F_0(\mathbf{K}) = \sum_{\alpha_j > \alpha_{c0}} (\alpha_j - \alpha_{c0})^2 + M \sum_{\xi_j < \xi_{c0}} (\xi_{c0} - \xi_j)^2 \quad (4-4)$$

$$F_1(\mathbf{K}) = \sum_{\alpha_j > \alpha_{c1}} (\alpha_j - \alpha_{c1})^2 + M \sum_{\xi_j < \xi_{c1}} (\xi_{c1} - \xi_j)^2 \quad (4-5)$$

$$F_n(\mathbf{K}) = \sum_{\alpha_j > \alpha_{cn}} (\alpha_j - \alpha_{cn})^2 + M \sum_{\xi_j < \xi_{cn}} (\xi_{cn} - \xi_j)^2 \quad (4-6)$$

where \mathbf{K} stands for the PSS parameter vector; $K_{\min}, T_{1,\min}, T_{2,\min}, T_{3,\min}$ and $T_{4,\min}$ are the minimum limits of PSS parameters; $K_{\max}, T_{1,\max}, T_{2,\max}, T_{3,\max}$ and $T_{4,\max}$ are the maximum limits of PSS parameters; $F_0(\mathbf{K})$ represents the objective function of pre-contingency condition; $F_1(\mathbf{K})$ to $F_n(\mathbf{K})$ represent the objective function of n different post-contingency conditions, which are ranked according to the contingency's severity degree, from the most severe to the least severe condition. α_{c0} and ξ_{c0} are damping threshold values for pre-contingency condition, α_{cj} and ξ_{cj} ($j = 1, \dots, n$) denote damping threshold values for post-contingency condition. In particular, α_{c0} should be set to be less than α_{cj} and ξ_{c0} larger than ξ_{cj} so that the SSSA criteria under pre-contingency condition are more rigorous than that of the post-contingency condition. More generally, $\alpha_{c0} \leq \alpha_{c1} \leq \dots \leq \alpha_{cn}$ and $\xi_{c0} \geq \xi_{c1} \geq \dots \geq \xi_{cn}$ are set so that different criteria are specified for different contingencies according to their degree of severity. M is a weighting constant and set to 10 according to the studies in Reference [1].

There are several multi-objective optimization methods to obtain the Pareto optimality of optimization problem in (4-3), such as the weighted sum method, Lexicographic method, min-max method and so on [102]. In this chapter, the min-max approach will be utilized to transform problem (4-3) into a single objective optimization problem, because the expected goals of the objective functions (4-4)-(4-6) are known in advance such that the parameters necessary for min-max approach can be easily set. The min-max approach consists of minimizing the maximum of the $n+1$ objective functions $F_0(\mathbf{K})$, $F_1(\mathbf{K})$, \dots , $F_n(\mathbf{K})$. In practice, it is often implemented as the minimization of the maximum (weighted) difference between the objectives and the specified value of the expected goals $F_{0,0}$, \dots , $F_{n,0}$ for each objective. Mathematically, the multi-objective optimization problem can be transformed into the following single optimization problem:

$$F(\mathbf{K}) = \max_{j=0,\dots,n} \frac{F_j(\mathbf{K}) - F_{j,0}}{w_j} \quad (4-7)$$

Minimize $F(\mathbf{K})$

such that the parameter constraints in problem (4-3) are satisfied.

The weights w_j (for $j = 0, \dots, n$) indicate the desired direction of search in the objective space, and are often set to the absolute value of the goals [102]. The smaller the weight, the easier the corresponding objective reaches the goal compared to other objectives. The specification of w_j equal to the goal value is able to provide proper priority order of contingencies according to their importance in PSS design.

For mere PSS tuning under pre-contingency condition, the objective function is formulated in model (4-4) and only those “weak” eigenvalues ($\alpha_j > \alpha_{c0}$ or $\xi_j < \xi_{c0}$) are included so that those unstable or poorly damped electromechanical oscillation modes are relocated into a more stable region. If problem (4-4) is solvable (i.e. a feasible solution exists), all eigenvalues should be located in the D-shape region S^* in Figure 2-2 and the value of $F_0(\mathbf{K})$ will be equal to zero ultimately. That means $F_{0,0}$, the expected goal value of $F_0(\mathbf{K})$, is zero. More generally, if a feasible PSS tuning scheme for model (4-7) exists, it could satisfy all stability criteria under different conditions, including post-contingency conditions. That means

$$[F_{0,0}, F_{1,0}, \dots, F_{n,0}] = [0, 0, \dots, 0] \quad (4-8)$$

Since equation (4-8) may lead to a ‘divided by zero’ situation, it is more reasonable to set the following relationship:

$$0 < F_{0,0} \leq F_{1,0} \leq \dots \leq F_{n,0} \approx 0 \quad (4-9)$$

For example, $[F_{0,0}, F_{1,0}, \dots, F_{n,0}] = [10^{-5}, 10^{-3}, 2 \times 10^{-3}, \dots]$. If an ideal PSS tuning scheme is obtained, both the pre-contingency and the post-contingency criteria can be satisfied so that $F_0(\mathbf{K}) = F_1(\mathbf{K}) = \dots = F_n(\mathbf{K}) = 0.0$ and $F(\mathbf{K}) = -1.0$ holds.

4.3 Solution by the BLX- α GA

It is a computational challenge to obtain the overall optimal solution of the problem in model (4-7), since it is a highly nonlinear and multi-modal optimization problem (i.e., there exists more than one local optimum). In Reference [1], a real-coded GA based on

a blend crossover operator (BLX- α) has been reported to be able to achieve prominent performance in PSS design. However, the PSS design model in Reference [1] did not include a systematic way to handle the system contingencies. Thus, the PSS design by the BLX- α GA approach will be extended to consider the system contingencies by optimization model (4-7). The BLX- α GA in the thesis are composed of a blend crossover operator (BLX- α) and a non-uniform mutation operator. This section describes the principal components of the BLX- α GA and its application in solving the problem (4-7).

4.3.1 Principal components of the BLX- α GA

The principal components of the BLX- α GA algorithm different from DE in Chapter 3 are introduced as follows:

A The blend crossover (BLX- α) [50, 61, 107]

The specified probability of crossover p_c gives the expected $NP \times p_c$ number of chromosomes which will undergo the crossover operation. The BLX- α operator begins by choosing the parameter α to determine the distance outside the bounds of the two parent variables that the offspring variable may exist, as shown in Figure 4-2. For the j -th variable of parents pair ($i1, i2$), $x_{i1,j}$ and $x_{i2,j}$, the offspring variables are randomly generated from the interval $[x_{i1,j} - \alpha(x_{i2,j} - x_{i1,j}), x_{i2,j} + \alpha(x_{i2,j} - x_{i1,j})]$. Thus this operator allows new values outside the range of the parents generated without letting the algorithm stray too far. To ensure the balance between exploitation and

exploration of the search space, $\alpha=0.5$ is selected for the studies in the thesis. An illustration of this operator is depicted in Figure 4-2.

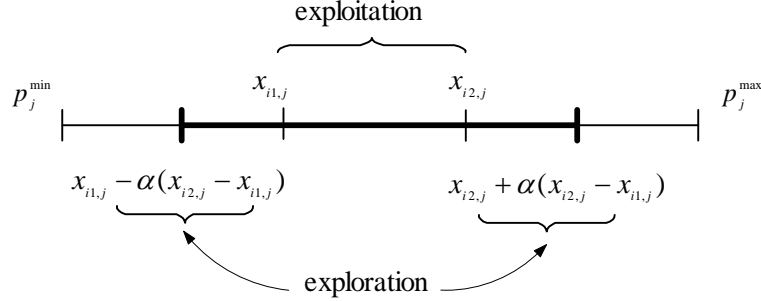


Figure 4-2. The BLX- α operation of the real-coded GA

B The non-uniform mutation

The specified probability of mutation p_{mr} gives the expected $NP \times D \times p_{mr}$ number of mutated bits. In this operator, if $X_i^{(g)} = [x_{i,1}, x_{i,2}, \dots, x_{i,D}]$ is a chromosome at the g -th generation and the j -th element $x_{i,j}$ was selected for this mutation, the result is a vector

$X_i^{(g+1)} = [x_{i,1}, x_{i,j}^{(g+1)}, \dots, x_{i,D}]$. The new value $x_{i,j}^{(g+1)}$ after mutation is given as,

$$x_{i,j}^{(g+1)} = \begin{cases} x_{i,j}^{(g)} + \Delta(g, p_j^{\max} - x_{i,j}^{(g)}) & \text{if a random digit is 0,} \\ x_{i,j}^{(g)} - \Delta(g, x_{i,j}^{(g)} - p_j^{\min}) & \text{if a random digit is 1,} \end{cases} \quad (4-10)$$

$$\text{and } \Delta(g, y) = y \cdot \left(1 - r \cdot \left(\frac{(1 - \frac{g}{g_{\max}})^{\beta}}{g_{\max}} \right) \right)$$

where r is a uniformly distributed random value over the range of $[0, 1]$; g_{\max} is the maximum number of generations. β is a system parameter determining the degree of dependency on iteration number and $\beta=5$ is selected in the thesis [1]. The function $\Delta(g, y)$ returns a value in the range $[0, y]$ such that the probability of $\Delta(g, y)$ being close to 0 increases as g increases. This property causes this operator to search the space

uniformly initially (when g is small), and very locally at later stages; thus increasing the probability of generating the new number closer to its successor than a random choice.

C The ranking selection

A ranking selection strategy is employed in the studies with the following characteristics: chromosomes are selected proportionally to their rank; the rank of chromosomes is decided by their corresponding values of objective function and no explicit fitness values are actually needed [107].

4.3.2 GA steps

The problem (4-7) can be solved by the BLX- α GA according to the following steps:

Step 1 Initialization: initialize NP individuals/chromosomes in the population according to equation (3-3) of Chapter 3, which act as the initial parent population.

Step 2 Generate the next generation of NP chromosomes in the following way:

Step 2.1 Evaluate the objective function of the chromosomes in the current generation using equation (4-7). In the present work, the fittest chromosome (i.e. the individual with the minimum value of the objective function) in the current generation is always retained in the next generation.

Step 2.2 Selection: select two chromosomes as the parents by the ranking selection method.

Step 2.3 Crossover: with the specified crossover probability, p_c , apply the BLX- α crossover to the two selected parents in the current generation when the value of a random number generated between 0 and 1, $rand [0, 1]$, is less than p_c . Otherwise,

the two parents are retained and are taken as the child chromosomes in the next generation. Repeat the selection step in Step 2.2 and the present step until NP child chromosomes are formed in the next generation.

Step 2.4 Mutation: for each chromosome in the next generation, apply the non-uniform mutation to the elements of the chromosome when the mutation probability, p_{mr} , is greater than $rand [0, 1]$. Otherwise, the chromosome will remain intact.

Step 3: The next generation formed in Step 2 is now taken to be the current generation. New generations are produced by repeating the solution process starting from Step 2 until the specified maximum number of generations is reached or the objective function becomes -1 .

4.3.3 Design procedure

The overall procedure for the contingency-based PSS design is given in the flow chart in Figure 4-3. The critical contingency screening process is performed and the initial tuning conditions are first obtained. Then the GA is applied to solve the optimization problem (4-7) according to the procedures in Section 4.3.2. If the post-contingency criteria are not all satisfied under some contingent conditions, then the most severe contingency will be added to the previous tuning conditions and the PSSs parameters need to be retrofitted on the basis of existing results, i.e., the GA will proceed into the second “round”. This process will continue until the prescribed post-contingency criteria are all satisfied. Thus in this process, the BLX- α GA algorithm may be applied

recursively. The stop criterion is either the maximum number of generations or a solution with an objective function equal to -1 .

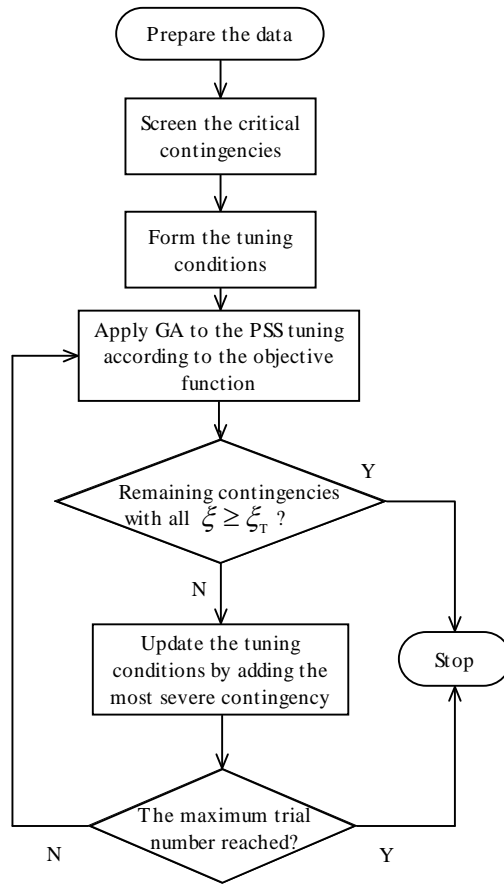


Figure 4-3. Flow chart for contingency-based PSS design

4.4 Case Studies

The eight-machine system (system II) of Figure 2-6 in Chapter 2 will be used to demonstrate the effectiveness of the proposed method. In this study, the top 4 ($k=4$) most severe contingencies will be selected into a contingency pool for each operating condition. The most stressed operating condition, specified as the peak load condition in this chapter, is selected as the unique pre-contingency condition in equation (4-4) and the criteria for all pre-contingency conditions are $\xi_{c0} = 0.1$ and $\alpha_{c0} = 0$. The criterion for critical contingency screening is $\xi_T = 0.1$ and all post-contingency threshold

values are set equal to $\xi_c = 0.1$. The parameter configuration of the BLX- α GA is listed in Table 4-1.

Table 4-1. The BLX- α GA parameter configuration

Parameter	Configuration
Maximum generation	150
Population size	400
Selection operator	rank-based selection
Crossover operator	BLX- α crossover with $\alpha = 0.5$ and probability 0.9
Mutation operator	Non-uniform mutation with probability 0.01

4.4.1 System configuration

All generators are represented as sixth-order models and equipped with IEEE-Type I exciters and speed governors. System loads are represented by constant impedances. All network parameters, nodal powers, control system parameters are listed in Appendix C2.

Similar to Chapter 2 and 3, each nodal power and PV bus voltage is assigned with standardized daily operating curves as given in Appendix C2. From these curves, 480 operating samples are created and they correspond to 480 operating conditions. The post-contingency modes of this open-loop test system under 480 operating conditions are illustrated in Figure 4-4. A brief summary of these post-contingency modes is presented in Table 4-2, which are ranked in the ascending sequence of their $\bar{\xi}$. The following information is included in the table: the contingency line index; the averaged least damping ratio $\bar{\xi}$ and the averaged mode frequency \bar{f} (Hz); the percentage of the contingency listed in the $k \times T$ size contingency pool, in which those prominent

contingencies have large percentage; the operating condition, which is the time period when the damping of the contingency ranked the lowest in the contingency pool; and the most associated state variables. Besides, the top 5 least-damping contingencies in the contingency pool are summarized in Table 4-3.

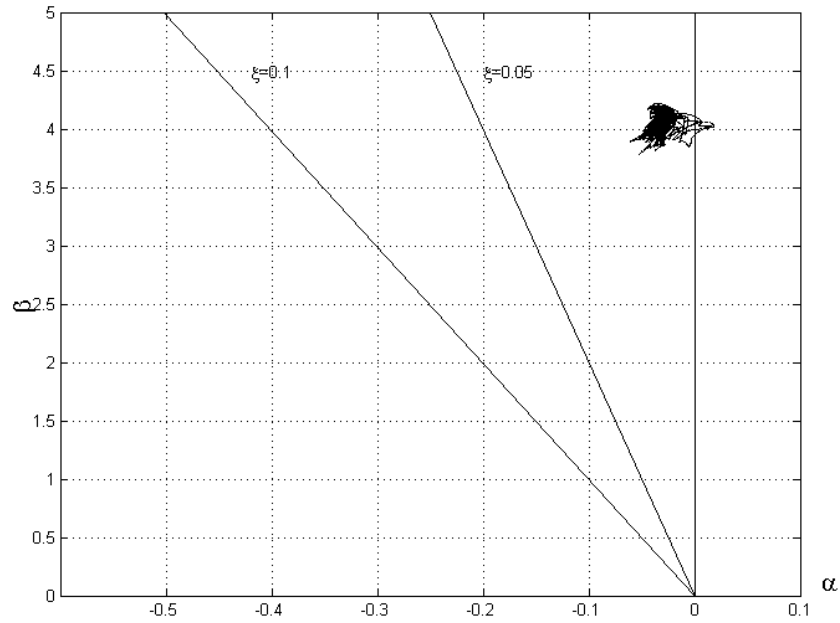


Figure 4-4. Post-contingency modes of the open-loop system **II** under 480 operating conditions

Table 4-2. Post-contingency profiles of the open-loop system **II**

No.	Contingency Line (From-To)	$\bar{\xi}$	\bar{f}	Operating Condition	Percentage (%)	Dominant States
1	9-12	0.00076	0.640	301	25.00	$\delta_7, \delta_5, \omega_8$
2	13- 9	0.00585	0.634	121	23.59	$\delta_7, \delta_5, \omega_8$
3	7-13	0.00582	0.634	121	23.70	$\delta_7, \delta_5, \omega_8$
4	15-12	0.00573	0.650	301	25.00	$\delta_7, \delta_5, \omega_8$
5	15- 8	0.00801	0.636	330	2.71	$\delta_7, \delta_5, \omega_8$

Table 4-3. The top 5 least-damping contingencies

No.	Contingency Line (From-To)	ξ	f	Operating Condition	Dominant States
1	9-12	-0.0044	0.640	301	$\delta_7, \delta_5, \omega_8$
2	9-12	-0.0044	0.640	300	$\delta_7, \delta_5, \omega_8$
3	9-12	-0.0044	0.640	299	$\delta_7, \delta_5, \omega_8$
4	9-12	-0.0044	0.641	298	$\delta_7, \delta_5, \omega_8$
5	9-12	-0.0044	0.641	297	$\delta_7, \delta_5, \omega_8$

As shown in Table 4-2, the first four contingencies related to lines 9-12, 13-9, 7-13 and 15-12 respectively are prominent contingencies, which in total occupy 97.29 percent of all contingencies in the contingency pool. All five contingencies in Table 4-2 are related to an inter-area oscillation mode with frequency around 0.6Hz, in which G5, G7 and G8 are involved. From Figure 4-4, it can be observed that all post-contingency modes in Table 4-2 are lightly damped; some of them even have negative ξ , as shown in Table 4-3. The top 5 lowest ξ in the contingency pool are all related to line 9-12, which indicates that line 9-12 is a potential weakness of this interconnected system.

From Table 4-2, lines 9-12, 7-13, 13-9 and 15-12 along with the corresponding operating conditions are finally selected as the contingent tuning conditions. That means these 4 contingencies ($n=4$) are regarded as the initial contingent tuning conditions. To enhance system damping level, six power-signal based PSSs at G1, G2, G3, G5, G6, and G7 have been identified in Chapter 2.

4.4.2 Algorithm performance

The whole process of contingency-based PSS tuning experiences two rounds: in the first round, the solution for problem (4-7) is found by GA and part of those remaining contingencies are added into the tuning condition after eigenvalue analysis; in the second round, the solution for problem (4-7) is obtained and no unsatisfactory post-contingency damping remains. Their convergence processes are shown Figure 4-5 and Figure 4-6. When the first GA round is finished, the global minimum has become -1.0 . The second GA round starts on the basis of the first tuning results and the updated contingent tuning conditions. The global minimum is greater than -1.0 initially under these conditions. When the second tuning is finished, this value has reached -1.0 again.

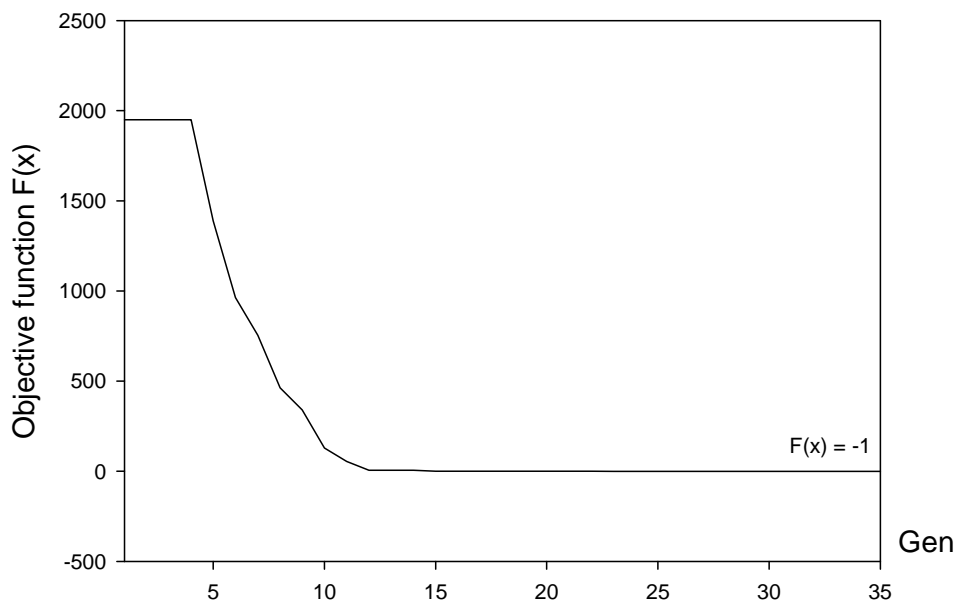


Figure 4-5. Objective function evolution in the first GA round

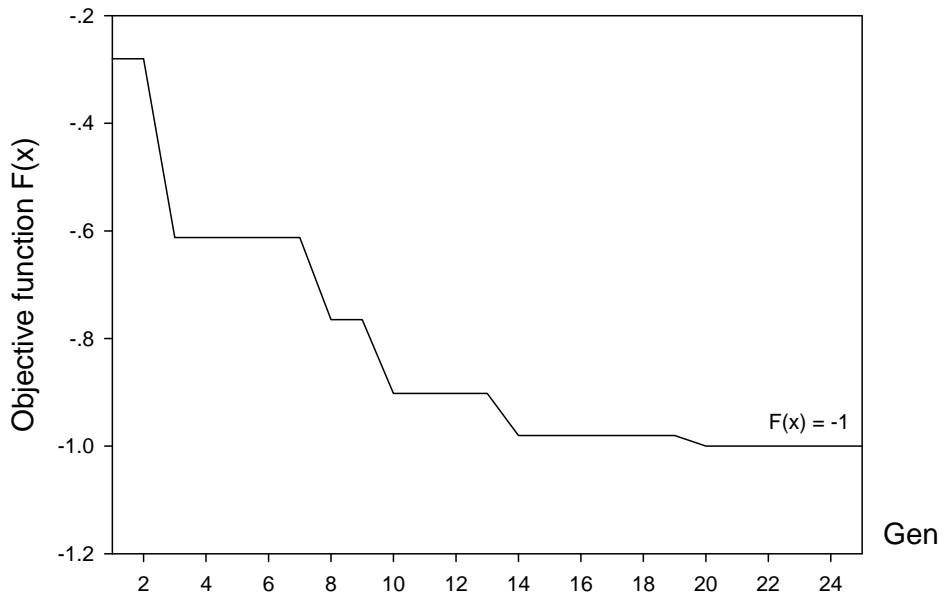


Figure 4-6. Objective function evolution in the second GA round

4.4.3 The first tuning results

The results of the first GA round for this closed-loop system are given in Table 4-4. A collection of post-contingency modes under all operating conditions are plotted in Figure 4-7 and a brief summary of them is listed in Table 4-5.

Table 4-4. PSS parameters after the first GA round

	K_{PSS}	T_1	T_2	T_3	T_4
PSS1	-0.100	0.523	0.052	0.400	0.040
PSS2	-0.100	1.151	0.164	0.431	0.043
PSS3	-0.100	1.394	0.157	1.577	0.200
PSS5	-0.193	0.060	0.176	0.392	0.043
PSS6	-0.045	0.447	0.097	0.327	0.040
PSS7	-0.592	0.805	0.089	0.060	0.200

Table 4-5. Post-contingency modes after the first GA round

No.	Contingency Line (From-To)	$\bar{\xi}$	\bar{f}	Operating Condition	Percentage (%)	Dominant States
1	7-16	0.05259	0.418	201	0.57	δ_3, E'_{q3}
2	6-7	0.06201	0.428	338	10.10	δ_3, E'_{q3}
3	7-13	0.07734	0.471	301	15.52	δ_3, E'_{q3}
4	13-9	0.07866	0.469	201	16.61	δ_3, E'_{q3}
5	2-4	0.08590	0.561	201	11.04	δ_3, E'_{q3}

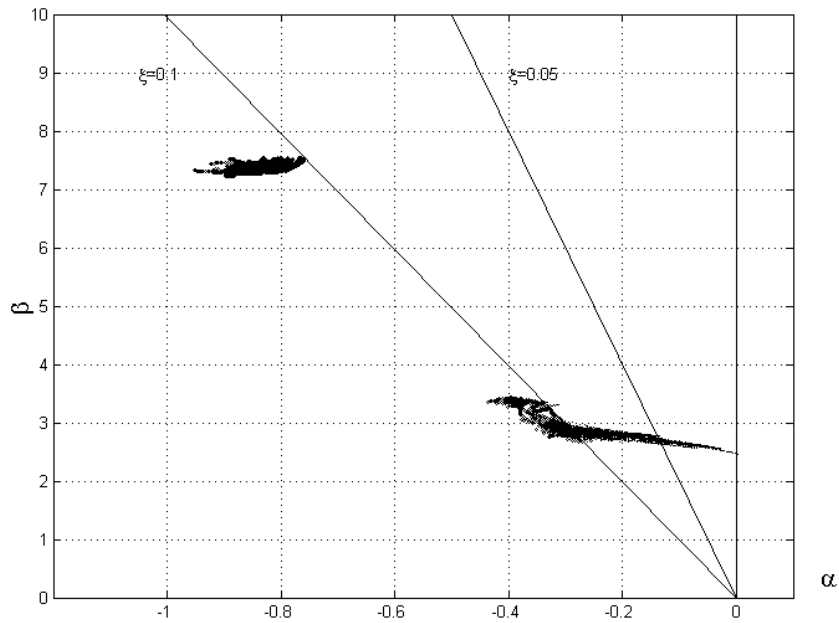


Figure 4-7. Post-contingency modes of the closed-loop system **II** after the first GA round

It is clear that the post-contingency damping ratios have been significantly enhanced by the first tuning of PSSs in this closed-loop system. The lowest $\bar{\xi}$ of post-contingency system has been raised from 0.00076 at line 9-12 in Table 4-3 to 0.05259 at line 7-16 in Table 4-5. Before PSS tuning, those least-damping modes are some inter-area modes;

after the first tuning, the least-damping modes are some local electro-mechanical oscillation modes. The above evidence indicates that the test system damping has been significantly improved by the help of the resulting PSSs after the first GA round. It is also revealed from Table 4-5 that there are some contingencies with $\bar{\xi}$ less than ξ_c (less than 0.1). In Table 4-5, contingent cases related to line 7-16 has very small proportion (0.57%) among the contingency pool, thus the contingent tuning conditions are updated by tentatively adding line 6-7 along with its operating condition in Table 4-5. Thus the system damping need to be further improved in the second tuning below.

4.4.4 The second tuning results

The results of the second round GA for this closed-loop system are given in Table 4-6. The corresponding post-contingency modes of this system under all operating conditions are provided in Figure 4-8 and a brief summary of them is listed in Table 4-7. As can be observed in Table 4-7 and Figure 4-8, the lowest $\bar{\xi}$ has been increased to greater than ξ_T . This confirms that the damping of all post-contingency conditions has been successfully satisfied through the second tuning.

Table 4-6. PSS parameters after the second GA round

	K_{PSS}	T_1	T_2	T_3	T_4
PSS1	-0.105	0.437	0.056	0.159	0.040
PSS2	-0.619	0.298	0.162	0.424	0.042
PSS3	-0.102	0.060	0.164	0.809	0.200
PSS5	-0.495	0.060	0.128	0.060	0.040
PSS6	-0.042	0.354	0.099	0.340	0.053
PSS7	-0.274	0.487	0.105	0.060	0.164

Table 4-7. Post-contingency modes after the second tuning

No.	Contingency Line (From-To)	$\bar{\xi}$	\bar{f}	Operating Condition	Percentage (%)	Dominant States
1	1-3	0.11119	1.16	197	25.00	δ_4, ω_4
2	13-9	0.11167	1.01	197	5.31	δ_4, ω_4
3	2-3	0.11173	1.16	198	23.65	δ_4, ω_4
4	1-2	0.11199	1.15	321	24.17	δ_4, ω_4
5	7-13	0.11265	0.93	198	3.44	δ_4, ω_4

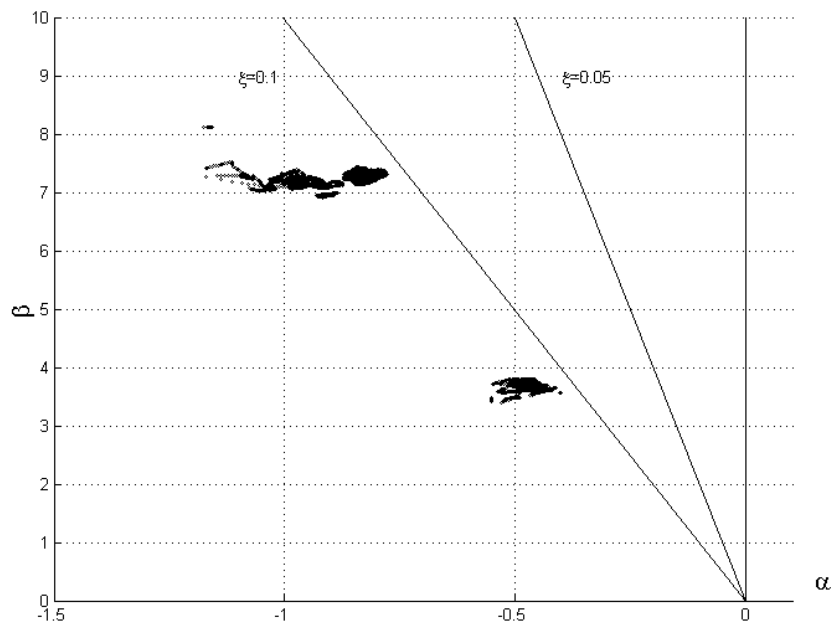


Figure 4-8. Post-contingency modes of the closed-loop system **II** after the second GA round

4.4.5 Transient simulation

To assess nonlinear behavior of the test system with the proposed PSS tuning approach, a group of transient stability simulations was performed on the test cases in

Table 4-8. These test cases are concerned with those severe operating conditions and critical line outages, which usually correspond to extreme conditions from the stability point of view. To simulate a large disturbance imposed on the system, at $t = 0.1$ s a six-cycle three-phase-to-earth fault happens at the sending end of each line (e.g. bus 9 of line 9-12), respectively. The fault is then cleared by line isolation without reclosure, making the corresponding line out of service.

Similar to the transient performance index defined in Chapter 3, another two indices on the basis of multi-operating conditions and system contingencies are defined here:

$$J'_1 = \frac{1}{N} \sum_{n=1}^N \int_{t=0}^{t=t_{sim}} |\Delta \varepsilon(t)| dt \quad (4-11)$$

$$J'_2 = \frac{1}{N} \sum_{n=1}^N \int_{t=0}^{t=t_{sim}} t \cdot \Delta^2 \varepsilon(t) dt \quad (4-12)$$

where equations (4-11) and (4-12) here are almost identical to the performance indices equations (3-6) and (3-7), except that N is the total number of test cases that is different from that in Chapter 3. Similarly, the lower the values of these indices, the smaller deviation of the signal will present in response to disturbance.

Table 4-8. Test cases for transient stability simulation

Case No	Operating Condition	Contingency Line (From-To)	Case No	Operating Condition	Contingency Line (From-To)
1	301	9-12	10	121	8-11
2	121	7-13	11	121	2-3
3	121	13-9	12	121	11-9
4	301	15-12	13	121	7-16
5	121	1-3	14	121	1-2
6	301	15-8	15	121	4-10
7	121	6-7	16	121	3-4
8	121	10-8	17	121	2-4
9	121	9-8	18	121	4-11

A nonlinear behavior comparison of the proposed method with the gradient-based conventional optimization method (GPSS) in Chapter 3 is conducted. The latter is designed under the worst scenario of 480 operating conditions and using the same damping criteria as that in this chapter. The performance indices of machine electrical powers in the system are given in Table 4-9. M1 and M2 denote the ATV value calculated by GPSS and the proposed method in this chapter respectively. The electrical power curves of G8 are plotted in Figure 4-9 (a)-(f), which corresponds to the first six cases in Table 4-8. As shown in Table 4-9, most of ATV values with the proposed method are less than the conventional method and the simulation curves are consistent with the performance index analysis. As shown in Figure 4-9, both PSS schemes can damp out the system oscillation, yet it is observed that the proposed PSS scheme is more robust than the conventional PSSs over a wide range of operating conditions.

Table 4-9. Performance indices of the test cases

		P_{e1}	P_{e2}	P_{e3}	P_{e4}	P_{e5}	P_{e6}	P_{e7}	P_{e8}
J'_1	M1	0.01244	0.01864	0.03048	0.02249	0.03057	0.03833	0.04892	0.12098
	M2	0.01123	0.01583	0.02630	0.01974	0.01921	0.03032	0.03737	0.06452
J'_2	M1	0.00106	0.00126	0.00275	0.00098	0.00195	0.00515	0.00197	0.00836
	M2	0.00106	0.00124	0.00271	0.00097	0.00178	0.00489	0.00172	0.00280

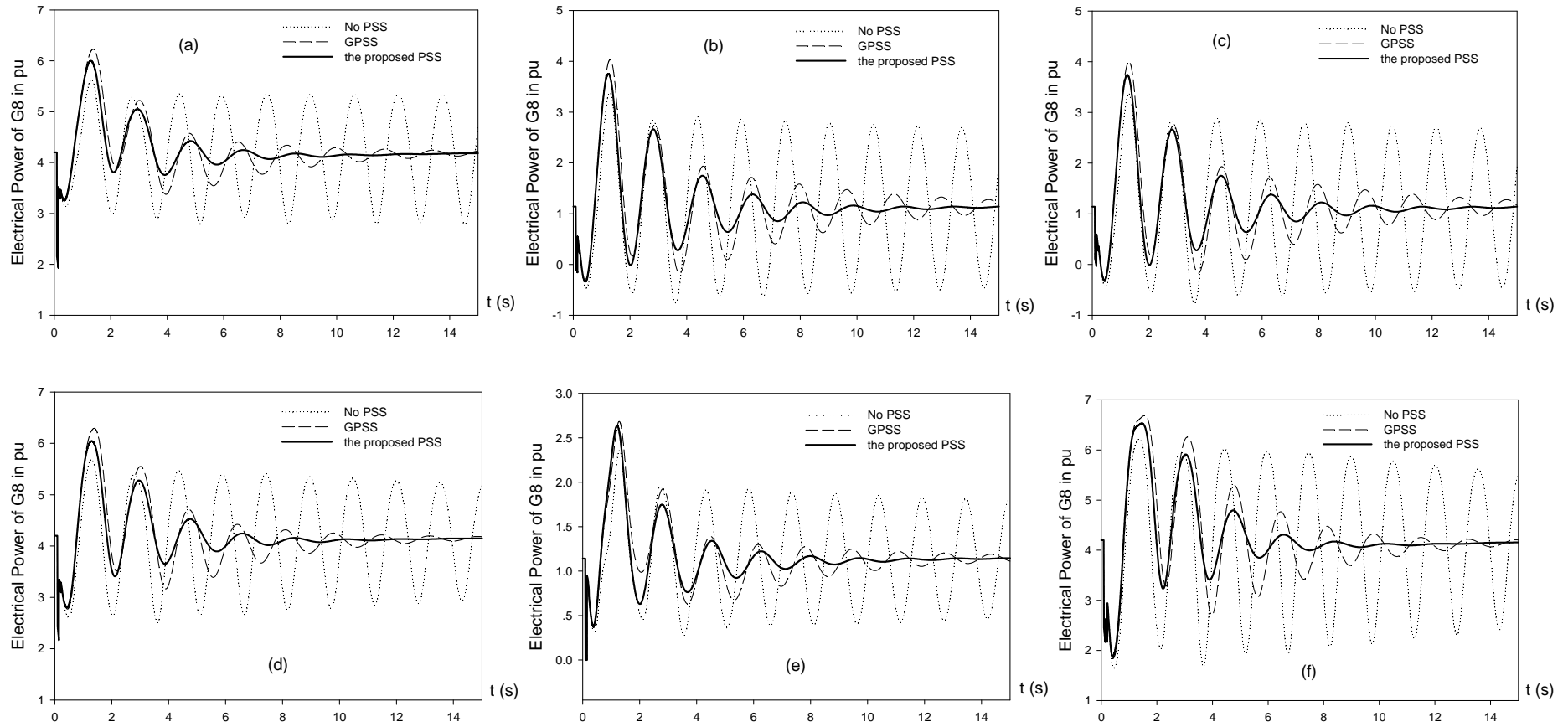


Figure 4-9. Transient simulation curves in different cases

4.5 Summary

A PSS design approach that can systematically consider system contingencies is proposed in this chapter. A critical contingency screening is first conducted according to a post-contingency small signal stability index. Then a multi-objective optimization model is formulated to pursue the effective system damping with contingencies taken into account. A min-max method is adopted to transform it into a single-objective optimization model and a recursive GA is employed to solve this problem. Case studies show that all post-contingency criteria can be satisfied by the recursive GA approach. Transient simulation experiments show that the proposed approach can more effectively enhance post-contingency damping compared to a conventional method. In the next chapter, the idea of handling the system contingencies will be extended to the probabilistic PSS design under a wide range of operating conditions.

5 PROBABILISTIC PSS DESIGN CONSIDERING SYSTEM CONTINGENCIES

5.1 Introduction

In Chapter 4, a systematic contingency-based PSS tuning approach is developed. To consider different operating conditions in this approach, it is necessary to perform the same procedure repeatedly and the computation burden will be increased with repetition. In this chapter, the idea of how to deal with the system contingencies in Chapter 4 will be extended to the probabilistic PSS design. Similarly, a critical contingency screening is conducted according to a post-contingency probabilistic small signal stability index. The probabilistic PSS design problem is formulated as an optimization model with contingencies taken into account.

Kennedy and Eberhart first introduced particle swarm optimization (PSO) as a new heuristic method in 1995 [78] and hereafter PSO has been extended to numerous field applications [117, 118]. PSO is a swarm intelligence algorithm that mimics the movement of individuals (fishes, birds, or insects) within a group (school, flock, and swarm) [38, 79]. One attractive feature of PSO is that it potentially has smaller population-size requirement than some EAs such as GA and EP [45]. This is a highlighted advantage when these kinds of population-based algorithms are applied to those highly complex problems that require time-consuming simulations to determine

the fitness value (Each fitness evaluation may require several minutes of CPU time). The probabilistic PSS design considering system contingencies, proposed in this chapter, is a very complex problem that might require a large amount of computing time for calculation. Hence, a PSO approach is employed to solve this optimization model. The effectiveness of the proposed approach is demonstrated on an eight-machine system under a wide range of operating conditions and a comparison study of PSO with the DE and the BLX- α GA is primarily conducted.

5.2 Contingency-based Probabilistic PSS Design

5.2.1 Critical contingency screening

The critical contingency screening in this chapter differs from that in Chapter 4 mainly on that a probabilistic small signal stability index is introduced here to measure the contingency severity degree. Under the framework of probabilistic eigenvalue analysis in Chapter 2, equations (5-1) and (5-2) are used for robust stability evaluation. The post-contingency least damping $\xi_{(j)}^*$ is employed to measure the severity of the j -th contingency under multi-operating conditions, which is defined in equation (5-3),

$$\alpha_{j,k}^* = -(\bar{\alpha}_{j,k} - \alpha_{j,C}) / \sigma_{\alpha_{j,k}} \geq \kappa \quad (5-1)$$

$$\xi_{j,k}^* = (\bar{\xi}_{j,k} - \xi_{j,C}) / \sigma_{\xi_{j,k}} \geq \kappa \quad (5-2)$$

$$\xi_{(j)}^* = \min_k \{ \xi_{j,k}^* \} \quad (5-3)$$

where different threshold values $\alpha_{j,C}$, $\xi_{j,C}$ are introduced in equations (5-1) and (5-2) to cater for the requirement of different criteria for different contingency conditions.

$\alpha_{0,C}$ and $\xi_{0,C}$ are damping threshold for pre-contingency condition, $\alpha_{j,C}$ and $\xi_{j,C}$ ($j = 1, \dots, n$) denote the damping threshold for n contingency conditions. In particular, $\alpha_{0,C}$ should be set to be less than $\alpha_{j,C}$ and $\xi_{0,C}$ larger than $\xi_{j,C}$ so that the damping criteria under pre-contingency condition are more rigorous than that under contingency condition. More generally, $\alpha_{0,C} \leq \alpha_{1,C} \leq \dots \leq \alpha_{n,C} \leq 0$ and $\xi_{0,C} \geq \xi_{1,C} \geq \dots \geq \xi_{n,C} > 0$ are set so that different criteria are specified for different contingencies according to their degree of severity. Similarly, $\xi_{(j)}^* \geq \kappa$ means the system under the j -th contingency condition satisfy the $\kappa\sigma$ criteria. The lower is the value of $\xi_{(j)}^*$, the weaker is the damping effect in the power system when the j -th contingency happens, and hence the system is less robustly stable.

During the screening process, the stability index (5-3) will be calculated for all contingency conditions one by one. However, the study will not regard all those contingencies with $\xi_{(j)}^* < \kappa$ as tuning conditions, but only the top n (usually 3-5) most severe contingencies will be selected as the critical contingencies.

5.2.2 Optimization model

The probabilistic PSS tuning problem is formulated as a multi-objective problem in model (5-4).

$$\text{Minimize } [F_0(\mathbf{K}), F_1(\mathbf{K}), \dots, F_n(\mathbf{K})] \quad (5-4)$$

s.t.

$$K_{\min} \leq K_i \leq K_{\max}$$

$$T_{1,\min} \leq T_{1i} \leq T_{1,\max}, \quad T_{2,\min} \leq T_{2i} \leq T_{2,\max}$$

$$T_{3,\min} \leq T_{3i} \leq T_{3,\max}, \quad T_{4,\min} \leq T_{4i} \leq T_{4,\max}$$

The objective function set are listed as follows:

$$F_0(\mathbf{K}) = \sum_{\alpha_{0,i}^* < \kappa} (\alpha_{0,i}^* - \kappa)^2 + \sum_{\xi_{0,i}^* < \kappa} (\xi_{0,i}^* - \kappa)^2 \quad (5-5)$$

$$F_j(\mathbf{K}) = \sum_{\alpha_{j,i}^* < \kappa} (\alpha_{j,i}^* - \kappa)^2 + \sum_{\xi_{j,i}^* < \kappa} (\xi_{j,i}^* - \kappa)^2 \quad (5-6)$$

$$F_n(\mathbf{K}) = \sum_{\alpha_{n,i}^* < \kappa} (\alpha_{n,i}^* - \kappa)^2 + \sum_{\xi_{n,i}^* < \kappa} (\xi_{n,i}^* - \kappa)^2 \quad (5-7)$$

where the parameters K_i , T_{1i}/T_{2i} , T_{3i}/T_{4i} , K_{\max}/K_{\min} , $T_{1,\max}/T_{1,\min}$, $T_{2,\max}/T_{2,\min}$, $T_{3,\max}/T_{3,\min}$, $T_{4,\max}/T_{4,\min}$ and vector \mathbf{K} has the same meaning as those in problem (4-3) of Chapter 4; $\alpha_{j,i}^*$ and $\xi_{j,i}^*$ represent damping profiles of the i -th electromechanical mode under the j -th contingency condition; $F_0(\mathbf{K})$ represents the objective function of pre-contingency condition; $F_1(\mathbf{K})$ to $F_n(\mathbf{K})$ represent the objective function of n different post-contingency conditions, which are ranked according to the contingency's severity degree. The same min-max approach used in Chapter 4 will be applied to transform problem (5-4) into a single objective optimization problem (5-8).

$$F(\mathbf{K}) = \max_{j=0,\dots,n} \frac{F_j(\mathbf{K}) - F_{j,0}}{w_j} \quad (5-8)$$

Minimize $F(\mathbf{K})$

such that the parameter constraints in problem (5-4) are satisfied.

The similar strategies of Section 4.2.2 on how to set the weighting constants w_j (for $j = 0, \dots, n$) and the expected goals $F_{0,0}, \dots, F_{n,0}$ will be employed. If an ideal PSS tuning scheme is obtained, both the pre-contingency and the post-contingency criteria can be satisfied so that $F_0(\mathbf{K}) = F_1(\mathbf{K}) = \dots = F_n(\mathbf{K}) = 0.0$ and $F(\mathbf{K}) = -1.0$ holds.

5.3 Solution by PSO

Particle swarm optimization (PSO) is a swarm intelligence algorithm that mimics the movement of individuals (fishes, birds, or insects) within a group (school, flock, and swarm). It has been applied to many power system problems, such as economic dispatch/unit commitment, optimal power flow problem, power system controller design, generation/transmission expansion planning and so on [7], covering the continuous and/or discrete optimization problems.

5.3.1 Basic algorithm

Similar to GA, a PSO consists of a population that can refine its knowledge of a given search space by particles moving. In short, PSO can be summarized as a population consisting of NP particles, each particle has D variables (dimensions) which have its own ranges for each value, the particle's velocity and position is updated at each time step until the termination conditions are satisfied. The set of the particles in the space is called a swarm. At each time step, each particle i is described by the following features

- its position vector $X_i = [x_{i,1}, x_{i,2}, \dots, x_{i,D}]$
- its velocity vector $V_i = [v_{i,1}, v_{i,2}, \dots, v_{i,D}]$
- its best position found so far $p_i = [p_{i,1}, \dots, p_{i,D}]$
- Particle's "informant group", sometimes called its neighborhood. This is effectively a set of links to other particles, which indicates who informs who in the swarm. These links are often defined at the beginning of a run and are kept fixed thereafter.

- the best position found by its neighbors $g_i = [g_{i,1}, \dots, g_{i,D}]$

For every generation (iteration), each particle is updated by two “best” values: the first one is the best position/solution a particle has achieved so far; another “best” value is the best position/solution that any neighbor/informant of a particle has achieved so far.

The core of canonical PSO is the updating formulae of the particle, which can be represented in equations (5-9), (5-10).

$$v_{i,j}^t = w \cdot v_{i,j}^{t-1} + c_1 \cdot rand \cdot (g_{i,j} - x_{i,j}^{t-1}) + c_2 \cdot rand \cdot (p_{i,j} - x_{i,j}^{t-1}) \quad (5-9)$$

$$x_{i,j}^t = x_{i,j}^{t-1} + v_{i,j}^t \quad (5-10)$$

where $i \in \{1, \dots, NP\}$; $j \in \{1, \dots, D\}$; $v_{i,j}^t$ denotes the i -th particle’s velocity in the j -th dimension at time step t ; $rand$ is a $[0, 1]$ random number; c_1 and c_2 are learning factors which control the influence of p_i and g_i ; equation (5-9) is a general formula of particle’s velocity update of next time step; equation (5-10) represents the i -th particle’s position update of next time step; w is a inertia weight coefficient, which can improve search performance so as to better control PSO convergence as well as population diversity. There are two prevailing variants of (w, c_1, c_2) in general equation (5-9): one is the implementation of “inertia weight”, which was first reported in 1998 [131]; another is “constriction coefficients” that was developed by French mathematician Maurice Clerc in 1999 [37].

For PSO core formulae (5-9), the item related to $p_{i,j}$ is termed as cognition component and the item related to $g_{i,j}$ is termed as social component [79]; from the psychological standpoint, the former represents the tendency of individuals to duplicate past behaviors

that have been proven successful, whereas the latter represents the tendency to follow the successes of others [79]. In principle, PSO is a heuristic process of particles to adjust their positions based on their previous best positions and the best positions of their neighbors. The main parameters in PSO include learning factors c_1 and c_2 , inertia weight coefficient w , neighbor number/size K , particle number/size NP and maximum iteration. Some useful selection strategies of these parameters are discussed below and will be utilized in the thesis, more details can be found in [38, 79].

5.3.2 Parameter setting

A *The neighborhood size*

The number/size K of neighbors will affect the convergence speed of the algorithm. It is generally accepted that a larger neighbor size will make the particles converge faster, while a small neighbor size will help to prevent the particle from premature convergence. The neighborhood strategy adopted here is based on the *lbest* model [79], in which each particle is influenced by a small number of its neighbors. A robust linking with $K=3$ is adopted, where each particle has randomly initialized links (i.e. the number of linking neighbors is expected to be $K=3$) with other particles at the beginning of a run and then again each time the swarm is unable to find an improved solution during an iteration of the algorithm [38]. Those particles with links have neighborhood relationship. The initial links are established according to a linking probability p_a in equation (5-11).

$$p_a = 1 - \left(1 - \frac{1}{NP}\right)^K \quad (5-11)$$

B c_1, c_2 and w

The strategies on how to select the values of c_1 , c_2 and w in this chapter is presented in equations (5-12) and (5-13), which are derived from the stagnation analysis in PSO by M. Clerc [39] that can improve the convergence without self adapting its parameters.

$$w = \frac{1}{2 \ln 2} \cong 0.721 \quad (5-12)$$

$$c_1 = c_2 = \frac{1 + 2 \ln 2}{2} \cong 1.193 \quad (5-13)$$

C V_{max}

The maximum velocity V_{max} serves as a constraint to control the global exploration ability of a particle swarm. A rule of thumb on control particle velocity [40] in equations (5-14) and (5-15) will be adopted in this chapter.

$$\text{If } x_{i,j}^t > p_j^{\max} \text{ then } x_{i,j}^t = p_j^{\max} \text{ and } v_{i,j}^t = 0 \quad (5-14)$$

$$\text{If } x_{i,j}^t < p_j^{\min} \text{ then } x_{i,j}^t = p_j^{\min} \text{ and } v_{i,j}^t = 0 \quad (5-15)$$

In summary, the values of PSO parameters used in the study are listed in Table 5-1.

Table 5-1. PSO algorithm parameters

Parameter	Configuration
Maximum iteration	1000
Particles size NP	40
Inertia weight coefficient w	$w = \frac{1}{2 \ln 2} \cong 0.721$
Learning factors	$c_1 = c_2 = \frac{1 + 2 \ln 2}{2} \cong 1.193$
Neighbor size	$K=3$

5.3.3 Design procedure

The following steps explain the procedure of PSO served for solving the PSS design problem (5-8):

Step 1 Initialization: the iteration t is set to 0. The initial population position $X(0)$ and velocity $V(0)$ are randomly produced based on the PSS parameter ranges. For each particle i , its position $X_i(0)$ is mapped into a group of PSS parameters, then the probabilistic eigenvalue analysis is made and its objective function value is evaluated according to formula (5-8). The particle's best position found so far, p_i , is set as $X_i(0)$.

Step 2 Updating the best neighbors: the links between particles will be randomly established according to linking probability p_a under two situations: $t=0$ or there is no improvement on particle swarm's flying/moving toward global optimum from last time. For each particle i , the best position found by its neighbors, g_i , is updated by the one with best fitness (smallest objective function value) among its neighbors.

Step 3 Flying: let $t=t+1$; for each particle i , its velocity $V_i(t)$ and position $X_i(t)$ is updated according to equations (5-9), (5-10) and adjusted according to equations (5-14), (5-15) when needed. The new particle position $X_i(t)$ is mapped into a new group of PSS parameters and its objective function value is evaluated. The whole particle population is therefore updated.

Step 4 Updating the best positions: for each particle i , its position $X_i(t)$ is compared with p_i on their objective function value and it will become the new p_i once the former performs better.

Step 5 Stop criteria: new particle population is produced by repeating the process starting from Step 2 until the objective function becomes -1 or the specified maximum number of generations is reached.

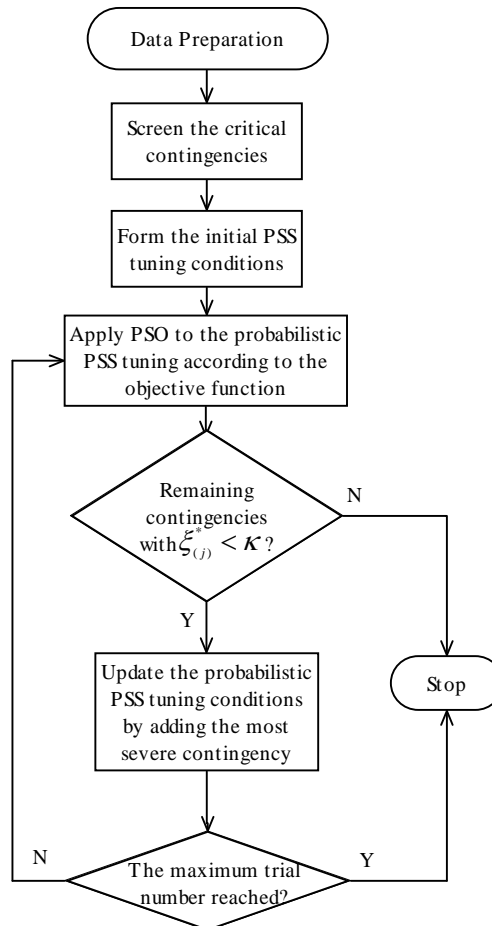


Figure 5-1. Flow chart of the contingency-based probabilistic PSS design

The overall procedure for the contingency-based probabilistic PSS design is given in Figure 5-1. Firstly, the critical contingency screening process is performed and the initial tuning conditions are formed. Then the PSO is applied to solve the optimization problem (5-8). If the post-contingency criteria are not all satisfied under some contingent conditions, then the most severe contingency will be added to the previous tuning conditions and the PSSs parameters need to be retrofitted on the basis of existing

results, i.e., the PSO will proceed into the second “round”. This process will continue until the prescribed post-contingency criteria are all satisfied or the maximum trial number is reached. The maximum trial number of the outer loop in Figure 5-1 is set to 10 in the study.

5.4 Numerical Experiments

In this section, the eight-machine system (system **II**) of Figure 2-6 in Chapter 3 will be used to test the proposed method. The top 4 ($n=4$) most severe contingencies will be selected as the initial contingent tuning conditions; the criteria for pre-contingency probabilistic eigenvalue analysis are $\alpha_c = 0$ and $\xi_c = 0.1$; the criteria for all post-contingency cases are also set to $\alpha_c = 0$ and $\xi_c = 0.1$, uniformly. The distribution constant κ is set to 3.5. Each nodal power and PV bus voltage is assigned with standardized daily operating curves as given in Appendix C2. From these curves, 480 operating samples are created and covariances of nodal injections are determined. Then the probabilistic eigenvalue analysis is performed on all contingencies independently.

Table 5-2. Post-contingency modes of the open-loop system

No.	Contingency Line (From-To)	$\bar{\alpha}$	$\bar{\beta}$	σ_α	α^*	$\bar{\xi}$	σ_ξ	$\xi_{(j)}^*$	Dominant States
1	15-8	-0.013	3.804	0.0060	2.10	0.0033	0.0016	-60.34	$\omega_8, \delta_7, \delta_5$
2	15-12	-0.027	3.856	0.0058	4.75	0.0071	0.0016	-59.86	$\omega_8, \delta_7, \delta_5$
3	9-12	-0.030	3.847	0.0061	4.95	0.0078	0.0016	-56.46	$\omega_8, \delta_7, \omega_7$
4	4-10	-0.034	3.885	0.0067	5.10	0.0089	0.0018	-50.59	$\omega_8, \delta_7, \delta_5$
5	8-11	-0.033	3.863	0.0067	4.91	0.0086	0.0018	-50.49	$\omega_8, \delta_7, \delta_5$

Only the top 5 least damping post-contingency modes of the open-loop system are given in Table 5-2, with the following information included: the contingency line index; the least-damping eigenvalue profiles, including expectation $\bar{\alpha}$, $\bar{\beta}$ and $\bar{\xi}$, standard deviation σ_{α} and σ_{ξ} , the damping constant α^* and the least damping ratio $\xi_{(j)}^*$; and the most associated state variables. These modes are ranked in the ascending sequence of $\xi_{(j)}^*$ and those unsatisfactory $\xi_{(j)}^*$ are highlighted in the table.

As shown in Table 5-2, the top 5 modes are all relevant to an inter-area oscillation mode with frequency around 0.6 Hz, in which G5, G7 and G8 are involved. It can be observed that all post-contingency modes in Table 5-2 are inadequate for robust stability with $\xi_{(j)}^* < \kappa$. From Table 5-2, line 15-8, 15-12, 9-12 and 4-10 are selected as initial contingent tuning conditions. To enhance system damping level, six power-signal based PSSs at G1, G2, G3, G5, G6, and G7 have been identified in Chapter 2.

5.4.1 Algorithm performance

The whole process of contingency-based probabilistic PSS tuning experiences two rounds: in the first round, the solution for problem (5-8) is found by PSO optimizer and the most severe contingency among remaining unsatisfactory contingencies is added into the tuning condition after the probabilistic eigenvalue analysis; in the second round, the solution for problem (5-8) is obtained and no unsatisfactory post-contingency damping remains. The convergence processes of two PSO rounds are shown in Figure 5-2 and Figure 5-3, respectively. In Figure 5-2, the initial objective function value is very large (10^9 level) because of the function of a weighting constant (10^{-4}). The first PSS round is finished when the final global minimum reaches -1.0 . The second PSS

round starts on the basis of the first tuning results and the updated PSS tuning conditions. The global minimum is greater than -1.0 initially. Likewise, the global minimum has reached -1.0 again when the second PSO round is finished.

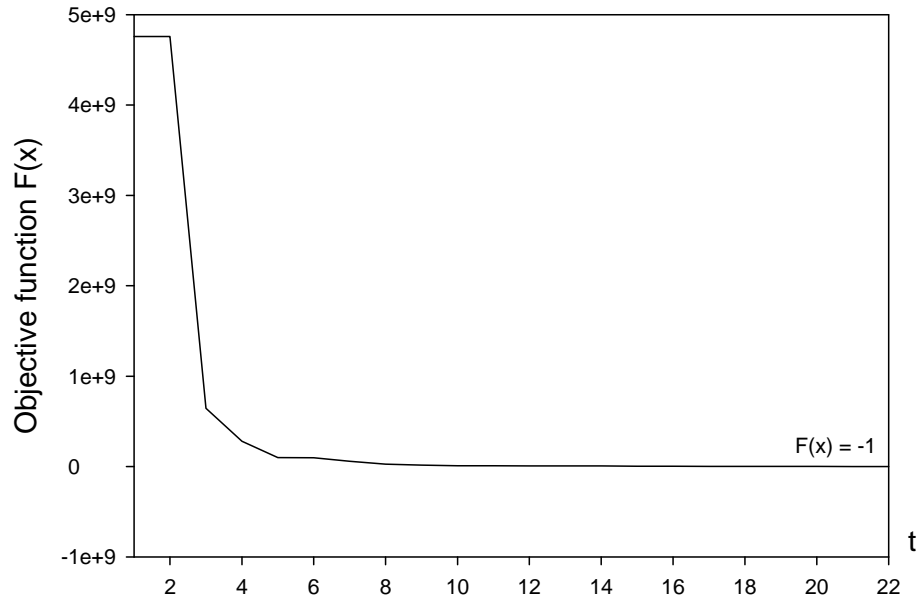


Figure 5-2. Objective function evolution in the first PSO round

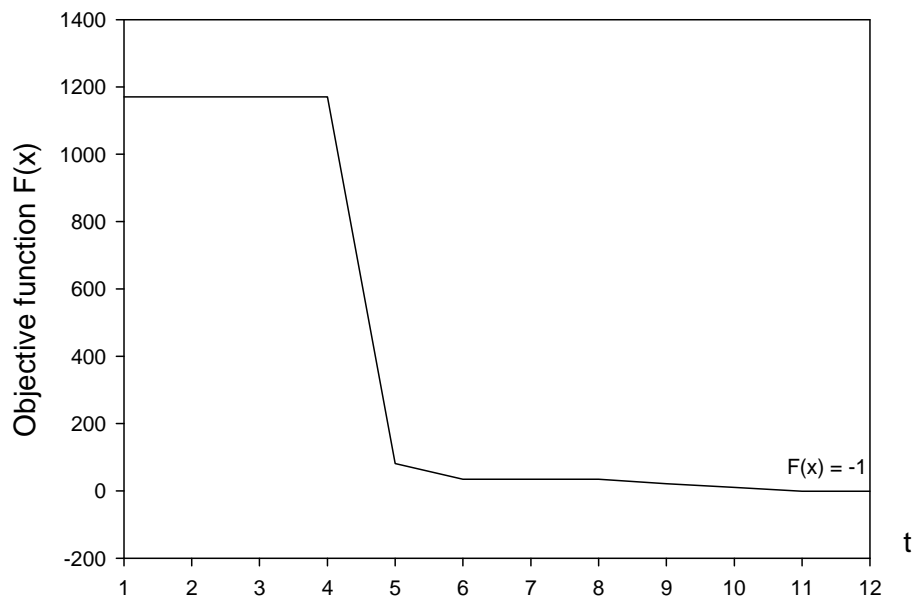


Figure 5-3. Objective function evolution in the second PSO round

5.4.2 The first tuning results

Table 5-3 shows the tuning results after the first PSO round for the closed-loop system. Table 5-4 gives a collection of the top 5 post-contingency modes when the PSSs in Table 5-3 are applied.

Table 5-3. PSS parameters after the first PSO round

	K_{PSS}	T_1	T_2	T_3	T_4
PSS1	-0.010	1.239	0.154	0.488	0.049
PSS2	-0.131	0.626	0.082	0.423	0.167
PSS3	-0.108	0.281	0.152	0.590	0.101
PSS5	-0.196	0.061	0.077	0.060	0.043
PSS6	-0.010	1.473	0.194	0.565	0.070
PSS7	-2.284	0.063	0.145	0.259	0.063

Table 5-4. Post-contingency modes after the first PSO round

No.	Contingency Line (From-To)	$\bar{\alpha}$	$\bar{\beta}$	σ_α	α^*	$\bar{\xi}$	σ_ξ	$\xi_{(j)}^*$	Dominant States
1	7-16	-2.972	16.214	0.4677	6.36	0.1803	0.0330	2.43	$\delta_1, \omega_1, E'_{q1}$
2	6-7	-2.947	16.247	0.4258	6.92	0.1785	0.0301	2.61	$\delta_1, \omega_1, E'_{q1}$
3	13-9	-0.406	2.872	0.0195	20.85	0.1399	0.0125	3.19	$\omega_8, \delta_7, \delta_6$
4	7-13	-0.406	2.872	0.0195	20.85	0.1399	0.0125	3.19	$\omega_8, \delta_7, \delta_6$
5	9-8	-2.828	16.531	0.2777	10.18	0.1686	0.0186	3.69	$\delta_1, \omega_1, E'_{q1}$

It is clear that the post-contingency probabilistic damping has been significantly enhanced by the use of PSSs in Table 5-3. The lowest $\xi_{(j)}^*$ of post-contingency modes

has been raised from -60.34 ($\xi_{(15-8)}^*$) in Table 5-2 to 2.43 ($\xi_{(7-16)}^*$) in Table 5-4. Before PSS tuning, those least-damping modes are some inter-area modes; after the first tuning, the least-damping modes are some local electro-mechanical oscillation modes. In Table 5-4, the first four modes still have $\xi_{(j)}^* < \kappa$ cases, thus the contingent tuning conditions are updated by tentatively adding line 7-16 for tuning process in succession.

5.4.3 The second tuning results

Table 5-5 shows the tuning results after the second PSO round for this closed-loop system. The corresponding top 5 post-contingency modes are given in Table 5-6. In Table 5-6, the lowest $\xi_{(j)}^*$ among the top 5 modes is greater than κ ($\xi_{(7-16)}^*=3.51$). The post-contingency criteria are satisfied and the post-contingency system damping is adequate for robust stability after the two PSO rounds.

Table 5-5. PSS parameters after the second PSO round

	K_{PSS}	T_1	T_2	T_3	T_4
PSS1	-0.010	0.766	0.077	0.402	0.047
PSS2	-0.239	0.473	0.101	0.216	0.130
PSS3	-0.053	0.169	0.120	0.367	0.121
PSS5	-0.243	0.061	0.068	0.074	0.045
PSS6	-0.010	1.375	0.199	0.504	0.056
PSS7	-2.460	0.067	0.185	0.246	0.091

Table 5-6. Post-contingency modes after the second PSO round

No.	Contingency Line (From-To)	$\bar{\alpha}$	$\bar{\beta}$	σ_{α}	α^*	$\bar{\xi}$	σ_{ξ}	$\xi_{(j)}^*$	Dominant States
1	7-16	-3.131	15.853	0.3594	8.71	0.1938	0.0267	3.51	$\delta_1, \omega_1, E'_{q1}$
2	3-4	-3.464	14.672	0.4835	7.17	0.2298	0.0341	3.81	E_{fd7}, V_{s7}
3	2-4	-3.463	14.660	0.4819	7.19	0.2299	0.0340	3.82	$\delta_1, \omega_1, E'_{q1}$
4	6-7	-3.122	15.877	0.3268	9.55	0.1929	0.0242	3.84	E_{fd7}, V_{s7}
5	1-3	-3.495	14.682	0.4557	7.67	0.2316	0.0329	4.00	E_{fd7}, V_{s7}

* V_{s7} represents a state variable of PSS7

5.4.4 Transient simulation

To complete the study, a group of transient stability simulations to assess nonlinear behavior of the test system is carried out. The test cases are composed of some fictitious contingencies listed in Table 5-7. These contingencies are related to those critical line outages, some of which correspond to extreme conditions in Table 5-2.

Table 5-7. Test cases for transient stability simulation

Case No.	Contingency Line (From-To)	Case No.	Contingency Line (From-To)
1	15-8	10	7-13
2	9-12	11	7-16
3	15-12	12	10-8
4	4-10	13	1-3
5	8-11	14	4-11
6	1-2	15	11-9
7	9-8	16	6-7
8	2-3	17	3-4
9	13-9	18	2-4

Performance of the proposed PSS design approach (denoted as CONT-PPSS) is evaluated and compared with the results of the DE-PPSS method and the GPSS method in Chapter 3. The study system with large disturbance impulsion will be tested under typical sampled operating conditions, which are composed of 24 operating conditions of each hour in the operating curve, with three methods independently applied. A nonlinear time domain simulation will be conducted for all test cases in Table 5-7 one by one. To simulate a large disturbance imposed on the system, at $t = 0.1$ s a six-cycle three-phase-to-earth fault happens at the sending end of a line (e.g. bus 15 of line 15-8) in Table 5-7. The fault is then cleared by line isolation without reclosure, making the corresponding line out of service.

Four performance indices are defined in equations (5-16)-(5-19) to measure the system transient performance under a wide range of operating conditions. The indices (5-16), (5-17) are similar to indices (3-6), (3-7) in Section 3.4.1. Indices (5-18) and (5-19) can measure the overall transient performance with all disturbances and all generators taken into account.

$$J_1 = \frac{1}{N} \sum_{n=1}^N \int_{t=0}^{t=t_{sim}} |\Delta \varepsilon(t)| dt \quad (5-16)$$

$$J_2 = \frac{1}{N} \sum_{n=1}^N \int_{t=0}^{t=t_{sim}} t \cdot \Delta^2 \varepsilon(t) dt \quad (5-17)$$

$$J_3 = \sum_{h=1}^H \sum_{p=1}^m J_1 \quad (5-18)$$

$$J_4 = \sum_{h=1}^H \sum_{p=1}^m J_2 \quad (5-19)$$

where N is the total number of samples; H is the number of test cases in Table 5-7; m is the number of machines. t_{sim} is the total simulation time; $\varepsilon(t)$ represents all the time response of the selected physical variables and $\Delta\varepsilon(t) = \varepsilon(t) - \varepsilon(t-1)$; It is obvious that the lower the values of these indices, the smaller deviation of the signal will present in response to disturbance.

The performance indices of machine electrical powers in the system are given in Table 5-8, where M1 and M2 denote the GPSS method and DE-PPSS method in Chapter 3, respectively; M3 denotes the proposed CONT-PPSS approach in this chapter. Only the results of the top 4 most severe contingencies are exhibited in the table. The values of J_3 with respect to three methods are 4.42693, 2.91577 and 2.82653, respectively; while the values of J_4 are 0.38843, 0.28978 and 0.28906, respectively. This confirms the conclusion in Chapter 3 that DE-PPSS method is superior to the GPSS method in terms of damping ability under a wide range of operating conditions; the proposed approach in this chapter further improve the DE-PPSS, especially under large disturbances (for example, 15-8) and stressed conditions, due to its effective consideration of all contingencies in the PSS synthesis process.

Table 5-8. Performance indices of the test cases

		J_1			J_2		
		M1	M2	M3	M1	M2	M3
15-8	G1	0.0770	0.0759	0.0632	0.00660	0.00681	0.00655
	G2	0.0571	0.0428	0.0425	0.00230	0.00198	0.00198
	G3	0.1414	0.0765	0.0801	0.01460	0.00956	0.00962
	G4	0.0845	0.0607	0.0634	0.00580	0.00473	0.00479
	G5	0.1208	0.0777	0.0673	0.01240	0.00932	0.00904
	G6	0.0678	0.0519	0.0505	0.00330	0.00290	0.00290
	G7	0.2051	0.1087	0.1028	0.01750	0.00506	0.00496
	G8	0.4106	0.1385	0.1347	0.10690	0.01212	0.01077
15-12	G1	0.0188	0.0181	0.0157	0.00178	0.00179	0.00176
	G2	0.0157	0.0119	0.0120	0.00087	0.00085	0.00085
	G3	0.0434	0.0240	0.0262	0.00475	0.00434	0.00436
	G4	0.0292	0.0224	0.0251	0.00233	0.00225	0.00230
	G5	0.0424	0.0286	0.0274	0.00473	0.00445	0.00442
	G6	0.0203	0.0159	0.0156	0.00141	0.00138	0.00138
	G7	0.0540	0.0276	0.0300	0.00196	0.00103	0.00112
	G8	0.1246	0.0387	0.0445	0.01141	0.00242	0.00254
9-12	G1	0.0127	0.0121	0.0104	0.00079	0.00079	0.00078
	G2	0.0192	0.0165	0.0168	0.00212	0.00210	0.00211
	G3	0.0312	0.0175	0.0195	0.00237	0.00216	0.00217
	G4	0.0204	0.0147	0.0161	0.00089	0.00084	0.00085
	G5	0.0289	0.0181	0.0177	0.00175	0.00157	0.00157
	G6	0.0185	0.0156	0.0164	0.00149	0.00148	0.00149
	G7	0.0363	0.0188	0.0203	0.00080	0.00038	0.00044
	G8	0.0939	0.0329	0.0373	0.00769	0.00301	0.00307
4-10	G1	0.0096	0.0090	0.0075	0.00034	0.00034	0.00033
	G2	0.0096	0.0076	0.0075	0.00031	0.00031	0.00031
	G3	0.0255	0.0126	0.0150	0.00112	0.00094	0.00096
	G4	0.0138	0.0096	0.0097	0.00031	0.00028	0.00028
	G5	0.0204	0.0125	0.0113	0.00063	0.00053	0.00052
	G6	0.0251	0.0223	0.0230	0.00360	0.00359	0.00359
	G7	0.0467	0.0305	0.0318	0.00605	0.00573	0.00576
	G8	0.0749	0.0277	0.0300	0.00429	0.00137	0.00139
		J_3			J_4		
		4.42693	2.91577	2.82653	0.38843	0.28978	0.28906

5.5 Methodology Comparison

In this section, a comparison among the PSO method of this chapter, the DE method of Chapter 3 and the BLX- α GA method of Chapter 4 on problem (5-8) is conducted, based on 15 trial simulations. For comparison purpose, some parameters of the three algorithms are listed in Table 5-9; other parameters can be found in respective chapters.

Table 5-9. Parameter configuration of three methods

Method	Maximum iteration	Population size NP
DE	150	200
the BLX- α GA	150	200
PSO	750	40

The evaluation times (i.e., the total iteration number of each DE/GA/PSO running) of three methods in 15 trials are investigated. The maximum, the minimum and the average evaluation times (i.e., the averaged evaluation times of each trial) are shown in Figure 5-4 and the average computing time consumed in each trial is presented in Table 5-10. It can be observed in Figure 5-4 that in these trials the average evaluation times of the PSO method, the DE method and the BLX- α GA method are about 1350, 2000, and 4500, respectively; the minimum evaluation times of three methods are about 960, 1600, and 2100, respectively; the maximum times of three methods are about 1800, 3000, and 6500, respectively. That means the PSO method here undergoes less objective function evaluation than other two methods on problem (5-8). Due to the complexity of problem (5-8), each objective function evaluation consumes about 3.28 second of CPU time in an Intel P4 2.66 GHz CPU and 1G RAM computer. In Table 5-10, the average

computing time for each simulation is 73.7 minutes, 110.1 minutes and 178.5 minutes for the PSO, the BLX- α GA, and the DE, respectively, which show that the proposed PSO method converges more quickly than the BLX- α GA method and the DE method on this problem.

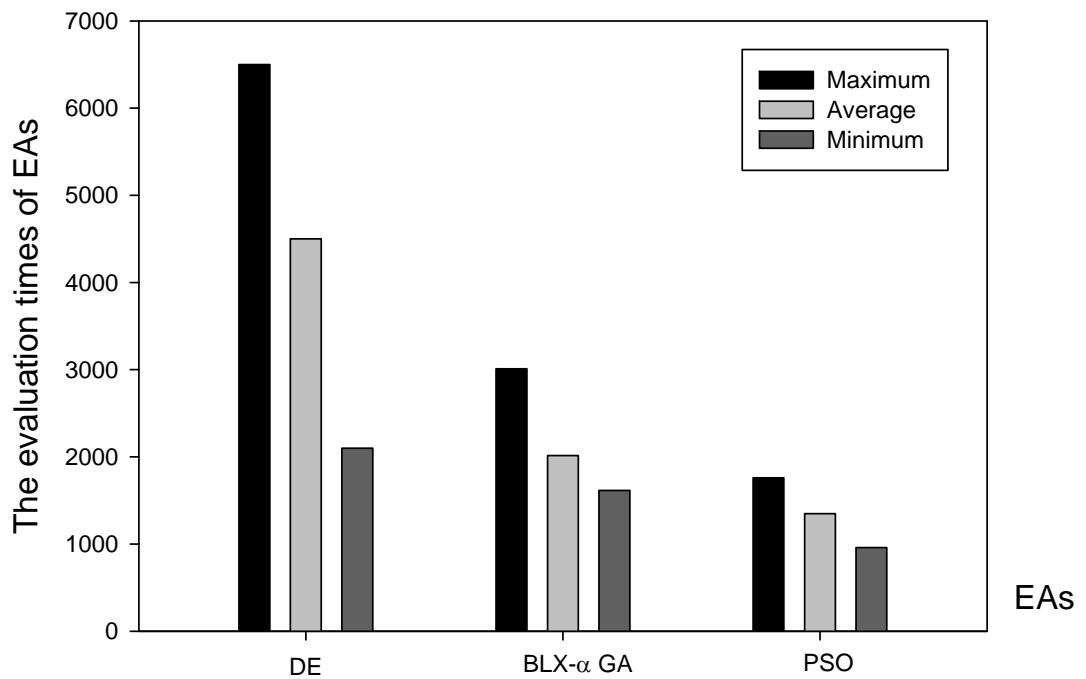


Figure 5-4. Histogram of convergence performance statistics

Table 5-10. Computing time of three methods

Parameter	Average evaluation times	Computing time (min.)
DE	4500	178.5
the BLX- α GA	2015	110.1
PSO	1348	73.7

5.6 Summary

In this chapter, the probabilistic PSS design has been extended by synthesizing system contingencies into the parameter optimization model. The critical contingency screening is first performed to select the top n (usually 3-5) most severe contingencies based on a probabilistic small signal stability index. The PSS tuning problem has been converted into a multi-objective optimization model and further transformed into a single-objective optimization model. A recursive PSO-based algorithm is used to solve this problem. Numerical experiments on the 8-machine system with multiple contingencies and a wide range of load conditions imposed have shown that the PSO consumes less computing time than the DE and the BLX- α GA and the proposed model can further improve system performance compared to the probabilistic PSS design model in Chapter 3.

6 PROBABILISTIC POWER SYSTEM STABILIZER DESIGN CONSIDERING OPTIMAL SITING

6.1 Introduction

As discussed in Chapter 1, some approaches or indices based on open-loop system model have been proposed and successfully used to select proper PSS sites, such as participation factor analysis [119], residue method [104], mode analysis [140], and sensitivity coefficients [170], etc. These methods can provide fast indication of proper places to install PSSs. Some of the above methods have the following features: (i) PSS sites and parameters are decided by a sequential method, which considers the damping enhancement of just one critical electromechanical mode at a time; (ii) the eigenanalysis is performed on the open-loop system, which only considers the open-loop eigenvalues and eigenvectors to determine the PSS sites; (iii) some of these PSS siting schemes are independent of changes of the power system operating conditions.

Based on above background, the purpose of this chapter is to carry out a study to solve the following issues: (i) eigenanalysis of the open-loop system can only convey part of information on how the control input affects the modes of the system. To gain the full knowledge of the effects of the controller on the modes, it is desirable to know the effectiveness of PSS in changing the closed-loop eigenvalues associated with the selected modes [98]; (ii) it is often desirable to identify sites for installing PSSs so that

several modes are damped out simultaneously in an effective way [112]; (iii) a wide range of operating conditions and uncertainties will be considered so that the PSS design will not be limited to deterministic condition with a particular load level; (iv) considering the optimal PSS siting, i.e., the minimum number of PSSs, to meet the requirement of power system damping criteria among a given group of PSS candidates is of particular interest so that the cost and complexity of controller design can be decreased to some extent.

The probabilistic PSS design approach in Chapter 3 will be extended to include the optimal PSS siting topic in this chapter. The problem will be first described as a combination optimization problem, which can determine the optimal PSS siting and PSS parameters among a group of PSS candidates so that the design criteria are satisfied. A recursive GA based on a mixed integer-binary coding and a partially matched crossover operator is then developed to solve the problem. The proposed approach is finally tested on two test systems.

6.2 Probabilistic PSS Design with Optimal Siting

For description purpose, it is assumed there are N_{PSS} potential PSS sites (i.e. N_{PSS} PSS candidates) that are numbered in integer sequence $1, 2, \dots, N_{\text{PSS}}$, each number corresponds to a generator index that could be a possible PSS location; among them K_{PSS} sites ($\leq N_{\text{PSS}}$) constitute a PSS siting set Φ ,

$$\Phi = \{h_1, h_2, \dots, h_i, \dots, h_{K_{\text{PSS}}}\} \quad (6-1)$$

where $h_i \in \{1, 2, \dots, N_{\text{PSS}}\}$; each h_i ($i=1, \dots, K_{\text{PSS}}$) represents a tentative PSS location; and there are no two identical h_i in the set Φ obviously.

The probabilistic PSS design with optimal siting taken into account is formulated as,

$$\text{Min}_{\{\Phi, K_{\text{PSS}}\} \cup \{K_i, T_{1i}, T_{2i}, T_{3i}, T_{4i}\}} f(\mathbf{P}) = \sum_{\alpha_k < \kappa} (\alpha_k^* - \kappa)^2 + \sum_{\xi_k^* < \kappa} (\xi_k^* - \kappa)^2 \quad (6-2)$$

s.t.

$$K_{\min} \leq K_i \leq K_{\max}$$

$$T_{1,\min} \leq T_{1i} \leq T_{1,\max}, \quad T_{2,\min} \leq T_{2i} \leq T_{2,\max}$$

$$T_{3,\min} \leq T_{3i} \leq T_{3,\max}, \quad T_{4,\min} \leq T_{4i} \leq T_{4,\max}$$

where K_{PSS} , Φ , K_i , T_{1i}/T_{2i} and T_{3i}/T_{4i} ($i \in \Phi$) are to be determined; the PSS parameters have the same meaning as those in problem (3-2).

To avoid the curse-of-dimension difficulty generally in combination optimization, gradual increment of the PSS number (i.e. number of tentative PSS sites) is to be evaluated recursively until the damping criteria are satisfied, which will be discussed in next section; and as a result the optimal-siting PSSs and their optimal parameters are determined. The problem (6-2) is a complex optimization problem characterized by an implicit objective function of discrete-continuous variables. Besides, it is related to the evaluation of probabilistic eigenvalues. Thus it is very difficult to resolve it using conventional methods, because the continuity of the objective function does not exist and its Jacobian matrix cannot be easily obtained.

As mentioned before, GA is computationally simple and easy to implement, besides it is very powerful and flexible in handling those optimization problems with mixed discrete-continuous variables. When the probabilistic PSS design considers the optimal

siting in problem (6-2), it can be described as an optimization problem with mixed discrete-continuous variables. Hence, a mixed integer-binary coded GA will be applied to the optimal-siting probabilistic PSS design in the chapter.

6.3 Optimization by the Mix-coding GA

Techniques such as tabu search [2], simulated annealing [3], and GA [57] have been applied to the controller design research of power systems. These heuristic algorithms can obtain optimal or near-optimal solutions of a problem by searching over a subspace. The most important advantage of heuristic algorithms is that they are not limited by assumptions such as continuity, availability of derivative of objective function, etc. GA is based on the mechanism of natural selection. It often produces high quality solutions.

The overall procedure for the optimal-siting probabilistic PSS design is illustrated in Figure 6-1 and explained below. The inner loop of Figure 6-1 is the GA search process, which is mainly composed of crossover, mutation and selection operation. To ascertain the optimal PSS siting, the effect of a given number of PSSs is to be evaluated recursively, as shown in the outer loop of Figure 6-1. The value of K_{PSS} (i.e., there are K_{PSS} tentative PSS installed), is first initialized simply as one or some pre-specified number (e.g., one third of total number). Proper selection of initial value of K_{PSS} can reduce the number of GA computation (i.e. the number of outer loop in Figure 6-1). Then the proposed GA is employed to solve the optimization problem. If the solution is not satisfactory to pre-specified damping criteria, then the number of PSSs will be increased and the GA search process will be restarted. The update of K_{PSS} and the GA

search process continues until the system damping criteria are all satisfied or the maximum trial number is reached. The outer loop process will stop under two conditions: the objective function becomes zero, i.e. damping criteria are satisfied; or the maximum number of potential PSS locations are finished checking. For each GA search process, two independent stop criteria are adopted: 1) the specified maximum number of generations is reached; 2) There occurs a severe stagnancy phenomenon, i.e., the best value of objective function found so far has not changed over the past 20 iterations/generations.

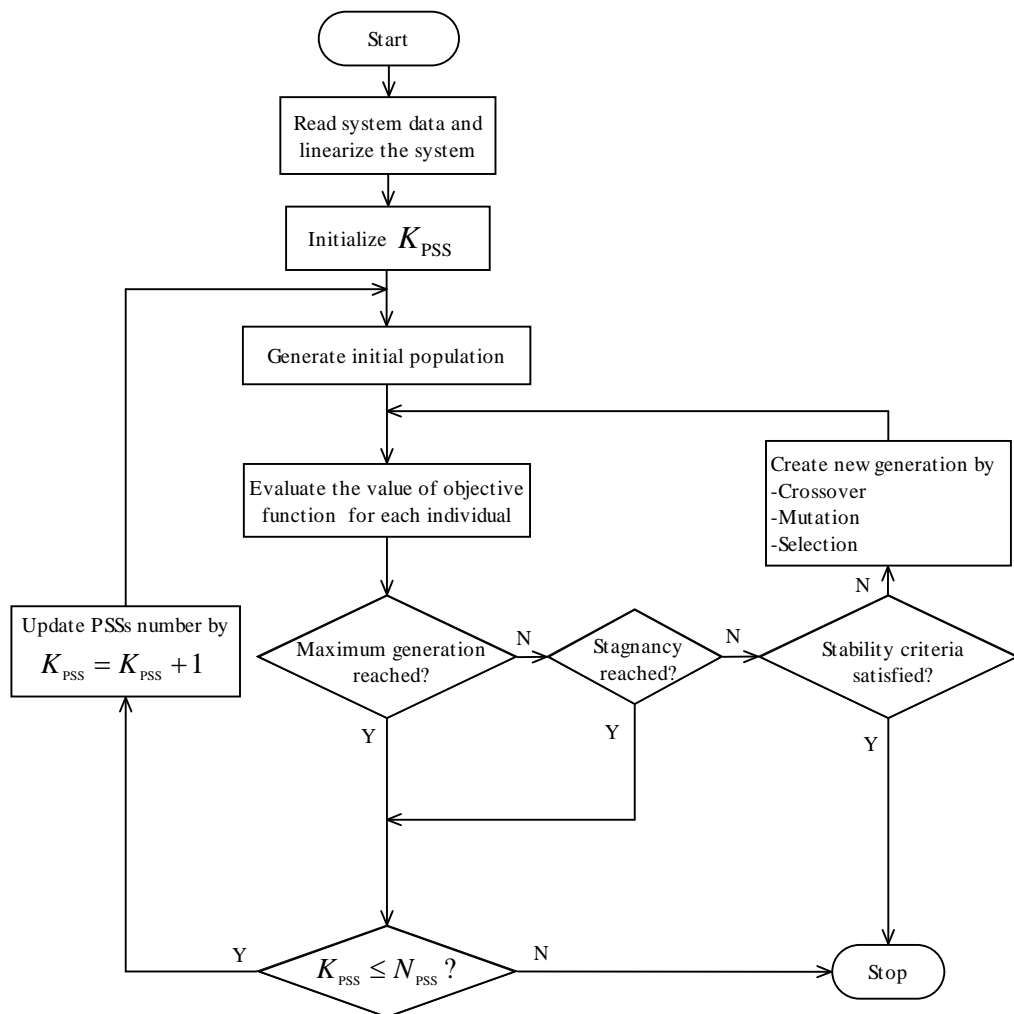


Figure 6-1. Flow chart of the recursive GA

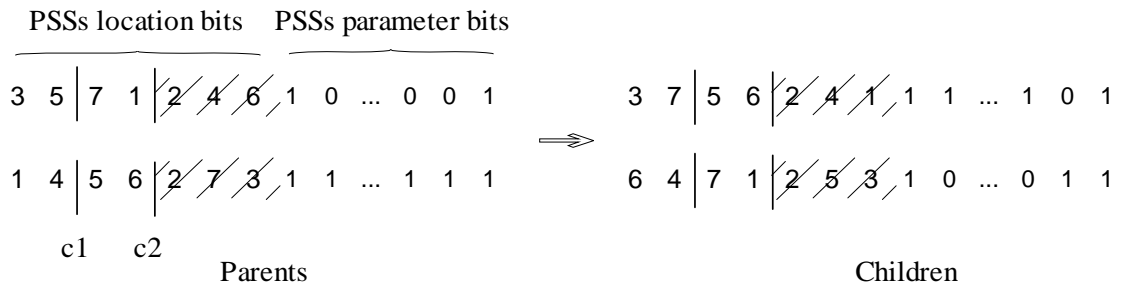
6.3.1 GA coding scheme

A configuration of K_{PSS} PSSs is composed of two types of parameters: the location index of PSSs (integer number) and PSS parameters (real number). A particular GA coding scheme is developed to match them. Correspondingly, there are two types of bits in the GA chromosome, integer bits and binary bits, as shown in Figures 6-2 (a)-(e) that correspond to an example of $K_{\text{PSS}}=4$ and $N_{\text{PSS}}=7$.

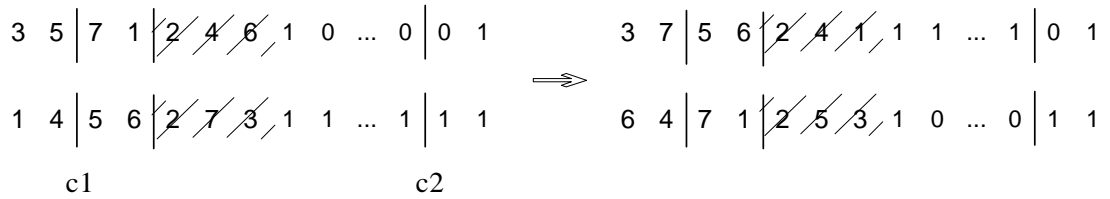
There are two portions in the integer bits. The first portion is called PSS-site bits, as shown in the first K_{PSS} length parts of the chromosomes in Figures 6-2 (a)-(e). PSS-site bits are composed of K_{PSS} length integers; each integer ($\leq N_{\text{PSS}}$) represents a location index in set Φ that will install a PSS. The second portion next to PSS-site bits is called dumb-PSS-site bits, as shown in the shadow parts in Figures 6-2 (a)-(e). Dumb-PSS-site bits are composed of $(N_{\text{PSS}} - K_{\text{PSS}})$ length integers; each integer represents a potential location index that is not contained in set Φ . Each PSS-site bit as well as dumb-PSS-site bit could appear at maximum once in the string. The order of integer bits in the string is not important for a given configuration, but could have its importance when applying the operator of crossover [57]. The dumb-PSS-site bits are not putting any effect on the configuration, but are indispensable to keeping the diversity of GA population and assisting the crossover and mutation operations. The binary bits in the remaining parts of chromosomes correspond to all potential PSS parameters, which are coded in binary bits. There are also some dumb parameter bits in them, which have no effect in the calculation of the value of objective function (6-2)

temporarily; but only those binary bits that are related to PSS-site bits will be involved in the calculation.

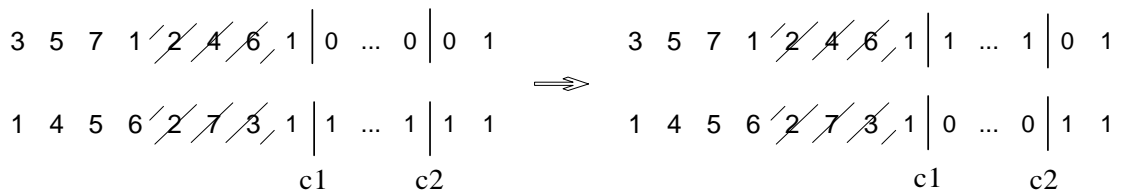
As a simple illustration, in Figure 6-2 (a) there is a pair of parents with four tentative PSS sites ($K_{\text{PSS}}=4$) among seven potential locations ($N_{\text{PSS}}=7$). In the first parent of Figure 6-2 (a), four PSS-site bits 3, 5, 7, 1 represent that the PSSs are tentatively installed at generator index 1, 3, 5 and 7. The three dumb-PSS-site bits are 2, 4 and 6. The remaining 0-1 codes correspond to all potential PSS parameters arranged in sequence.



(a) $c1 < c2 \leq K_{\text{PSS}}$



(b) $c1 \leq K_{\text{PSS}} < c2$



(c) $K_{\text{PSS}} < c1 < c2$

$$\begin{array}{l}
3 \mid 5 \ 7 \ 1 \ \cancel{2} \ \cancel{4} \ \cancel{6} \mid 1 \ 0 \ \dots \ 0 \ 0 \ 1 \\
1 \mid 4 \ 5 \ 6 \ \cancel{2} \ \cancel{7} \ \cancel{3} \mid 1 \ 1 \ \dots \ 1 \ 1 \ 1 \\
c1=c2
\end{array}
\Rightarrow
\begin{array}{l}
3 \mid 7 \ 4 \ 6 \ \cancel{2} \ \cancel{5} \ \cancel{1} \mid 1 \ 1 \ \dots \ 1 \ 1 \ 1 \\
6 \mid 5 \ 7 \ 1 \ \cancel{2} \ \cancel{4} \ \cancel{3} \mid 1 \ 0 \ \dots \ 0 \ 0 \ 1
\end{array}$$

$$(d) \ c1 = c2 \leq K_{PSS}$$

$$\begin{array}{l}
3 \ 5 \ 7 \ 1 \ \cancel{2} \ \cancel{4} \ \cancel{6} \mid 1 \ 0 \ \dots \ 0 \mid 0 \ 1 \\
1 \ 4 \ 5 \ 6 \ \cancel{2} \ \cancel{7} \ \cancel{3} \mid 1 \ 1 \ \dots \ 1 \mid 1 \ 1 \\
c1=c2
\end{array}
\Rightarrow
\begin{array}{l}
3 \ 5 \ 7 \ 1 \ \cancel{2} \ \cancel{4} \ \cancel{6} \mid 1 \ 0 \ \dots \ 0 \mid 1 \ 1 \\
1 \ 4 \ 5 \ 6 \ \cancel{2} \ \cancel{7} \ \cancel{3} \mid 1 \ 1 \ \dots \ 1 \mid 0 \ 1
\end{array}$$

$$(e) \ K_{PSS} < c1 = c2$$

Figure 6-2. Cases of the PMX operation with $K_{PSS}=4$ and $N_{PSS}=7$

6.3.2 GA operators

A Crossover

1) Introduction

The main crossover operator used here is a variant of two-point crossover with the specified probability p_c , called partially matched crossover (PMX) [61, 107]. For an ordinary two-point crossover of binary GA, two crossover positions are generated at random for the parents. Then the bits within the two positions of each parent are swapped. In this chapter, the PMX will be utilized in view of the particularity of the coding scheme discussed in last section. PMX is a bit-by-bit crossover operator, which can repair bit conflict problem. Taken an example of two integer GA strings in Figures 6-3 (a)-(b), two crossover positions $c1$ and $c2$ define a matching section that is used to affect a cross through position-by-position/bit-by-bit exchange operations. PMX

proceeds by bitwise exchanges. First, mapping string B to string A, the 5 and the 2, the 3 and the 6, and the 10 and the 7 exchange places. Similarly mapping string A to string B, the 5 and the 2, the 6 and the 3, and the 7 and the 10 exchange places. The final result of PMX is given in Figure 6-3 (b).

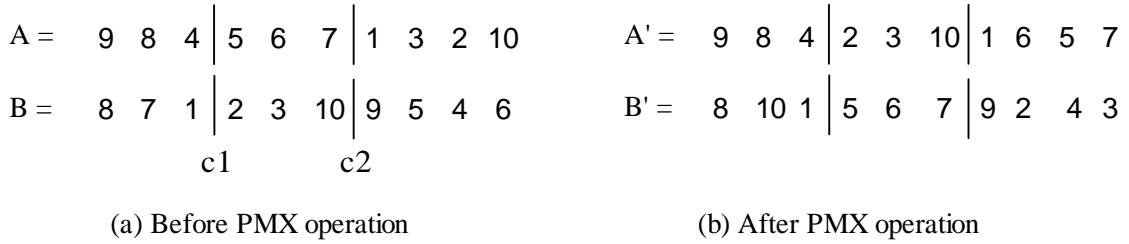


Figure 6-3. PMX operation of integer-coded GA strings [61]

2) Application

The application of PMX is illustrated in Figures 6-2 (a)-(e) and explained below. In the figures, each GA string consists of K_{PSS} PSS-site bits, $(N_{PSS} - K_{PSS})$ dumb-PSS-site bits and the remaining ℓ PSS-parameter bits. ℓ is the total length of binary string, which is data precision dependent [61, 107]. Two crossover positions $c1$ and $c2$ are generated over $[1, K_{PSS} + \ell]$ at random with $1 \leq c1 \leq c2 \leq K_{PSS} + \ell$. The dumb-PSS-site bits do not participate in but assist in the crossover operation of PSS-site bits. There are five crossover strategies summarized as follows,

(i). If $c1 < c2 \leq K_{PSS}$, as illustrated in Figure 6-2 (a), since each PSS candidate could appear at maximum once in the GA string, then a PMX operator will be adopted. The PMX-based repair will executed bit by bit in case there is bit conflict. In Figure 6-2 (a), the integer bits within $c1$ and $c2$ of two parents are swapped: specifically, when 7 is swapped with 5 and there is conflict happened with two 5 in the first parent and two 7 in

the second parent; for the first parent, the PMX repairs the conflict by replacing the 5 before $c1$ with 7; for the second parent, the PMX repairs the conflict by replacing the duplicate 7 in the dumb-PSS-site bits with 5. During this process, there is an implicit bit swap happened between the dumb-PSS-site bits and the PSS-site bits of the second parent. This operation will be applied for remaining bits one by one until the swapping of all bits within $c1$ and $c2$ is finished.

(ii). If $c1 \leq K_{\text{PSS}} < c2$, as illustrated in Figure 6-2 (b), the first position $c1$ and an implicit position K_{PSS} are the two cutting positions for PMX operation on the PSS-site bits. The second position $c2$ defines a cutting position for an ordinary one-point crossover on the PSS parameter bits.

(iii). If $K_{\text{PSS}} < c1 < c2$, as illustrated in Figure 6-2 (c), there is no operation on any integer bits. An ordinary two-point crossover is executed according to two cutting positions $c1$ and $c2$.

(iv). If $c1 = c2 \leq K_{\text{PSS}}$, as illustrated in Figure 6-2 (d), the position $c1$ ($c2$) and an implicit position K_{PSS} define two cutting positions for PMX operation on the PSS-site bits.

(v). If $K_{\text{PSS}} < c1 = c2$, as illustrated in Figure 6-2 (e), the position $c1$ ($c2$) defines a cutting position for an ordinary one-point crossover operated on the PSS parameter bits.

B Mutation

There are two types of mutation operators supported in the study: swap mutation and bit-flipping mutation. A single-bit swap mutation is supported between PSS-site bits and dumb-PSS-site bits with the specified probability p_{ms} . In Figure 6-4 one position

$x1$ is selected at random in the PSS-site bits; another one $x2$ is selected at random in the dumb-PSS-site bits. The bits at two positions are swapped so that new PSS configuration is produced. Another mutation operator is a bit-flipping mutation performed on the binary bits [107], which implement a bitwise bit-flipping with the specified probability p_{mr} . Different mutation probability is arranged because of the two mutation operators are independent of each other.

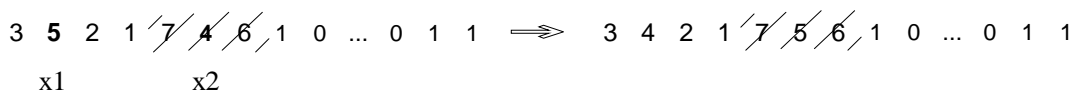


Figure 6-4. Swap mutation on the integer bits

C Selection

In the study, the ranking selection strategy in Chapter 4 will be employed. Besides, an elitism mechanism is adopted in the GA implementation.

6.3.3 Design procedure

The problem (6-2) can be solved by the proposed GA according to the following steps:

Step 1 Initialization: initialize NP individuals/chromosomes in the population in the following way:

Step 1.1 For each chromosome, make a random permutation of N_{PSS} site indexes for the first N_{PSS} -length integer bits.

Step 1.2 For each 0-1 bit in the remaining ℓ -length binary GA string, when the value of a random number generated between 0 and 1, $rand [0, 1]$, is less than 0.5, the corresponding binary bit is 0; otherwise, 1.

Step 2 Generate the next generation of NP chromosomes in the following way.

Step 2.1 Evaluate the objective function of the chromosomes in the current generation using equation (6-2). In the present work, the fittest chromosome in the current generation is always retained in the next generation.

Step 2.2 Selection: select two chromosomes as the parents by the ranking selection method.

Step 2.3 Crossover: generate two crossover positions $c1$ and $c2$ at random, apply the PMX to the two selected parents in the current generation when $rand [0, 1]$ is less than p_c . Otherwise, the two parents are retained and are taken as the child chromosomes in the next generation. Repeat the selection step in Step 2.2 and the present step until NP child chromosomes are formed in the next generation.

Step 2.4 Mutation: for each chromosome in the next generation, apply the swap mutation to the integer bits of the chromosome when the swap mutation probability, p_{ms} , is greater than $rand [0, 1]$; otherwise, the integer bits will remain intact. Apply the bit-flipping mutation to every binary bit one by one when the bit-flipping mutation probability p_{mr} is greater than $rand [0, 1]$; otherwise, the binary bit will remain intact.

Step 3: The next generation formed in Step 2 is now taken to be the current generation. New generations are produced by repeating the solution process starting from Step 2 until the specified maximum number of generations is reached or the objective function becomes zero.

6.4 Case Studies

In this section the same two test systems as those in Chapter 2, system **I** and system **II**, will be employed to test the effectiveness of the proposed method. In addition, the same dynamic stability criteria will be adopted as well, i.e., $\xi_c = 0.1$ and $\alpha_c = 0$ for both system and κ values are set to 4.0 and 3.5 for system **I** and system **II** respectively. The influence of algorithm parameters on the convergence performance of the proposed method in Section 6.3 will follow, including different combination of the crossover probability p_c , the bit-flipping mutation probability p_{mr} and the swap mutation probability p_{ms} . The pre-specified parameters for two test systems are listed in Table 6-1.

Table 6-1. The pre-specified parameters

Parameter	system I	system II
Maximum generation	100	100
Population size	50	200
Initial K_{PSS}	1	3
N_{PSS}	2	7

6.4.1 System I

A GA parameter experiments

The three-machine nine-bus system is shown in Figure 2-3 of Chapter 2. To improve the system damping, G1 and G2 are two potential sites for PSS installation. Since crossover and mutation probability have great impacts on the performance of canonical GA [61], several experiments on investigating the influence of different combination

$\{p_c, p_{mr}, p_{ms}\}$ on the convergence performance of the proposed method will be carried out and empirically excellent parameters from these experiments will hence be adopted for further studies. When applying K_{PSS} number of PSSs, if stagnancy happens, the GA will be restarted (in Figure 6-1). In this section, the stagnancy analysis of the proposed method with respect to $\{p_c, p_{mr}, p_{ms}\}$ is to be discussed. The values used for each parameter were: $p_c \in \{0.50, 0.75, 0.90\}$, $p_{mr} \in \{0.01, 0.05, 0.1, 0.3\}$, and $p_{ms} \in \{0.001, 0.005, 0.01, 0.05\}$. The parameters were investigated for 50 trial simulations in succession according to three scenarios: (a) altering p_c with $p_{mr}=0.01$ and $p_{ms}=0.005$; (b) altering p_{mr} with $p_c=0.9$ and $p_{ms}=0.005$; (c) altering p_{ms} with $p_c=0.9$ and $p_{mr}=0.05$. The reasons for above arrangement are to be explained hereinafter.

Table 6-2. The results of GA parameter experiments in system I

p_c ($p_{mr} = 0.01$ and $p_{ms} = 0.005$)	Evaluation times			Trial statistics (%)	
	Max.	Min.	Avg.	$K_{PSS}=1$	$K_{PSS}=2$
0.50	2374	88	494	88	12
0.75	1995	93	483	86	14
0.90	2474	96	476	88	12
p_{mr} ($p_c = 0.90$ and $p_{ms} = 0.005$)	Evaluation times			Trial statistics (%)	
	Max.	Min.	Avg.	$K_{PSS}=1$	$K_{PSS}=2$
0.05	1615	98	235	98	2
0.10	2304	99	326	94	6
0.30	2991	99	382	92	8
p_{ms} ($p_c = 0.90$ and $p_{mr} = 0.05$)	Evaluation times			Trial statistics (%)	
	Max.	Min.	Avg.	$K_{PSS}=1$	$K_{PSS}=2$
0.001	1807	99	339	90	10
0.01	2450	99	253	96	4
0.05	2055	99	363	92	8

The summary of the experiment results is given in Table 6-2 and the convergence curves of average $F(x)$ are shown in Figures 6-5, 6-6 and 6-7.

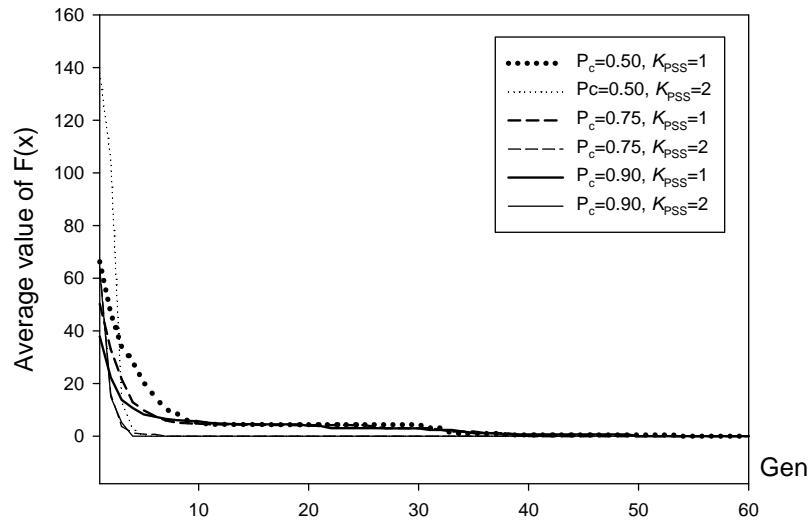


Figure 6-5. The influence of p_c on the recursive GA

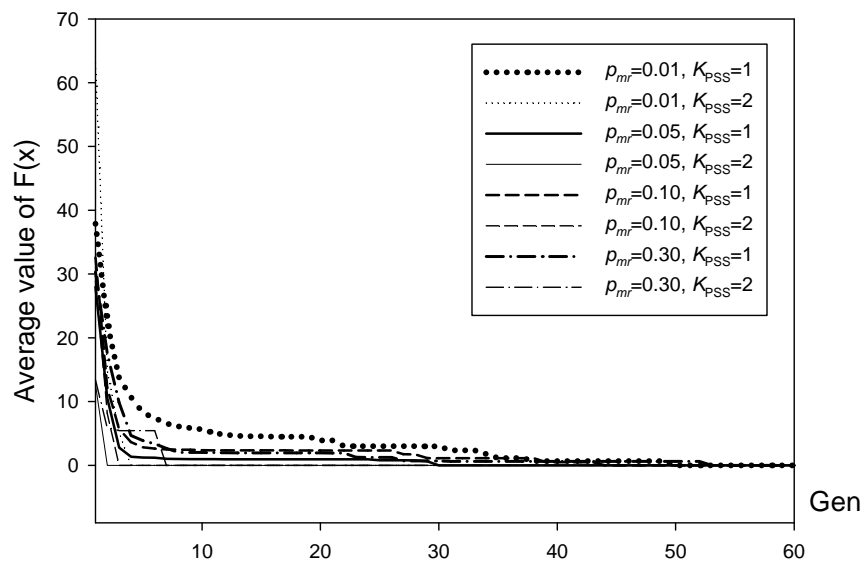


Figure 6-6. The influence of p_{mr} on the recursive GA

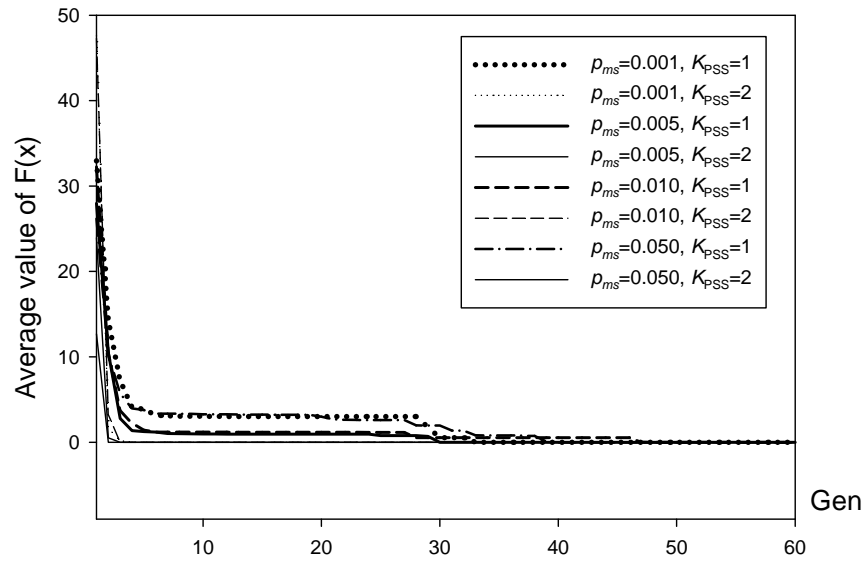


Figure 6-7. The influence of p_{ms} on the recursive GA

In Table 6-2, different cases are compared on the GA evaluation times, with the maximum, the minimum and the average evaluation times of total simulations given. Apparently, the less the average evaluation times, the faster does the algorithm converge. Statistics information on the proportion of the proposed method that can converge in one PSS ($K_{PSS}=1$) and in two PSSs ($K_{PSS}=2$) are also given in Table 6-2. Similarly, the larger proportion in case $K_{PSS}=1$, the faster does the algorithm converge. In Figures 6-5, 6-6 and 6-7, the highlighted/bold curves are those cases that can converge in case $K_{PSS}=1$, while those normal curves are related to those that can only converge in case $K_{PSS}=2$. In common, the simulation process in case $K_{PSS}=2$ runs faster than that in case $K_{PSS}=1$ for the same configuration of $\{p_c, p_{mr}, p_{ms}\}$, but the convergence performance between different cases of $K_{PSS}=2$ are trivial. So only the cases with $K_{PSS}=1$ are utilised to evaluate the algorithm performance in the study. The highlighted solid line in each figure is the curve corresponding to a preferable parameter

setting in each scenario. From the experiment results in Table 6-2 and Figures 6-5, 6-6 and 6-7, there are the following observations:

(i) When $p_{mr}=0.01$ and $p_{ms}=0.005$, altering p_c in turn and it is observed that $p_c=0.9$ is the best setting, which corresponds to the curve that converges most rapidly in $K_{PSS}=1$. The crossover probability experiments here show that $p_c=0.9$ is preferable to other p_c candidates. In the remaining experiments of scenario (b) and (c), $p_c=0.9$ will be adopted.

(ii) When $p_c=0.9$ and $p_{ms}=0.005$, altering p_{mr} and it is found that $p_{mr}=0.05$ is preferable to other p_{ms} candidates. In the remaining experiments of scenario (c), $p_{mr}=0.05$ will be adopted.

(iii) When $p_c=0.9$ and $p_{mr}=0.05$, altering p_{ms} and $p_{ms}=0.005$ in (ii) is preferable to other p_{ms} candidates.

(iv) From above discussions, parameters $\{p_c, p_{mr}, p_{ms}\}$ equal to $\{0.90, 0.05, 0.005\}$ is tentatively applied for the studies hereinafter.

B Tuning result

The resulting PSS settings are given in Table 6-3, and all closed-loop electro-mechanical modes shown in Table 6-4 are adequate for robust stability. When compared with the original open-loop eigenvalues in Table 2-1 of Chapter 2, the system stability is much improved. In Chapter 4, PSSs are installed on G1 and G2 and the system damping are satisfactorily improved. By comparison with the proposed method, only G1 is adequate to meet the robust stability requirement.

Table 6-3. Final PSS parameters for system I

Site	K_{PSS}	T_1	T_2	T_3	T_4
G1	3.532	0.650	0.183	0.136	0.044

Table 6-4. Electromechanical modes of the closed-loop system I

No.	$\bar{\alpha}$	$\bar{\beta}$	σ_α	α^*	P_α	$\bar{\xi}$	σ_ξ	ξ^*	P_ξ
1	-1.945	8.434	0.1337	14.54	1.00	0.2247	0.0300	4.15	1.00
2	-4.391	7.413	0.9290	4.73	1.00	0.5096	0.0967	4.24	1.00

C Transient performance

To complete the study, the performance of the proposed optimal-siting probabilistic PSS design (OS-PPSS) considering optimal siting is evaluated by time domain simulation and compared with that of the results in Section 3.4.1. The same three-phase-to-earth fault near bus 6 as that in Section 3.4.1 is applied, and the transient performance indices J_1 and J_2 in equations (3-6), (3-7) are calculated.

Table 6-5. Performance indices of system I

		δ_1	δ_2	v_{f1}	v_{f2}	v_{f3}	v_{t1}	v_{t2}	v_{t3}
J_1	M1	0.0492	0.0586	0.0390	0.0291	0.0206	0.0022	0.0030	0.0033
	M2	0.0711	0.0727	0.0710	0.0317	0.0251	0.0024	0.0031	0.0033
J_2	M1	0.0018	0.0032	0.0014	0.00069	0.00045	0.00005	0.00012	0.00016
	M2	0.0074	0.0088	0.0088	0.00105	0.00065	0.00005	0.00012	0.00016

The ATV comparison between OS-PPSS and DE-PPSS method in Chapter 3 is listed in Table 6-5, where M1 and M2 denote DE-PPSS method and OS-PPSS, respectively. Though it is observed that OS-PPSS here is slightly less robust than DE-PPSS, but the proposed PSS scheme here has satisfactorily acceptable performance index values compared with those of GPSS in Chapter 3 (see Table 3-5), as can also be confirmed in Figure 6-8. The reason is that the two normalized damping ratio ξ^* in Table 3-3 are 10.40 and 23.92 while the corresponding values in Table 6-4 are lower with 4.15 and 4.24, respectively. Typical transient response curves of rotor angles of G1 and G2 at light, medium and heavy load conditions in Figure 6-8 validate this observation.

6.4.2 System II

The 8-machine 24-bus system is shown in Figure 2-6 of Chapter 2. To improve the system damping, G1–G7 are seven potential sites for power-signal PSS installation. The resulting PSS parameters and electro-mechanical modes are listed in Tables 6-6 and 6-7, with the system damping effectively enhanced. In Chapter 3, PSSs are installed on G1, G2, G3, G5, G6, and G7, and the system damping are satisfactorily improved. By comparison, PSSs on G3, G5, G6 and G7 in this chapter are adequate to meet the robust stability requirement with the proposed method. The number of PSS has been reduced from 6 to 4.

Table 6-6. PSS parameters for system II

Site	K_{PSS}	T_1	T_2	T_3	T_4
G3	-1.299	0.102	0.068	0.075	0.180
G5	-0.195	0.266	0.196	0.176	0.158
G6	-0.020	0.161	0.162	1.959	0.075
G7	-1.104	0.146	0.164	0.097	0.166

Table 6-7. Electromechanical modes of the closed-loop system II

No.	$\bar{\alpha}$	$\bar{\beta}$	σ_α	α^*	P_α	$\bar{\xi}$	σ_ξ	ξ^*	P_ξ
1	-1.959	15.465	0.081	24.34	1.00	0.126	0.007	3.68	1.00
2	-1.417	11.67	0.046	30.51	1.00	0.121	0.006	3.57	1.00
3	-1.317	10.850	0.063	20.86	1.00	0.121	0.005	4.01	1.00
4	-1.451	10.107	0.134	10.81	1.00	0.142	0.012	3.51	1.00
5	-0.939	7.448	0.027	35.44	1.00	0.125	0.003	8.22	1.00
6	-2.149	3.099	0.078	27.61	1.00	0.570	0.032	14.63	1.00
7	-0.721	2.882	0.056	12.82	1.00	0.243	0.034	4.23	1.00

Similarly, the same three-phase-to-earth fault near bus 15 as that in Section 3.4.2 is applied and the deviations of generators' electrical power in p.u. are investigated. The performance indices are presented in Table 6-8; and the electrical power responses of G8 are plotted in Figure 6-9. Despite slightly less robust than DE-PPSS, the proposed OS-PPSS scheme is satisfactorily acceptable compared with GPSS, as can also be confirmed in Figure 6-9. The reason is that the lower least damping ratio ξ^* achieved in Table 6-7 is 3.51; by comparison, the corresponding value in Table 3-7 is 3.97.

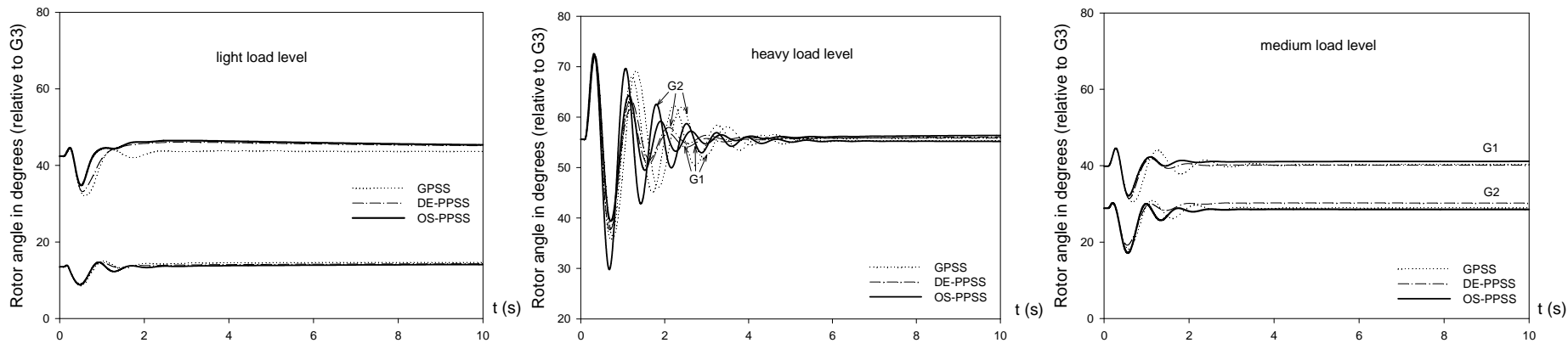


Figure 6-8. Transient responses of system I under typical load conditions

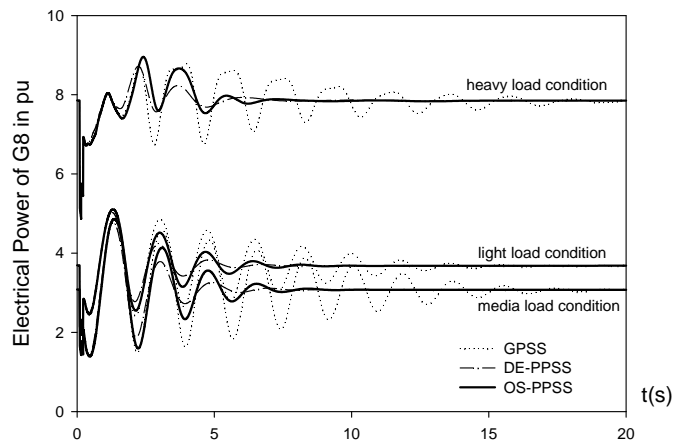


Figure 6-9. Transient responses of G8 of system II under typical operating conditions

Table 6-8. Performance indices of system II

		P_{e1}	P_{e2}	P_{e3}	P_{e4}	P_{e5}	P_{e6}	P_{e7}	P_{e8}
J_1	M1	0.0759	0.0428	0.0765	0.0607	0.0777	0.0519	0.1087	0.1385
	M2	0.0802	0.0337	0.0718	0.0568	0.0930	0.0506	0.1194	0.2052
J_2	M1	0.0068	0.0020	0.0096	0.0047	0.0093	0.0029	0.0051	0.0121
	M2	0.0069	0.0018	0.0093	0.0046	0.0096	0.0029	0.0053	0.0187

6.5 Summary

Under the framework of probabilistic eigenvalue analysis, the probabilistic PSS design considering optimal siting is investigated. A combination optimization model is proposed and a recursive GA is developed to solve this problem. The outstanding characteristics of the present GA can be summarized as: a) a mixed integer-binary coding is adopted to handle the discrete and continuous variables; b) the PMX-based crossover operator is used to resolve the integer bit conflict. Case studies show that the proposed optimal-siting probabilistic PSS design method can also achieve adequate robust stability compared to the method in Chapter 3, but the number of PSS installed has been reduced.

7 CONCLUSIONS AND FUTURE WORK

7.1 Summary

The past decades have witnessed a growing attention with poorly-damped, low frequency oscillation problems in interconnected power systems. Power system stabilizers have been widely employed to solve oscillation problems as a very cost-effective damping controller. In this thesis, the robust and coordinated PSS design has been deeply investigated with the application of some evolutionary algorithms.

Under multiple operating conditions, power system nodal voltages and nodal admittances are chosen as basic variables and the probabilistic eigenvalue analysis is introduced to evaluate eigenvalue expectation and covariance under the assumption of normal distribution. Two probabilistic sensitivity indices are derived and adopted to determine robust PSS siting. The results of PSIs are consistent with the results of mode analysis in case studies. The probabilistic eigenvalue analysis in Chapter 2 lays the foundation for most studies in the thesis.

A probabilistic eigenvalue-based optimization model has been formulated by probabilistic eigenvalue analysis to consider a wide range of operating conditions in Chapter 3. To overcome some limitations of previous gradient-based optimization

methods, such as high demand on initialization and trapping in local optimum, differential evolution (DE), as a new branch of EAs, has been introduced to solve the highly nonlinear optimization problem. Studies show that DE is not remarkably sensitive to its control parameters over specified ranges. This makes it easy to select its parameters for the probabilistic PSS design problem. A comprehensive comparison study between the proposed DE-based approach and a gradient-based conventional PSS (GPSS) indicates that the former is more robust than the latter.

In Chapter 4, a systematic method that can consider system contingencies in PSS design has been developed. A three-stage critical contingency screening process is first conducted to reduce the number of contingencies according to a post-contingency small signal stability index. In the first stage, the stability indices for all post-contingency cases are calculated one by one for one time period. In the second stage, the top k (usually 3-5) most severe contingencies for each time period t are accumulated into a contingency pool and ranked according to their stability index. In the third stage, the final n contingencies are selected as initial contingent tuning conditions based on some strategies, such as the ranking of averaged least damping ratio, etc. A multi-objective optimization model is developed and a min-max method is adopted to transform it into a single-objective optimization model. A BLX- α GA is recursively used until all post-contingency criteria are satisfied or some other termination condition is met. Case studies show that all post-contingency criteria can be satisfied by the recursive GA approach. Transient simulation experiments are conducted based on a prescribed set of

contingencies, which correspond to some extreme conditions from the stability point of view. The results show that this approach can more effectively enhance post-contingency damping compared to a conventional method.

The system contingencies are further concluded in the probabilistic PSS design model by a multi-objective optimization model in Chapter 5. To reduce the number of contingencies, the critical contingency screening is first performed to select the top n contingencies based on a post-contingency probabilistic small signal stability index. A PSO technique is recursively used until all post-contingency criteria are satisfied or some other termination condition is met. Numerical experiments over multiple contingencies and a wide range of load conditions show that the PSO consumes less computing time than the DE and the BLX- α GA and the proposed model can further improve system performance compared to the probabilistic PSS design model in Chapter 3.

To settle the optimal siting problem, i.e., the minimum number of PSS locations, in the probabilistic PSS design, a combination optimization model has been proposed in Chapter 6. A special GA with a mixed integer-binary coding and a PMX-based crossover operator is developed to handle the discrete and continuous variables in the optimization model and resolve the integer bit conflict. Case studies show that the proposed optimal-siting probabilistic PSS design method can also achieve adequate

robust stability compared to the method in Chapter 3, but the number of PSS installed has been reduced.

7.2 Recommendation for Future Work

Lessons from several cascading outages during the past several years have called for the recommendation of new technologies being applied in power systems, such as distributed generation technologies, wide area measurement system (WAMS) [9], which are on the way of rapid expansion. On the other hand, the new power system environment with competitive power market introduced further has great impact on the power system operation patterns. Thus the following issues on damping controller design merit attention in future studies.

1. At present, some elementary models have been developed to consider damping controller design in distributed generation environment [70, 71, 110]. However, the stochastic characteristic of wind power is not considered in these publications. Thus the probabilistic PSS design could be further extended to include the variation characteristics of wind power generation in the model.

2. Some fundamental studies have been conducted on how to consider nonlinear effects in damping controller design of small signal analysis [95, 127] under stressed operating conditions. Yet these still exhibit spaces for improvement, for example, applying the

EAs to the damping controller design with high order terms of SSSA taken into account; considering the time-delay effect in the WAMS-based PSS design.

3. FACTS device and HVDC system are more complicated than PSS and they are being applied more and more widely. The probabilistic controller design in [13] can be further extended to consider system contingencies in these sophisticated power electronic equipments, which should be more challenging.

4. In recent years, an advanced evolutionary algorithm, coevolutionary computation has been applied in unit commitment [25], strategic interaction in electricity markets [26], reactive power optimization [93], etc. The decomposition and coordination idea in the coevolutionary architecture is very attractive so that convergence performance of classical EAs can be particularly improved. An investigation study on the effectiveness of applying the coevolutionary computation to the probabilistic PSS design is of particular interest.

5. To release the computing burden, a hybrid method of EAs and Heffron-Philips Model could be considered in PSS design. On the one hand, the lead/lag time constants of PSS can be derived from the GEP(s) phase compensation [53, 59]; on the other hand, only the PSS gains are tuned by EAs so that the search space can be considerably reduced.

APPENDIX A PROBABILISTIC EIGENVALUE ANALYSIS

A1 Power System Model

A1.1 Framework

The power system models in this thesis will be constructed under the GMT/PMT framework [31, 139], where the machines, system components and the associated control devices are represented by only two types of elementary transfer blocks (first and zero order) as shown in Figures A-1 (a)-(b). Any standard power system components could be easily and versatily 'plugged' in to form a small perturbation state space model irrespective of the complexity of the system.

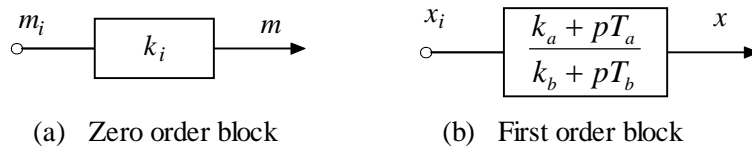


Figure A-1. Two types of elementary transfer blocks

By eliminating the zero-order input vector \mathbf{M}_i through proper substitution, here vectors \mathbf{X}_i , \mathbf{X} and \mathbf{M} are used to collect all the x_i , x and m variables of Figures A-1 (a)-(b), the following system connection matrix could be constructed.

$$\begin{bmatrix} \mathbf{X}_i \\ \mathbf{Y}_o \\ \mathbf{0} \end{bmatrix} = \begin{bmatrix} \mathbf{L}_1 & \mathbf{L}_2 & \mathbf{L}_3 \\ \mathbf{L}_4 & \mathbf{L}_5 & \mathbf{L}_6 \\ \mathbf{L}_7 & \mathbf{L}_8 & \mathbf{L}_9 \end{bmatrix} \begin{bmatrix} \mathbf{X} \\ \mathbf{R} \\ \mathbf{M} \end{bmatrix} \quad (\text{A-1})$$

where \mathbf{R} and \mathbf{Y}_o are input and output vectors. The constructions of sub-matrix \mathbf{L}_1 to \mathbf{L}_9 are described detailed in [31, 139]. The first order transfer block in Figure A-1 (b) can be represented as

$$(\mathbf{K}_b + p)\mathbf{X} = (\mathbf{K}_a + p\mathbf{K}_t)\mathbf{X}_i \quad (\text{A-2})$$

where \mathbf{K}_a , \mathbf{K}_b and \mathbf{K}_t are diagonal matrices collecting parameters k_a/T_b , k_b/T_b and T_a/T_b in Figure A-1 (b), respectively. Thus from equation (A-1) and (A-2), the state space equation is obtained by eliminating the non-state vector \mathbf{M} .

$$\begin{cases} \dot{\mathbf{X}} = \mathbf{A}\mathbf{X} + \mathbf{B}\mathbf{R} + \mathbf{E}\dot{\mathbf{R}} \\ \mathbf{Y}_o = \mathbf{C}\mathbf{X} + \mathbf{D}\mathbf{R} \end{cases} \quad (\text{A-3})$$

where $\mathbf{A} = \mathbf{S}(\mathbf{K}_a\mathbf{F} - \mathbf{K}_b)$ with $\mathbf{S} = (\mathbf{I} - \mathbf{K}_t\mathbf{F})^{-1}$, $\mathbf{F} = \mathbf{L}_1 + \mathbf{L}_3\mathbf{H}\mathbf{L}_7$ and $\mathbf{H} = (-\mathbf{L}_9^{-1})$.

In the thesis it is assumed that the state vector \mathbf{X} is a n dimensional vector; \mathbf{R} is a r dimensional vector representing the input signals; \mathbf{A} is a $n \times n$ state matrix; \mathbf{B} is a $n \times r$ input matrix; \mathbf{C} is a $m \times n$ output matrix; \mathbf{D} is a $m \times r$ feedforward matrix. It should be mentioned that the $\mathbf{E}\dot{\mathbf{R}}$ term is often avoided in the usual representation of power system components [31, 139].

A1.2 Network equation

The nodal admittance matrix \mathbf{Y} is usually used to describe the network configuration and parameters of a power system. The network equation used in eigenvalue analysis can be expressed by \mathbf{Y} of entire system as

$$\mathbf{I} = \mathbf{Y}\mathbf{V} \quad (\text{A-4})$$

$$\Delta\mathbf{I} = \mathbf{Y}\Delta\mathbf{V} \quad (\text{A-5})$$

A1.3 Load model

The voltage dependency of load characteristic is represented by an exponential function

$$S_{Li} = P_{Li} + jQ_{Li} = P_{Li0} (V_i/V_{i0})^a + jQ_{Li0} (V_i/V_{i0})^b \quad (\text{A-6})$$

For the constant impedance load adopted in the thesis, $a = b = 2$.

A2 Probabilistic Eigenvalue Analysis

A2.1 Probabilistic eigenvalue analysis

In the probabilistic eigenvalue analysis, the statistical nature of nodal voltages is determined by the probabilistic load flow calculation [150]. If the nodal voltage vector \mathbf{V} is defined in rectangular coordinates, nodal injected power vector will be a quadratic function of nodal voltages. By accurately expanding $S(\mathbf{V})$ in Taylor series, the second-order terms will have the same form as $S(\mathbf{V})$. Considering $\bar{\mathbf{V}} = 0$, the power expectation can be expressed as equation (A-7) which takes into account the correction of covariances

$$\bar{\mathbf{S}} = \overline{S(\mathbf{V})} + \overline{S(\Delta\mathbf{V})} = g(\dots, \overline{V_i V_j} + C_{V_i, j}, \dots) \quad (\text{A-7})$$

where $C_{V_i, j}$ is the covariance between voltages V_i and V_j . Consequently, the correcting equations used in probabilistic load flow calculation are given as,

$$\begin{cases} \Delta\bar{\mathbf{S}} = \mathbf{J}_V \Delta\bar{\mathbf{V}} \\ \mathbf{C}_V = \mathbf{J}_V^{-1} \mathbf{C}_S (\mathbf{J}_V^{-1})^T \end{cases} \quad (\text{A-8})$$

where \mathbf{J}_V is the Jacobian matrix.

Under the assumption of the normal distribution, eigenvalue expectations are computed from the expectations of nodal voltages, which is similar to that in the

conventional deterministic eigenvalue analysis. To determine eigenvalue variances, eigenvalue λ is regarded as a nonlinear function of nodal voltages with the linearized expression as

$$[\Delta\lambda] = \mathbf{J}_\lambda \Delta\mathbf{V} \quad (\text{A-9})$$

where \mathbf{J}_λ denotes the first-order partial derivative matrix of eigenvalues. The eigenvalue variances \mathbf{C}_λ are derived as

$$\mathbf{C}_\lambda = \mathbf{J}_\lambda \mathbf{C}_V \mathbf{J}_\lambda^T \quad (\text{A-10})$$

A2.1 First and second sensitivity analysis

The general formulations for the first and second order sensitivities of an eigenvalue λ_k are [148, 167]:

$$\frac{\partial \lambda_k}{\partial x_i} = \mathbf{W}_k^T \frac{\partial \mathbf{A}}{\partial x_i} \mathbf{U}_k \quad (\text{A-11})$$

$$\frac{\partial^2 \lambda_k}{\partial x_i \partial x_j} = \mathbf{W}_k^T \frac{\partial^2 \mathbf{A}}{\partial x_i \partial x_j} \mathbf{U}_k + \frac{\partial \mathbf{W}_k^T}{\partial x_i} \frac{\partial \mathbf{A}}{\partial x_j} \mathbf{U}_k + \frac{\partial \mathbf{W}_k^T}{\partial x_j} \frac{\partial \mathbf{A}}{\partial x_i} \mathbf{U}_k \quad (\text{A-12})$$

where x_i and x_j denotes parameter variables, the left and right eigenvectors \mathbf{W}_k and \mathbf{U}_k responding to mode k , satisfy $\mathbf{W}_k^T \mathbf{U}_k = 1$. In equation (A-12), the derivative of the left eigenvector \mathbf{W}_k^T is a linear combination of all eigenvectors:

$$\frac{\partial \mathbf{W}_k^T}{\partial x_i} = \sum_{\substack{m=1 \\ m \neq k}}^n \left(\frac{1}{\lambda_k - \lambda_m} \mathbf{W}_k^T \frac{\partial \mathbf{A}}{\partial x_i} \mathbf{U}_m \mathbf{W}_m^T \right) \quad (\text{A-13})$$

To calculate the PSIs in Section 2.3, the sensitivity of $\bar{\alpha}$ in equation (2-5) can be obtained by equation (A-11), which is similar to the conventional eigenvalue sensitivity

calculation [148, 167], but the sensitivity of σ_{α_k} in equation (2-5) have to be derived from the second-order sensitivities in equation (A-12).

The covariances C_{α_k, α_k} , C_{α_k, β_k} , C_{β_k, α_k} and C_{β_k, β_k} of an eigenvalue $\lambda_k = \alpha_k + j\beta_k$ are calculated from C_V by equation (A-14), which could be generally denoted as C_{γ_k, η_k} with (γ_k, η_k) standing for the four combinations of α_k and β_k .

$$C_{\gamma_k, \eta_k} = \sum_{i=1}^{N,N} \sum_{j=1}^{N,N} \left(\frac{\partial \gamma_k}{\partial \mathcal{V}_i} \frac{\partial \eta_k}{\partial \mathcal{V}_j} C_{V_{i,j}} \right) \quad (\text{A-14})$$

where N is the number of power system network nodes. The covariance sensitivity with respect to m -th PSS gain K_m can be derived as

$$\frac{\partial C_{\gamma_k, \eta_k}}{\partial K_m} = \sum_{i=1}^{N,N} \sum_{j=1}^{N,N} \left[C_{V_{i,j}} \left(\frac{\partial^2 \gamma_k}{\partial \mathcal{V}_i \partial K_m} \frac{\partial \eta_k}{\partial \mathcal{V}_j} + \frac{\partial \gamma_k}{\partial \mathcal{V}_i} \frac{\partial^2 \eta_k}{\partial \mathcal{V}_j \partial K_m} \right) \right] \quad (\text{A-15})$$

Considering $\sigma_{\alpha_k}^2 = C_{\alpha_k, \alpha_k}$ and $\gamma_k = \eta_k = \alpha_k$ in equation (A-15), the sensitivity of the standard deviation σ_{α_k} is simply with

$$\frac{\partial \sigma_{\alpha_k}}{\partial K_m} = \frac{1}{2\sigma_{\alpha_k}} \frac{\partial C_{\alpha_k, \alpha_k}}{\partial K_m} \quad (\text{A-16})$$

By linearizing the damping ratio of an eigenvalue at the expectation point,

$\bar{\lambda}_k = \bar{\alpha}_k + j\bar{\beta}_k$, then

$$\Delta \xi_k = D_{Ak} \Delta \alpha_k + D_{Bk} \Delta \beta_k \quad (\text{A-17})$$

with

$$D_{Ak} = -\bar{\beta}_k^2 / |\bar{\lambda}_k|^3, \quad D_{Bk} = \bar{\alpha}_k \bar{\beta}_k / |\bar{\lambda}_k|^3 \quad (\text{A-18})$$

The variance of ξ_k is then derived as

$$C_{\xi_k, \xi_k} = D_{Ak}^2 C_{\alpha_k, \alpha_k} + D_{Bk}^2 C_{\beta_k, \beta_k} + 2D_{Ak} D_{Bk} C_{\alpha_k, \beta_k} \quad (\text{A-19})$$

and the variance sensitivity of m -th PSS parameter will be

$$\begin{aligned}
\frac{\partial \mathcal{C}_{\xi_k, \xi_k}}{\partial \mathcal{K}_m} &= D_{Ak}^2 \frac{\partial \mathcal{C}_{\alpha_k, \alpha_k}}{\partial \mathcal{K}_m} + D_{Bk}^2 \frac{\partial \mathcal{C}_{\beta_k, \beta_k}}{\partial \mathcal{K}_m} + 2D_{Ak} D_{Bk} \frac{\partial \mathcal{C}_{\alpha_k, \beta_k}}{\partial \mathcal{K}_m} \\
&\quad + 2(D_{Ak} C_{\alpha_k, \alpha_k} + D_{Bk} C_{\alpha_k, \beta_k}) \frac{\partial D_{Ak}}{\partial \mathcal{K}_m} \\
&\quad + 2(D_{Bk} C_{\beta_k, \beta_k} + D_{Ak} C_{\alpha_k, \beta_k}) \frac{\partial D_{Bk}}{\partial \mathcal{K}_m} \tag{A-20}
\end{aligned}$$

where

$$\begin{aligned}
\frac{\partial D_{Ak}}{\partial \mathcal{K}_m} &= -\frac{3}{\bar{\alpha}_k} D_{Ak} \bar{\xi}_k^2 \frac{\partial \bar{\alpha}_k}{\partial \mathcal{K}_m} - \left[\frac{2}{\bar{\alpha}_k} - \frac{3}{\bar{\xi}_k} D_{Ak} \right] D_{Bk} \frac{\partial \bar{\beta}_k}{\partial \mathcal{K}_m} \\
\frac{\partial D_{Bk}}{\partial \mathcal{K}_m} &= [1 - 3\bar{\xi}_k^2] \frac{D_{Bk}}{\bar{\alpha}_k} \frac{\partial \bar{\alpha}_k}{\partial \mathcal{K}_m} + \left[\frac{1}{\bar{\beta}_k} + \frac{3}{\bar{\xi}_k} D_{Bk} \right] D_{Bk} \frac{\partial \bar{\beta}_k}{\partial \mathcal{K}_m} \tag{A-21}
\end{aligned}$$

The sensitivity of the standard deviation σ_{ξ_k} is then obtained from $\sigma_{\xi_k}^2 = C_{\xi_k, \xi_k}$ in equation (A-22)

$$\frac{\partial \sigma_{\xi_k}}{\partial \mathcal{K}_m} = \frac{1}{2\sigma_{\xi_k}} \frac{\partial \mathcal{C}_{\xi_k, \xi_k}}{\partial \mathcal{K}_m} \tag{A-22}$$

Therefore, the probabilistic sensitivity indices determined in equations (2-5), (2-6) can be calculated. To reduce the computation requirement and the accumulative error, sparsity technique becomes important in this study and is employed for the partial derivative calculation of system matrix A by: a) properly arranging the computing sequence of partial derivatives for different system variables; b) using the sparse and symmetrical nature of the nodal admittance matrix, the covariance matrix and the second order sensitivity matrix.

APPENDIX B MACHINE MODELS

B1 Fourth-order Generator Model

The fourth-order generator model is used in the thesis for modeling the d -axis and q -axis transient dynamics with the following ODE equations [128].

$$p\delta / \omega_0 = \omega - \omega_{ref} \quad (\text{B-1.1})$$

$$p\omega = [P_m - P_e] / M \quad (\text{B-1.2})$$

$$pE'_q = [E_{fd} - (X_d - X'_d)I_d - E'_q] / T'_{dq0} \quad (\text{B-1.3})$$

$$pE'_d = [(X_q - X'_q)I_q - E'_d] / T'_{dq0} \quad (\text{B-1.4})$$

The GMT/PMT representation of the model is given in Figure B-1.

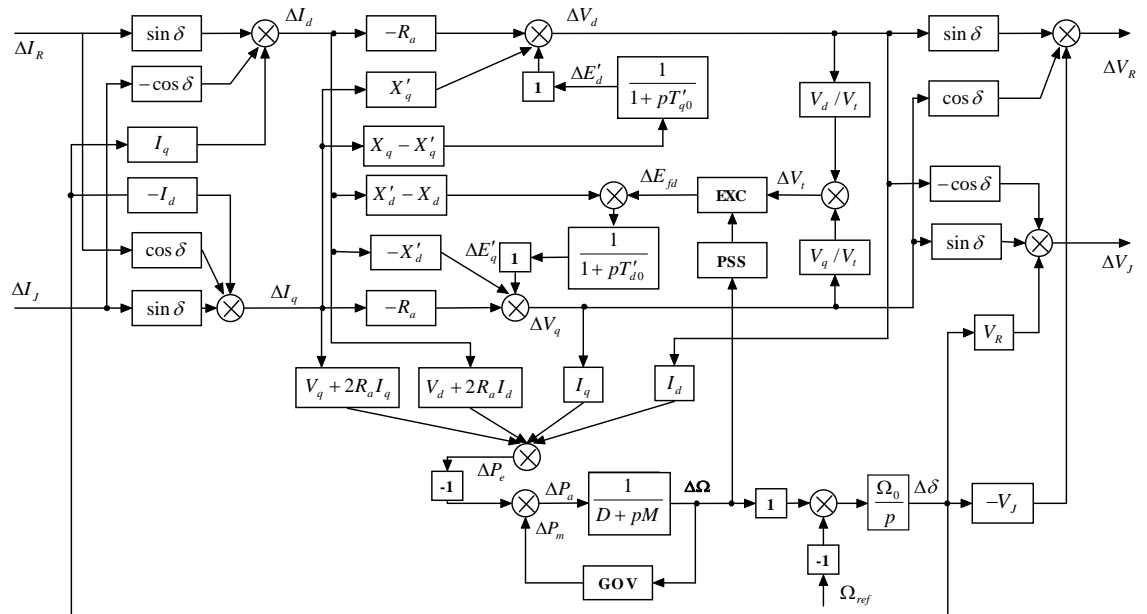


Figure B-1. GMT/PMT representation of the fourth-order generator model

B2 Sixth-order Generator Model

The sixth-order generator model used in the thesis is a subtransient generator model that assumes the presence of a field circuit and an additional circuit along the d -axis and two additional circuits along the q -axis and with the saturation effect neglected. The block diagram of this model is given in Figure B-2 [125, 129] and its GMT/PMT diagram is shown in Figure B-3. A group of its ODE equations can be referred to in [128].

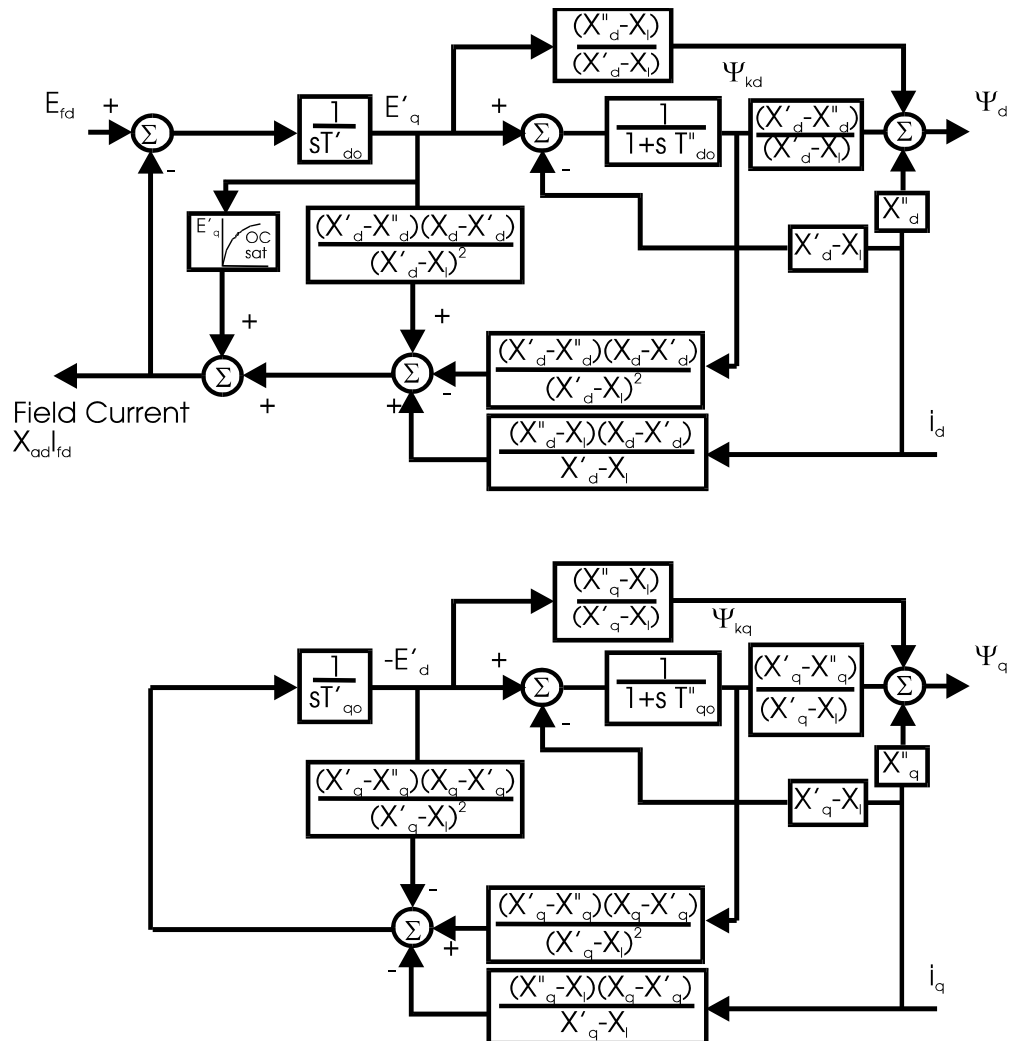


Figure B-2. Block diagram of sixth-order generator model

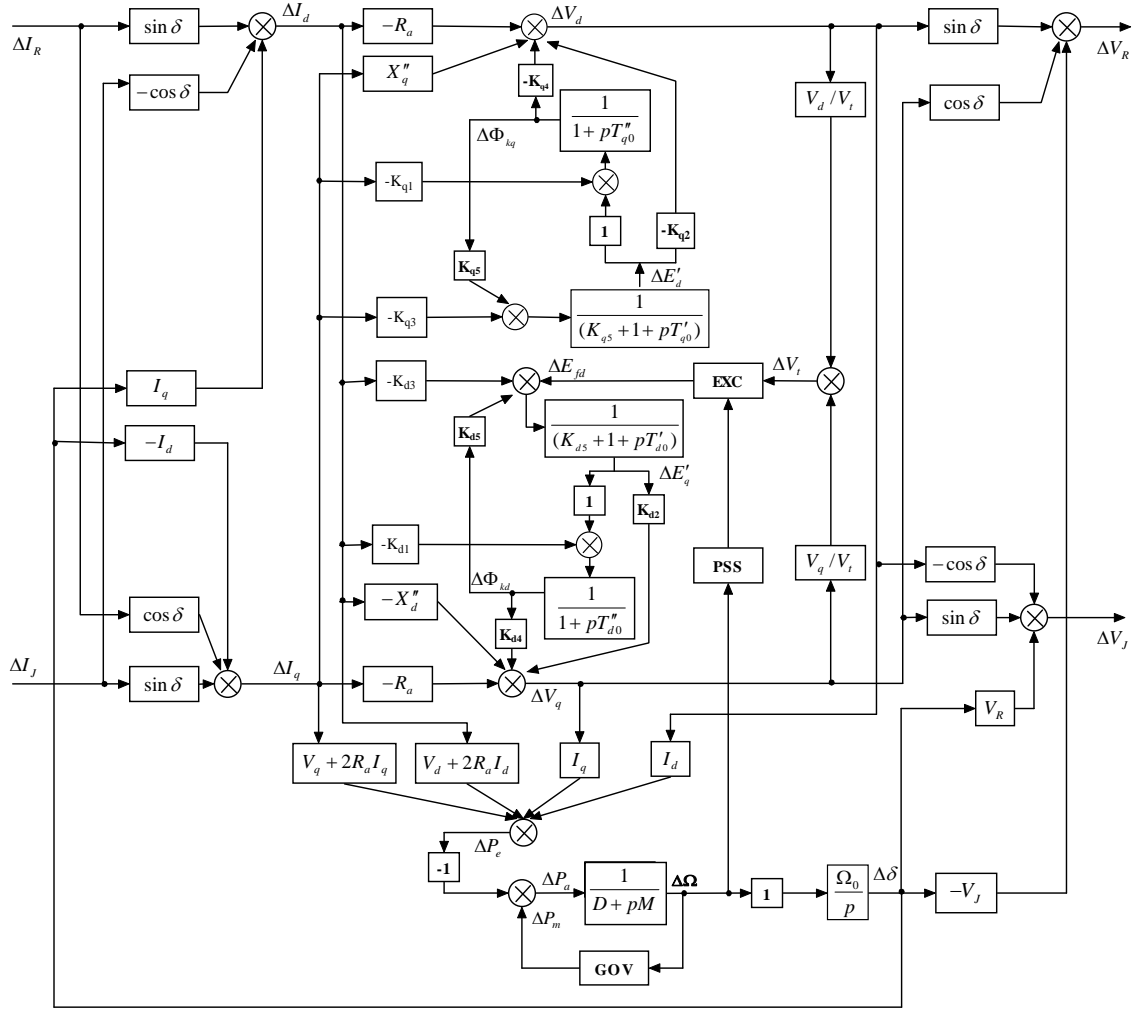


Figure B-3. GMT/PMT representation of the sixth-order generator model

The constants in Figure B-3 are defined as follows,

$$K_{d1} = X_d - X_l,$$

$$K_{q1} = X_q - X_l,$$

$$K_{d2} = \frac{(X_d'' - X_l)}{(X_d - X_l)},$$

$$K_{q2} = \frac{(X_q'' - X_l)}{(X_q - X_l)},$$

$$K_{d3} = \frac{(X_d - X_d')(X_d'' - X_l)}{(X_d - X_l)},$$

$$K_{q3} = \frac{(X_q - X_q')(X_q'' - X_l)}{(X_q - X_l)},$$

$$K_{d4} = \frac{(X_d' - X_d'')}{(X_d - X_l)},$$

$$K_{q4} = \frac{(X_q' - X_q'')}{(X_q - X_l)},$$

$$K_{d5} = \frac{(X_d - X_d')(X_d' - X_d'')}{(X_d - X_l)^2},$$

$$K_{q5} = \frac{(X_q - X_q')(X_q' - X_q'')}{(X_q - X_l)^2}$$

APPENDIX C TEST SYSTEM DATA

The three-machine system (system **I**) are shown in Figure 2-3 and the eight-machine system (system **II**) are in Figure 2-6. In the following tables, except for the dynamic data, all per unit data are on 100MVA base for both systems. Transformer's primary and secondary voltage ratio is specified on the 'From' side of transformer branch.

C1 Three-machine System (System I)

Table C-1. Bus data of system **I**

	Bus No.	P (p.u.)	Q (p.u.)	Curve No.	PV-Voltage	Curve No.
Load A	4	1.250	0.500	3	-	-
Load B	5	1.000	0.350	8	-	-
Load C	6	0.900	0.300	20	-	-
G1	7	1.130	0.000	3	1.000	1
G2	8	0.850	0.000	21	1.025	1
G3	9	0.000	0.000	-	1.040	31

Table C-2. Line data of system **I**

No.	From	To	Branch Number	R (p.u.)	X (p.u.)	B/2 (p.u.)	Transformer Ratio
1	1	5	1	0.0085	0.0720	0.0745	-
2	5	2	1	0.0119	0.1008	0.1045	-
3	1	4	1	0.0320	0.1610	0.1530	-
4	4	3	1	0.0100	0.0850	0.0880	-
5	2	6	2	0.0390	0.1700	0.3580	-
6	3	6	2	0.0340	0.0184	0.3160	-
7	1	7	1	0.0000	0.0625	0.0000	1.0000
8	2	8	1	0.0000	0.0586	0.0000	1.0000
9	3	9	1	0.0000	0.0576	0.0000	1.0000

Table C-3. Generator parameters of system I

Parameter	Machine		
	G1	G2	G3
Capacity (MVA)	250	250	1200
H (pu)	3.20	3.01	1.97
D (pu)	0.01	0.01	0.01
x_d (pu)	1.796	1.9688	1.752
x_q (pu)	1.725	1.8867	1.1628
x'_d (pu)	0.2396	0.272	0.7296
x'_q (pu)	0.2396	0.272	0.7296
T'_{do} (s)	6.00	5.89	8.96
T'_{qo} (s)	0.535	0.6	0.31

* Generator's per unit data are on its capacity base

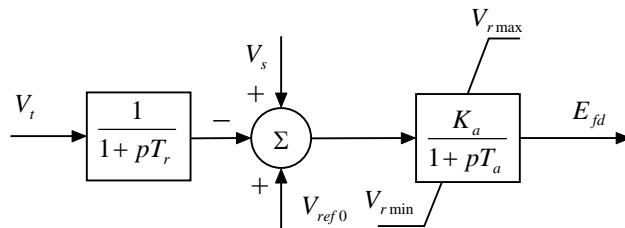


Figure C-1. Block diagram of static exciters in system I

Table C-4. Exciter parameters of system I

Parameter	Exciter		
	EXC1	EXC2	EXC3
K_a (pu)	100	100	100
T_a (s)	0.05	0.05	0.05
T_r (s)	0.02	0.02	0.02

C2 Eight-machine System (System II)

Table C-5. Bus data of system II

	Bus No.	P (p.u.)	Q (p.u.)	Curve No.	PV-Voltage	Curve No.
L1	2	2.870	1.440	1	-	-
L2	3	3.760	2.250	4	-	-
L3	4	2.270	2.690 (1.419)*	6	-	-
L4	8	5.000	2.300	2	-	-
L5	9	0.864 (1.324)*	0.662	5	-	-
L6	10	0.719	0.474	1	-	-
L7	11	0.700	0.500	1	-	-
L8	14	4.300 (3.225)*	2.200 (1.32)*	3	-	-
L9	15	5.200	2.500	2	-	-
L10*	1	1.200	0.800	1	-	-
G1	17	2.000	0.000	3	1.00	1
G2	18	1.600	0.000	5	1.02	32
G3	19	4.300	0.000	2	1.00 (1.03)*	1 (32)*
G4	20	2.250	0.000	2	1.00	1
G5	21	3.060	0.000	2	1.00	1
G6	22	6.000	0.000	30	1.01	33
G7	23	3.100	0.000	1	1.00	1
G8	24	0.000	0.000	-	1.00	31

(*) Data used in Chapter 4

Table C-6. Shunt capacitor of system II

Bus No.	G (p.u.)	B (p.u.)
7	0.000	-1/0.732
7	0.000	-1/0.732
8	0.000	1.0

Table C-7. Line data of system II

No.	From	To	Branch Number	R (p.u.)	X (p.u.)	B/2 (p.u.)	Transformer Ratio
1	1	24	1	0.0000	0.0150	0.0000	1.0750
2	1	2	2	0.2120	0.1480	0.0000	-
3	1	3	2	0.0294	0.2080	0.0000	-
4	2	4	1	0.0540	0.1900	0.1650	-
5	4	23	1	0.0000	0.0124	0.0000	1.0750
6	3	22	1	0.0000	0.0217	0.0000	1.0750
7	2	3	2	0.0068	0.0262	0	-
8	3	4	1	0.0559	0.2180	0.1954	-
9	4	10	1	0.0214	0.0859	0.3008	-
10	4	11	1	0.0150	0.0607	0.2198	-
11	6	1	1	0.0000	0.0180	0.0000	1.0250
12	6	7	2	0.0066	0.0686	0.93985	-
13	7	7	1	0.0000	0.7320	0.0000	-
14	7	7	1	0.0000	0.7320	0.0000	-
15	7	13	1	0.0000	0.0180	0.0000	1.0250
16	8	11	1	0.0037	0.1780	0.1640	-
17	13	9	1	0.0034	0.0200	0.0000	-
18	17	5	1	0.0000	0.0347	0.0000	-
19	8	5	1	0.0000	0.0010	0.0000	1.0270
20	16	5	1	0.0000	0.0100	0.0000	1.0270
21	7	16	2	0.0040	0.0500	0.6950	-
22	10	8	1	0.0165	0.0662	0.2353	-
23	11	9	1	0.0114	0.0370	0.0000	-
24	9	8	1	0.0578	0.2180	0.1887	-
25	14	8	1	0.0033	0.0333	0.0000	-
26	19	14	1	0.0000	0.0375	0.0000	1.0750
27	9	12	1	0.0196	0.0854	0.0810	-
28	15	8	2	0.0060	0.0260	0.0000	-
29	8	8	1	0.0000	-1.0000	0.0000	-
30	15	12	3	0.0090	0.1020	0.0550	-
31	12	20	1	0.0000	0.0438	0.0000	1.0250
32	9	18	1	0.0000	0.0640	0.0000	1.0250
33	12	21	1	0.0000	0.0328	0.0000	1.0250

Table C-8. Generator parameters of system II

Parameter	Machine							
	G1	G2	G3	G4	G5	G6	G7	G8
Capacity (MVA)	100.0	235.0	637.50	286.00	388.40	706.0	882.0	1880.0
H (pu)	2.620	3.336	3.075	3.846	4.196	2.124	4.507	3.745
D (pu)	0.0	0.0	0.0	0.0	0.0	0.0	0.0	0.0
r_a (pu)	0.0	0.0	0.0	0.0	0.0	0.0	0.0	0.0
x_l (pu)	0.0	0.0	0.0	0.0	0.0	0.0	0.0	0.0
x_d (pu)	1.6330	1.8100	1.9508	0.9046	0.7500	2.2663	1.2172	3.2148
x_q (pu)	1.6330	1.8100	1.9508	0.6401	0.6110	2.2663	0.5998	3.2148
x'_d (pu)	0.1970	0.2841	0.3060	0.3581	0.3061	0.2697	0.3493	3.2148
x'_q (pu)	1.6330	1.8100	1.9508	0.6401	0.6110	2.2663	0.5998	3.2148
x''_d (pu)	0.1480	0.1831	0.1983	0.2520	0.1961	0.1680	0.2496	3.2148
x''_q (pu)	0.1480	0.1831	0.1983	0.2520	0.1961	0.1680	0.2496	3.2148
T'_{d0} (s)	4.000	6.20	6.200	5.5300	5.9500	8.3750	7.2400	10.000
T'_{q0} (s)	9999.0	9999.0	9999.0	9999.0	9999.0	9999.0	9999.0	9999.0
T''_{d0} (s)	0.0600	0.1920	0.0500	0.0500	0.0500	0.2240	0.0500	0.1000
T''_{q0} (s)	0.2400	1.8900	0.5000	0.0500	0.0500	1.6600	0.2000	0.2000

* Generator's per unit data are on its capacity base

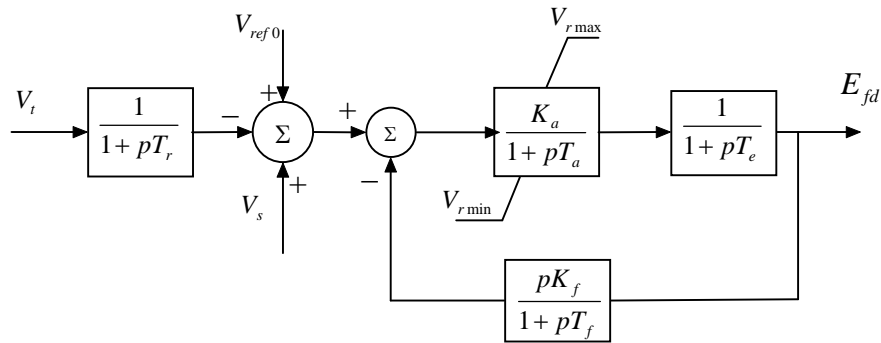


Figure C-2. Block diagram of IEEE-Type I exciter in system II

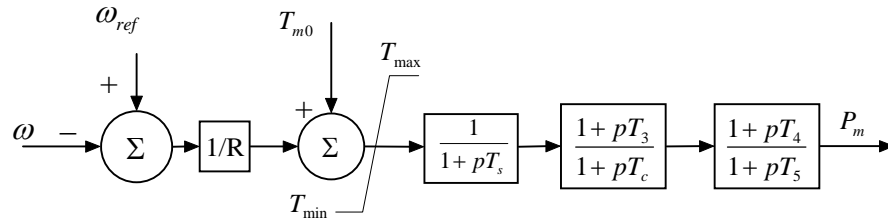


Figure C-3. Block diagram of speed-governor in system II

Table C-9. Exciter parameters of system II

Parameter	Exciter							
	EXC1	EXC2	EXC3	EXC4	EXC5	EXC6	EXC7	EXC8
K_a (pu)	50	50	50	20	20	50	50	50
T_a (s)	0.05	0.03	0.01	0.02	0.02	0.04	0.03	0.03
K_f (pu)	0.023	0.04	0.05	0.0	0.0	0.04	0.1	0.2
T_f (s)	0.8	0.715	0.715	0.0	0.0	0.715	0.715	0.715
T_e (s)	0.5	0.5	0.5	0.05	0.05	0.5	0.5	0.5
T_r (s)	0.03	0.03	0.03	0.03	0.03	0.03	0.03	0.03

Table C-10. Governor/turbine parameters of system II

Parameter	Governor/Turbine						
	GOV2	GOV3	GOV4	GOV5	GOV6	GOV7	GOV8
$1/R$ (pu)	20.00	20.00	25.00	25.00	20.00	25.00	20.00
T_{max} (pu)	3.53	9.56	4.29	5.83	10.60	13.20	28.20
T_s (s)	0.50	0.50	2.67	2.67	0.40	2.67	0.30
T_c (s)	0.20	0.20	11.70	11.70	0.20	11.70	0.05
T_3 (s)	0.00	0.00	5.00	5.00	0.00	5.00	0.00
T_4 (s)	1.00	1.00	-1.00	-1.00	1.00	-1.00	1.00
T_5 (s)	1.00	1.00	0.50	0.50	1.00	0.50	1.00

Table C-11. Typical daily operation curves [147, 161]

		hour of the day																							
		1	2	3	4	5	6	7	8	9	10	11	12	13	14	15	16	17	18	19	20	21	22	23	24
No.	1	1.00	1.00	1.00	1.00	1.00	1.00	1.00	1.00	1.00	1.00	1.00	1.00	1.00	1.00	1.00	1.00	1.00	1.00	1.00	1.00	1.00	1.00	1.00	1.00
	2	0.92	0.92	0.92	0.92	0.92	0.92	1.03	1.03	1.15	1.10	1.15	0.90	0.92	0.92	1.15	1.15	1.15	0.92	0.92	1.06	1.05	1.05	0.92	0.91
	3	0.62	0.62	0.61	0.61	0.61	0.91	0.91	0.91	1.08	1.37	1.67	0.60	0.60	0.91	1.21	1.67	1.67	1.67	0.76	1.21	1.21	0.93	0.91	0.75
	4	0.86	1.47	0.86	0.71	1.47	1.11	0.45	0.72	0.72	1.35	1.10	0.67	1.47	1.10	0.88	0.37	1.23	0.98	1.47	0.74	1.10	1.10	1.47	0.60
	5	1.47	1.19	1.09	0.52	0.52	0.95	1.30	1.30	0.65	0.65	0.26	0.26	1.35	1.43	1.56	1.56	1.43	1.43	0.26	0.52	0.52	1.30	1.30	1.18
	6	0.74	0.30	0.30	0.30	0.30	0.74	0.74	0.89	1.34	1.34	1.64	1.04	1.04	1.04	1.50	1.50	1.04	1.34	0.89	0.89	0.89	1.40	1.40	1.40
	7	0.53	0.11	0.11	0.11	0.11	0.36	0.79	0.79	2.15	2.38	1.85	1.06	0.53	1.59	1.86	1.85	1.08	1.38	1.32	1.06	1.06	0.79	0.79	0.34
	8	1.03	1.03	0.19	0.19	0.19	0.19	0.60	0.80	0.56	0.56	0.56	1.31	1.31	1.69	1.69	2.00	2.00	1.10	0.50	1.30	1.30	1.30	1.30	1.30
	9	1.07	0.53	0.18	0.18	0.18	0.53	0.53	1.07	1.07	2.14	1.74	0.53	0.89	1.07	0.89	0.53	0.55	1.60	1.60	1.07	2.14	1.42	1.41	1.08
	10	0.84	0.52	0.52	0.52	0.52	0.85	1.07	1.07	1.93	2.56	1.72	0.67	0.38	0.58	1.07	1.55	1.55	0.65	0.34	1.28	1.93	1.07	0.65	0.20
	11	0.52	0.52	0.26	0.26	0.15	0.36	1.29	1.80	0.54	0.52	2.32	0.26	0.26	0.71	1.29	2.32	0.26	0.26	1.29	2.58	2.58	1.80	1.29	0.56
	12	0.52	0.52	0.52	0.52	0.52	1.04	2.60	1.82	1.06	0.26	0.26	0.26	0.83	0.68	0.60	0.52	0.52	0.52	1.04	2.87	2.87	1.30	1.30	1.05
	13	0.41	0.34	0.57	0.50	0.34	0.54	0.81	1.01	0.68	1.51	1.85	1.49	1.49	1.14	1.34	1.24	0.81	1.01	1.17	1.17	1.68	1.51	0.85	0.54
	14	0.24	0.24	0.24	0.24	0.24	0.24	0.24	2.08	2.08	0.73	2.08	0.73	2.08	0.73	2.78	0.73	2.18	0.80	1.20	1.21	0.97	0.73	0.73	0.48
	15	0.67	0.67	0.67	0.67	0.67	0.67	0.67	1.33	1.33	1.33	1.33	1.33	1.33	1.33	0.67	0.67	1.33	1.33	1.33	1.33	1.33	1.33	0.67	0.67
	16	1.99	1.99	1.77	1.77	1.77	1.77	1.77	0.44	0.44	1.11	1.11	1.11	0.18	0.18	0.66	0.66	0.66	0.22	0.22	0.66	0.66	0.66	1.10	1.10
	17	0.36	0.36	0.36	0.36	0.36	0.36	0.36	0.36	0.70	1.96	1.60	1.60	1.24	1.40	1.60	1.96	1.96	1.60	1.60	0.71	0.71	0.89	0.89	0.90
	18	0.37	0.37	0.37	0.37	0.37	0.37	0.37	0.37	0.37	0.37	2.22	2.95	1.11	0.37	0.72	1.48	2.57	2.22	1.11	0.74	0.74	1.48	1.48	0.74
	19	0.19	0.19	0.19	0.19	0.29	1.94	1.94	1.94	0.04	0.04	0.04	0.04	1.97	1.97	1.97	1.97	1.97	1.97	1.99	0.79	0.79	0.79	0.39	0.39
	20	0.32	0.32	0.32	0.32	0.32	0.94	2.83	1.57	0.64	1.26	2.51	1.89	0.18	0.18	0.18	1.38	1.26	0.18	0.18	0.94	2.83	2.20	0.94	0.32
	21	0.21	0.21	0.21	0.21	0.21	0.82	1.23	0.41	0.82	2.26	2.26	0.41	0.41	1.23	2.26	2.26	2.26	1.23	0.41	1.02	1.64	1.42	0.41	0.21
	22	0.65	0.43	0.43	0.43	0.43	1.08	1.08	2.16	2.16	2.16	2.16	2.16	2.16	0.23	0.23	1.08	0.22	1.08	1.08	0.65	0.65	0.43	0.43	0.43
	23	0.23	0.23	0.23	0.23	0.23	0.91	0.91	1.36	1.36	2.70	2.70	0.40	0.05	0.45	1.58	2.49	1.81	0.68	0.68	1.36	1.36	0.91	0.91	0.23
	24	0.28	0.28	0.28	0.28	0.28	0.28	0.60	2.00	1.70	1.72	1.71	1.88	1.87	1.71	1.71	1.71	1.71	0.60	0.60	0.60	0.60	0.60	0.60	0.40
	25	0.37	0.37	0.37	0.37	0.37	0.37	0.37	0.37	0.37	1.48	1.48	2.95	2.95	0.37	0.37	0.37	0.48	1.95	2.95	0.37	0.84	1.89	1.85	0.37
	26	0.84	0.34	0.34	0.34	0.34	0.84	0.84	1.01	1.51	1.51	1.47	1.18	1.18	1.18	1.40	1.40	1.18	1.51	1.01	1.01	1.01	0.90	0.90	0.79
	27	0.67	0.62	0.62	0.67	0.70	0.77	1.03	1.13	1.24	1.24	1.19	1.03	1.13	1.13	1.08	1.13	1.13	1.03	0.98	1.03	1.24	1.29	1.08	0.82
	28	0.70	0.62	0.62	0.62	0.70	0.77	0.93	1.08	1.24	1.32	1.24	1.01	0.93	0.93	1.08	1.24	1.24	1.16	0.85	1.08	1.32	1.32	1.16	0.85
	29	0.79	0.79	0.68	0.56	0.68	0.68	0.79	1.01	1.35	1.46	1.24	0.79	0.68	0.68	1.24	1.35	1.35	1.24	0.79	0.90	1.46	1.35	1.13	1.01
	30	1.01	1.01	1.01	1.01	0.91	0.91	1.01	0.91	1.01	1.01	1.01	0.81	0.91	1.01	1.01	0.91	1.01	1.01	0.91	1.01	1.03	1.03	1.01	0.91
	31	1.01	1.01	1.02	1.02	1.02	1.02	1.01	1.00	1.00	0.99	0.98	0.98	0.99	1.00	1.00	0.99	0.99	0.98	0.99	1.00	1.00	1.00	1.00	0.99
	32	1.03	1.02	1.03	1.02	1.01	1.02	1.02	1.01	0.99	0.97	0.95	1.00	1.01	1.02	0.99	0.97	0.97	0.98	0.99	0.99	0.99	1.00	1.01	1.02
	33	1.04	1.02	1.03	1.04	1.01	1.00	1.03	1.02	1.02	0.97	0.98	1.00	0.98	0.99	1.00	1.02	0.98	1.00	0.97	1.01	1.00	0.99	0.98	1.03

REFERENCES

1. Abdel-Magid Y.L. and Abido M.A., "Optimal multiobjective design of robust power system stabilizers using genetic algorithms", *IEEE Transactions on Power Systems*, vol. 18, no. 3, pp. 1125-1132, Aug. 2003
2. Abdel-Magid Y.L., Abido M.A., and Mantaway A.H., "Robust tuning of power system stabilizers in multimachine power systems", *IEEE Transactions on Power Systems*, vol. 15, no. 2, pp. 735-740, May 2000
3. Abido M.A., "Robust design of multimachine power system stabilizers using simulated annealing", *IEEE Transactions on Energy Conversion*, vol. 15, no. 3, pp. 297-304, Sept. 2000
4. Abido M.A., "Optimal design of power-system stabilizers using particle swarm optimization", *IEEE Transactions on Energy Conversion*, vol. 17, no. 3, pp. 406-413, Sept. 2002
5. Abido M.A. and Abdel-Magid Y.L., "Optimal design of power system stabilizers using evolutionary programming", *IEEE Transactions on Energy Conversion*, vol. 17, no. 4, pp. 429-436, Dec. 2002
6. Aboulela M.E., Sallam A.A., McCalley J.D., and Fouad A.A., "Damping controller design for power system oscillations using global signals", *IEEE Transactions on Power Systems*, vol. 11, no. 2, pp. 767-773, May 1996

7. AlRashidi M.R. and El-Hawary M.E., "A survey of particle swarm optimization applications in electric power systems", *IEEE Transactions on Evolutionary Computation*, accepted for future publication, 2008
8. Alves J.E.R., Pilotto L.A.S., and Watanabe E.H., "An adaptive digital controller applied to HVDC transmission", *IEEE Transactions on Power Delivery*, vol. 8, no. 4, pp. 1851-1859, Oct. 1993
9. Andersson G., Donalek P., Farmer R., Hatziargyriou N., Kamwa I., Kundur P., Martins N., Paserba J., Pourbeik P., Sanchez-Gasca J., Schulz R., Stankovic A., Taylor C., and Vittal V., "Causes of the 2003 major grid blackouts in north America and Europe, and recommended means to improve system dynamic performance", *IEEE Transactions on Power Systems*, vol. 20, no. 4, pp. 1922-1928, Nov. 2005
10. Bäck T., *Evolutionary Algorithms in Theory and Practice: Evolution Strategies, Evolutionary Programming, Genetic Algorithms*, Oxford University Press, 1996
11. Basler M.J. and Schaefer R.C., "Understanding power system stability", in *Proceedings of the Conference Record of Annual Pulp and Paper Industry Technical Conference 2007*, Williamsburg, VA, USA, June 2007, pp. 37-47
12. Berube G.R., Hajagos L.M., and Beaulieu R., "Practical utility experience with application of power system stabilizers", in *Proceedings of the IEEE Power Engineering Society Summer Meeting*, vol. 1, Alberta, Canada, July 1999, pp. 104-109

13. Bian X.Y., "Probabilistic Robust Damping Controller Designs for FACTS Devices and PSS," The Hong Kong Polytechnic University, Hong Kong, China, 2006
14. Bomfim A.L.B. Do, Taranto G.N., and Falcao D.M., "Simultaneous tuning of power system damping controllers using genetic algorithms", *IEEE Transactions on Power Systems*, vol. 15, no. 1, pp. 163-169, Feb. 2000
15. Brandwajn V., Kumar A.B.R., Ipakchi A., Bose A., and Kuo S.D., "Severity indices for contingency screening in dynamic security assessment", *IEEE Transactions on Power Systems*, vol. 12, no. 3, pp. 1136-1142, Aug. 1997
16. Brucoli M., Torelli F., and Trovato M., "Probabilistic approach for power system dynamic stability studies", *IEE Proceedings-Generation, Transmission & Distribution*, vol. 128, no. 5, pp. 295-301, Sept. 1981
17. Burchett R.C. and Heydt G.T., "Probabilistic methods for power system dynamic stability studies", *IEEE Transactions on Power Apparatus and Systems*, vol. PAS-97, no. 3, pp. 695-702, May 1978
18. Burchett R.C. and Heydt G.T., "A generalized method for stochastic analysis of the dynamic stability of electric power system", in *Proceedings of the IEEE Power Engineering Society Summer Meeting*, 1978 (A78528)
19. Cai L.J. and Erlich I., "Simultaneous coordinated tuning of PSS and FACTS damping controllers in large power systems", *IEEE Transactions on Power Systems*, vol. 20, no. 1, pp. 294-300, Feb. 2005

20. Chaturvedi D.K. and Malik O.P., "Generalized neuron-based adaptive PSS for multimachine environment", *IEEE Transactions on Power Systems*, vol. 20, no. 1, pp. 358-366, Feb. 2005
21. Chaturvedi D.K., Malik O.P., and Kalra P.K., "Experimental studies with a generalized neuron-based power system stabilizer", *IEEE Transactions on Power Systems*, vol. 19, no. 3, pp. 1445-1453, Aug. 2004
22. Chaudhuri B., Majumder R., and Pal B.C., "Wide-area measurement-based stabilizing control of power system considering signal transmission delay", *IEEE Transactions on Power Systems*, vol. 19, no. 4, pp. 1971-1979, Nov. 2004
23. Chen C.L. and Hsu Y.Y., "Coordinated synthesis of multimachine power system stabilizer using an efficient decentralized modal control (DMC) algorithm", *IEEE Transactions on Power Systems*, vol. 2, no. 3, pp. 543-551, Aug. 1987
24. Chen G.P., Malik O.P., Hope G.S., Qin Y.H., and Xu G.Y., "An adaptive power-system stabilizer based on the self-optimizing pole shifting control strategy", *IEEE Transactions on Energy Conversion*, vol. 8, no. 4, pp. 639-645, Dec. 1993
25. Chen H. and Wang X., "Cooperative coevolutionary algorithm for unit commitment", *IEEE Transactions on Power Systems*, vol. 17, no. 1, pp. 128-133, Feb. 2002
26. Chen H., Wong K.P., Nguyen D.H.M., and Chung C.Y., "Analyzing oligopolistic electricity market using coevolutionary computation", *IEEE Transactions on Power Systems*, vol. 21, no. 1, pp. 143-152, Feb. 2006

27. Chow J.H. and Cheung K.W., "A toolbox for power system dynamics and control engineering education and research", *IEEE Transactions on Power Systems*, vol. 7, no. 4, pp. 1559-1564, Nov. 1992
28. Chow J.H. and Sanchez-Gasca J.J., "Pole-placement designs of power system stabilizers", *IEEE Transactions on Power Systems*, vol. 4, no. 1, pp. 271 -277, Feb. 1989
29. Chow J.H., Sanchez-Gasca J.J., Ren H., and Wang S., "Power system damping controller design-using multiple input signals", *IEEE Control Systems Magazine*, vol. 20, no. 4, pp. 82-90, Aug. 2000
30. Chung C.Y., Tse C.T., David A.K., and Rad A.B., "Partial pole placement of H_{∞} -based PSS design using numerator denominator perturbation representation", *IEE Proceedings-Generation, Transmission & Distribution*, vol. 148, pp. 413-419, Sept. 2001
31. Chung C.Y., Wang K.W., Cheung C.K., Tse C.T., and David A.K., "Machine and load modeling in large scale power industries", in *Proceedings of the Dynamic Modeling Control Applications for industry workshop*, IEEE Industry Applications Society, Apr. 1998, pp. 7-15
32. Chung C.Y., Wang K.W., Tse C.T., Bian X.Y., and David A.K., "Probabilistic eigenvalue sensitivity analysis and PSS design in multimachine systems", *IEEE Transactions on Power Systems*, vol. 18, no. 4, pp. 1439-1445, Nov. 2003
33. Chung C.Y., Wang K.W., Tse C.T., and Niu R., "Power system stabilizer (PSS) design by probabilistic sensitivity indexes (PSIs)", *IEEE Transactions on Power Systems*, vol. 17, no. 3, pp. 688-693, Aug. 2002

34. Chung C.Y., Wang L., Howell F., and Kundur P., "Generation rescheduling methods to improve power transfer capability constrained by small-signal stability ", *IEEE Transactions on Power Systems*, vol. 19, no. 1, pp. 524-530, Feb. 2004
35. CIGRE Task Force 38.01.07, "Analysis and Control of Power System Oscillations", 1996
36. CIGRE Task Force 38.02.16, "Impact of Interactions among power system controls", The CIGRE Brochure 166, 2000
37. Clerc M., "The swarm and the queen: towards a deterministic and adaptive particle swarm optimization", in *Proceedings of the IEEE Congress on Evolutionary Computation*, 1999, pp. 1951-1957
38. Clerc M., *Particle Swarm Optimization*, ISTE, 2006
39. Clerc M., "Stagnation analysis in particle swarm optimisation or what happens when nothing happens", <http://hal.archives-ouvertes.fr/hal-00122031>, accessed Nov. 2007
40. Clerc M., "Swissknife PSO: C source code", <http://clerc.maurice.free.fr/ps/>, accessed Nov. 2007
41. Czuba J.S., Hannett L.N., and Willis J.R., "Implementation of power system stabilizer at the Ludington pumped-storage plant", *IEEE Transactions on Power Systems*, vol. 1, no. 1, pp. 121-128, Feb. 1986

42. Demello F.P. and Concordia C., "Concepts of synchronous machine stability as affected by excitation control", *IEEE Transactions on Power Apparatus and Systems*, vol. PAS-88, no. 4, pp. 316-329, Apr. 1969
43. Duch W., "What is Computational Intelligence and where is it going?," in *Challenges for Computational Intelligence*, Duch W. and Mandziuk J. (Eds.), Springer, 2007, pp. 1-13.
44. Duran H., "A recursive approach to the cumulant method of calculating reliability and production cost", *IEEE Transactions on Power Apparatus and Systems*, vol. PAS-104, no. 1, pp. 82-90, Jan. 1985
45. Eberhart R. and Shi Y., "Particle swarm optimization: developments, applications and resources", in *Proceedings of the IEEE Congress on Evolutionary Computation 2001*, Seoul, Korea, 2001, pp. 81-86
46. Ejebe G.C., Irisarri G.D., Mokhtari S., Obadina O., Ristanovic P., and Tong J., "Methods for contingency screening and ranking for voltage stability analysis of power systems", *IEEE Transactions on Power Systems*, vol. 11, no. 1, pp. 350-356, Feb. 1996
47. Electric Power Research Institute of China, "Power system analysis software package (PSASP) manual" (in Chinese), 1993
48. Eliasson B.E., Hill D.J., Rudnick H., Andersson G., and Smed T., "Damping structure and sensitivity in the Nordel power system", *IEEE Transactions on Power Systems*, vol. 7, no. 1, pp. 97-105, Feb. 1992

49. ElMetwally K.A., Hancock G.C., and Malik O.P., "Implementation of a fuzzy logic PSS using a micro-controller and experimental test results", *IEEE Transactions on Energy Conversion*, vol. 11, no. 1, pp. 91-96, Mar. 1996
50. Eshelman L.J. and Schaffer J.D., "Real-coded genetic algorithms and interval-schemata," in *Foundations of Genetic Algorithms 2*, Whitley D.L. (Eds.), CA, Morgan Kaufman Publishers, 1993, pp. 187-202.
51. Fang S.L. and Zhu F., *Theory and applications of power system stabilizers* (in Chinese), Beijing: Electric Power Press, 1996
52. Feliachi A., "Optimal siting of power system stabilisers", *IEE Proceedings-Generation, Transmission & Distribution*, vol. 137, no. 2, pp. 101-106, Mar. 1990
53. Ferraz J.C.R., Martins N., and Taranto G.N., "Coordinated Stabilizer Tuning in Large Power Systems Considering Multiple Operating Conditions", in *Proceedings of the IEEE Power Engineering Society General Meeting*, Tamper, FL, USA, June 2007, pp. 1-8
54. Fogel D.B., *Evolutionary Computation: Toward a New Philosophy of Machine Intelligence*, New York: IEEE Press, 2000
55. Folly K.A., Yorino N., and Sasaki H., "Design of H_{∞} -PSS using numerator-denominator uncertainty representation", *IEEE Transactions on Energy Conversion*, vol. 12, no. 1, pp. 45-50, Mar. 1997

56. Fraile-Ardanuy J. and Zufiria P.J., "Design and comparison of adaptive power system stabilizers based on neural fuzzy networks and genetic algorithms", *Neurocomputing*, vol. 70, pp. 2902-2912, Oct. 2007
57. Gerbex S., Cherkaoui R., and Germond A.J., "Optimal location of multi-type FACTS devices in a power system by means of genetic algorithms ", *IEEE Transactions on Power Systems*, vol. 16, no. 3, pp. 537-544, Aug. 2001
58. Gerin-Lajoie L., Lefebvre D., Racine M., Soulieres L., and Kamwa I., "Hydro-Quebec experience with PSS tuning", in *Proceedings of the IEEE Power Engineering Society Summer Meeting*, vol. 1, Alberta, Canada, July 1999, pp. 88-95
59. Gibbard M.J., "Co-ordinated design of multimachine system stabilisers based on damping torque concepts", *IEE Proceedings-Generation, Transmission & Distribution*, vol. 135, no. 4, pp. 276-284, July 1988
60. Gibbard M.J., "Robust design of fixed-parameter power system stabilizers over a wide range of operating conditions", *IEEE Transactions on Power Systems*, vol. 6, no. 2, pp. 794-800, May 1991
61. Goldberg D.E., *Genetic Algorithms in Search, Optimization, and Machine Learning*, Mass.: Addison-Wesley, 1989
62. Hamdan A.M., "An investigation of the significance of singular value decomposition in power system dynamics", *International Journal of Electrical Power and Energy Systems*, vol. 21, no. 6, pp. 417-424, 1999

63. Hasanovic A., Feliachi A., Bhatt N.B., and DeGroff A.G., "Practical robust PSS design through identification of low-order transfer functions", *IEEE Transactions on Power Systems*, vol. 19, no. 3, pp. 1492-1500, Aug. 2004
64. Haupt R.L. and Haupt S.E., *Practical Genetic Algorithms*, New York: John Wiley & Sons, 1998
65. Hiyama T., "Coherency-based identification of optimum site for stabilizer applications", *IEE Proceedings-Generation, Transmission & Distribution*, vol. 130, no. 2, pp. 71-74, 1983
66. Hiyama T., "Rule-based stabilizer for multimachine power system", *IEEE Transactions on Power Systems*, vol. 5, no. 2, pp. 403-409, May 1990
67. Hiyama T., "Robustness of fuzzy logic power system stabilizers applied to multimachine power system", *IEEE Transactions on Energy Conversion*, vol. 9, no. 3, pp. 451-459, Sept. 1994
68. Holland J. H., *Adaptation in Natural and Artificial Systems*, Michigan: The University of Michigan Press, 1975
69. Hsu Y.Y. and Chen C.L., "Identification of optimum location for stabiliser applications using participation factors", *IEE Proceedings-Generation, Transmission & Distribution*, vol. 134, no. 3, pp. 238-244, 1987
70. Hughes F.M., Anaya-Lara O., Jenkins N., and Strbac G., "Control of DFIG-based wind generation for power network support", *IEEE Transactions on Power Systems*, vol. 20, no. 4, pp. 1958-1966, Nov. 2005

71. Hughes F.M., Anaya-Lara O., Jenkins N., and Strbac G., "A power system stabilizer for DFIG-based wind generation", *IEEE Transactions on Power Systems*, vol. 21, no. 2, pp. 763-772, May 2006
72. IEEE/CIGRE joint task force on stability terms and definitions, "Definition and classification of power system stability", *IEEE Transactions on Power Systems*, vol. 19, no. 3, pp. 1387-1401, Aug. 2004
73. IEEE Tutorial Course, *Power System Stabilization via Excitation Control*, 81 EHO 175-0 PWR, 1981
74. IEEE Tutorial Course, *Power System Stabilization via Excitation Control*, 07TP185, 2007
75. Kamwa I., Grondin R., and Hebert Y., "Wide-area measurement based stabilizing control of large power systems - A decentralized/hierarchical approach", *IEEE Transactions on Power Systems*, vol. 16, no. 1, pp. 136-153, Feb. 2001
76. Kamwa I., Trudel G., and Gerin-Lajoie L., "Robust design and coordination of multiple damping controllers using nonlinear constrained optimization", *IEEE Transactions on Power Systems*, vol. 15, no. 3, pp. 1084-1092, Aug. 2000
77. Karimpour A., Asgharian R., and Malik O. P., "Relative gain array and singular value decomposition in determination of PSS location", *European Transactions on Electrical Power*, vol. 15, no. 5, pp. 397-412, Sept. 2005

78. Kennedy J. and Eberhart R., "Particle Swam Optimization", in *Proceedings of the IEEE International Conference on Neural Networks*, vol. 4, Piscataway, NJ: IEEE Service Center, 1995, pp. 1942-1948
79. Kennedy J., Eberhart R., and Shi Y., *Swarm Intelligence*, CA: Morgan Kaufmann Publishers, 2001
80. Khaldi M.R., Sarkar A.K., Lee K.Y., and Park Y.M., "The modal performance measure for parameter optimization of power system stabilizers", *IEEE Transactions on Energy Conversion*, vol. 8, no. 4, pp. 660-666, Dec. 1993
81. Klein M., Le L.X., Rogers G.J., Farrokhpay S., and Balu N.J., "H_∞ damping controller design in large power systems", *IEEE Transactions on Power Systems*, vol. 10, no. 1, pp. 158-166, Feb. 1995
82. Klein M., Rogers G.J., and Kundur P., "A fundamental study of inter-area oscillations in power systems ", *IEEE Transactions on Power Systems*, vol. 6, no. 3, pp. 914-921, Aug. 1991
83. Kosterev D.N., Taylor C.W., and Mittelstadt W.A., "Model validation for the August 10, 1996 WSCC system outage", *IEEE Transactions on Power Systems*, vol. 14, no. 3, pp. 967-979, Aug. 1999
84. Kumar B.K., Singh S.N., and Srivastava S.C., "Placement of FACTS controllers using modal controllability indices to damp out power system oscillations", *IET Proceedings on Generation, Transmission & Distribution*, vol. 1, no. 2, pp. 209-217, Mar. 2007
85. Kundur P., *Power System Stability and Control*, New York: McGraw-Hill, 1994

86. Kundur P., "Effective use of power system stabilizers for enhancement of power system reliability", in *Proceedings of the IEEE Power Engineering Society Summer Meeting*, vol. 1, Alberta, Canada, July 1999, pp. 96-103
87. Kundur P., "Power System Stability," in *Power System Stability and Control, Electric Power Engineering Handbook Series*, Grigsby L. L. (Eds.), Boca Raton, FL, CRC Press, 2007.
88. Kundur P., Klein M., Rogers G.J., and Zywno M.S., "Application of power system stabilizers for enhancement of overall system stability", *IEEE Transactions on Power Systems*, vol. 4, no. 2, pp. 614-626, May 1989
89. Lampinen J. and Storn R., "Differential Evolution," in *New Optimization Techniques in Engineering*, Onwubolu G. and Babu B. (Eds.), Springer-Verlag, 2004.
90. Larsen E.V., Sanchez-Gasca J.J., and Chow J.H., "Concepts for design of FACTS controllers to damp power swings", *IEEE Transactions on Power Systems*, vol. 10, no. 2, pp. 948-956, May 1995
91. Larsen E.V. and Swann D.A., "Applying power system stabilizers, Part I: General concepts. Part II: Performance objectives and tuning concepts. Part III: Practical considerations", *IEEE Transactions on Power Apparatus and Systems*, vol. PAS-100, no. 6, pp. 3017-3046, June 1981
92. Lei X., Lerch E.N., and Povh D., "Optimization and coordination of damping controls for improving system dynamic performance", *IEEE Transactions on Power Systems*, vol. 16, no. 3, pp. 473-480, Aug. 2001

93. Liang C.H., Chung C.Y., Wong K.P., and Duan X.Z., "Parallel optimal reactive power flow based on cooperative co-evolutionary differential evolution and power system decomposition", *IEEE Transactions on Power Systems*, vol. 22, no. 1, pp. 249-257, Feb. 2007
94. Lim C.M. and Elangovan S., "A new stabiliser design technique for multimachine power systems", *IEEE Transactions on Power Apparatus and Systems*, vol. PAS-104, no. 9, pp. 2393-2400, Sept. 1985
95. Liu S., Messina A.R., and Vittal V., "Assessing placement of controllers and nonlinear behavior using normal form analysis", *IEEE Transactions on Power Systems*, vol. 20, no. 3, pp. 1486-1495, Aug. 2005
96. Liu S., Messina A.R., and Vittal V., "A normal form analysis approach to siting power system stabilizers (PSSs) and assessing power system nonlinear behavior", *IEEE Transactions on Power Systems*, vol. 21, no. 4, pp. 1755-1762, Nov. 2006
97. Loparo K. and Blankenship G., "A probabilistic mechanism for dynamic instabilities in electric power systems", in *Proceedings of the IEEE Power Engineering Society Winter Meeting*, New York, Feb. 1979 (A79053-0)
98. Lu J., Chiang H.-D., and Thorp J.S., "Identification of optimum sites for power system stabilizer applications", *IEEE Transactions on Power Systems*, vol. 5, no. 4, pp. 1302-1308, Nov. 1990
99. Majumder R., Chaudhuri B., and Pal B.C., "Implementation and test results of a wide-area measurement-based controller for damping interarea oscillations considering signal-transmission delay", *IET Proceedings-Generation Transmission & Distribution*, vol. 1, no. 1, pp. 1-7, Jan. 2007

100. Malik O.P., Mao C.X., Prakash K.S., Hope G.S., and Hancock G.C., "Tests with a microcomputer based adaptive synchronous machine stabilizer on a 400MW thermal unit", *IEEE Transactions on Energy Conversion*, vol. 8, no. 1, pp. 6-12, Mar. 1993
101. Margotin T. and Bourles H., "EDF experience with coordinated AVR+PSS tuning", in *Proceedings of the IEEE Power Engineering Society Summer Meeting*, vol. 1, Alberta, Canada, July 1999, pp. 47-52
102. Marler R.T. and Arora J.S., "Survey of multi-objective optimization methods for engineering", *Structural and Multidisciplinary Optimization*, vol. 26, no. 6, pp. 369-395, Mar. 2004
103. Martins N., Barbosa A.A., Ferraz J.C.R., and etc., "Retuning stabilizers for the north-south Brazilian interconnection", in *Proceedings of the IEEE Power Engineering Society Summer Meeting*, vol. 1, Alberta, Canada, July 1999, pp. 58-67
104. Martins N. and Lima L.T.G., "Determination of suitable locations for power system stabilizers and static VAR compensators for damping electromechanical oscillations in large power systems", *IEEE Transactions on Power Systems*, vol. 5, no. 4, pp. 1455-1463, Nov. 1990
105. Maslennikov V.A. and Ustinov S.M., "The optimization method for coordinated tuning of power system regulators", in *Proceedings of the 12th Power System Computation Conference*, Dresden, Germany, Aug. 1996, pp. 70-75

106. Maslennikov V.A. and Ustinov S.M., "Method and software for coordinated tuning of power system regulators", *IEEE Transactions on Power Systems*, vol. 12, no. 4, pp. 1419 -1424, Nov. 1997
107. Michalewicz Z., *Genetic Algorithms + Data Structures = Evolution Programs*, Springer, 1996
108. Mithulananthan N., Canizares C.A., Reeve J., and Rogers G.J., "Comparison of PSS, SVC, and STATCOM controllers for damping power system oscillations", *IEEE Transactions on Power Systems*, vol. 18, no. 2, pp. 786-792, May 2003
109. Nambu M. and Ohsawa Y., "Development of an advanced power system stabilizer using a strict linearization approach", *IEEE Transactions on Power Systems*, vol. 11, no. 2, pp. 813-818, May 1996
110. Nomikos B.M. and Vournas C.D., "Investigation of induction machine contribution to power system oscillations", *IEEE Transactions on Power Systems*, vol. 20, no. 2, pp. 916-925, May 2005
111. Onwubolu G.C. and Babu B.V., "Introduction," in *New Optimization Techniques in Engineering*, Onwubolu G. and Babu B. (Eds.), Springer-Verlag, 2004
112. Ostojic D.R., "Identification of optimum site for power system stabiliser applications", *IEE Proceedings-Generation, Transmission & Distribution*, vol. 135, no. 5, pp. 416-419, Sept. 1988
113. Ostojic D.R., "Stabilization of multimodal electromechanical oscillations by coordinated application of power system stabilizers", *IEEE Transactions on Power Systems*, vol. 6, no. 4, pp. 1439-1445, Nov. 1991

114. Pagola F.L., Ignacio J.P., and Verghese G.C., "On sensitivities, residues and participations, applications to oscillatory stability analysis and control", *IEEE Transactions on Power Systems*, vol. 4, no. 1, pp. 278-285, Feb. 1989
115. Pai M.A., Sen Gupta D.P., and Padiyar K.R., *Small Signal Analysis of Power Systems* UK: Apha Science, 2004
116. Paiva P.M., Soares J.M., Zeni N., Jr., and Pons F.H., "Extensive PSS use in large systems: the Argentinean case", in *Proceedings of the IEEE Power Engineering Society Summer Meeting*, vol. 1, Alberta, Canada, July 1999, pp. 68-75
117. Particle Swarm Central, <http://www.particleswarm.info/>, accessed Dec. 2007
118. Particle Swarm Optimization, <http://www.swarmintelligence.org/>, accessed Dec. 2007
119. Pérez-Arriaga I.J., Verghese G.C., and Schweppe F.C., "Selective modal analysis with applications to electric power systems, Part I: Heuristic introduction. Part II: The dynamic stability problem ", *IEEE Transactions on Power Apparatus and Systems*, vol. PAS-101, pp. 3117-3134, Sept. 1982
120. Pourbeik P. and Gibbard M.J., "Damping and synchronizing torques induced on generators by FACTS stabilizers in multimachine power systems", *IEEE Transactions on Power Systems*, vol. 11, no. 4, pp. 1920-1925, Nov. 1996
121. Pourbeik P. and Gibbard M.J., "Simultaneous coordination of power system stabilizers and FACTS device stabilizers in a multimachine power system for enhancing dynamic performance", *IEEE Transactions on Power Systems*, vol. 13, no. 2, pp. 473-479, May 1998

122. Price K.V., "Differential evolution: a fast and simple numerical optimizer ", in *Proceedings of the 1996 Biennial Conference of the North American Fuzzy Information Processing Society (NAFIPS 1996)*, Fuzzy Information Processing Society, June 1996, pp. 524-527
123. Price K.V., "An Introduction to Differential Evolution," in *New Ideas in Optimization*, Corne D., Dorigo M., and Glover F. (Eds.), UK, Mc Graw-Hill, 1999, pp. 79-108
124. Price K.V., Storn R.M., and Lampinen J.A., *Differential Evolution - A Practical Approach to Global Optimization*, Springer, 2005
125. Rogers G., *Power System Oscillations*, Norwell, MA: Kluwer, 2000
126. Samarasinghe V.G.D.C. and Pahalawaththa N.C., "Damping of multimodal oscillations in power systems using variable structure control techniques", *IEE Proceedings-Generation Transmission & Distribution*, vol. 144, no. 3, pp. 323-331, May 1997
127. Sanchez-Gasca J.J., Vittal V., Gibbard M.J., Messina A.R., Vowles D.J., Liu S., and Annakkage U.D., "Inclusion of higher order terms for small-signal (modal) analysis: committee report-task force on assessing the need to include higher order terms for small-signal (modal) analysis", *IEEE Transactions on Power Systems*, vol. 20, no. 4, pp. 1886-1904, Nov. 2005
128. Sauer P.W. and Pai M.A., *Power System Dynamics and Stability*, New Jersey: Prentice Hall, 1998

129. Schulz R.P., "Synchronous machine modeling", in *Proceedings of the IEEE Symposium on Adequacy and Philosophy of Modeling: System Dynamic Performance*, San Francisco, July 1972, pp. 24-28
130. Segal R., Kothari M.L., and Madnani S., "Radial basis function (RBF) network adaptive power system stabilizer", *IEEE Transactions on Power Systems*, vol. 15, no. 2, pp. 722-727, May 2000
131. Shi Y. and Eberhart R., "A modified particle swarm optimizer", in *Proceedings of the 1998 IEEE International Conference on Evolutionary Computation*, Piscataway, NJ, 1998, pp. 69-73
132. Simoes Costa A.J.A., Freitas F.D., and e Silva A.S., "Design of decentralized controllers for large power systems considering sparsity", *IEEE Transactions on Power Systems*, vol. 12, no. 1, pp. 144-152, Feb. 1997
133. Skogestad S. and Postlethwaite I., *Multivariable Feedback Control: Analysis and Design*, John Wiley, 2005
134. Stankovic A.M. and Lesieutre B.C., "A probabilistic approach to aggregate induction machine modeling", *IEEE Transactions on Power Systems*, vol. 11, no. 4, pp. 1983-1989, Nov. 1996
135. Storn R., "Designing Digital Filters with Differential Evolution," in *New Ideas in Optimization*, Corne D., Dorigo M., and Glover F. (Eds.), UK: Mc Graw-Hill, 1999, pp. 109-125.

136. Storn R. and Price K., "Differential evolution- a simple and efficient heuristic for global optimization over continuous spaces", *Journal of Global Optimization*, vol. 11, pp. 341-359, 1997
137. Taranto G.N., Chow J.H., and Othman H.A., "Robust redesign of power system damping controllers", *IEEE Transactions on Control Systems Technology*, vol. 3, no. 3, pp. 290-298, Sept. 1995
138. Trudnowski D.J., Smith J.R., Short T.A., and Pierre D.A., "An application of Prony methods in PSS design for multimachine systems", *IEEE Transactions on Power Systems*, vol. 6, no. 1, pp. 118-126, Feb. 1991
139. Tse C.T. and Tso S.K., "Approach of the study of small-perturbation stability of multimachine systems", *IEE Proceedings-Generation, Transmission & Distribution*, vol. 135, no. 5, pp. 396-405, Sept. 1988
140. Tse C.T. and Tso S.K., "Design optimisation of power system stabilisers based on modal and eigenvalue-sensitivity analyses", *IEE Proceedings-Generation, Transmission & Distribution*, vol. 135, no. 5, pp. 406-415, Sept. 1988
141. Tse C.T. and Tso S.K., "Refinement of conventional PSS design in multi-machine system by modal analysis", *IEEE Transactions on Power Systems*, vol. 8, no. 2, pp. 598-605, May 1993
142. Tse C.T., Wang K.W., Chung C.Y., and Tsang K.M., "Parameter optimization of robust power system stabilizers by probabilistic approach", *IEE Proceedings-Generation, Transmission & Distribution*, vol. 147, no. 2, pp. 69-75, Mar. 2000

143. Vassell G.S., "Northeast Blackout of 1965", *IEEE Power Engineering Review*, vol. 11, no. 1, pp. 4-8, Jan. 1991
144. Vournas C.D. and Papadias B.C., "Power system stabilization via parameters optimization application to the Hellenic interconnected system", *IEEE Transactions on Power Systems*, vol. 2, no. 3, pp. 615-622, Aug. 1987
145. Wang H.F., "On the connections among the electric torque, residue, functional sensitivity, participation and partial multi-modal decomposition", in *Proceedings of the UKACC International Conference on Control '98*, vol. 2, UK, Sept. 1998, pp. 1005-1010
146. Wang H.F., Swift F.J., and Li M., "Indices for selecting the best location of PSSs or FACTS-based stabilisers in multimachine power systems: A comparative study", *IEE Proceedings-Generation Transmission and Distribution*, vol. 144, no. 2, pp. 155-159, Mar. 1997
147. Wang K.W., "Robust PSS Design Based on Probabilistic Approach," Ph. D dissertation, The Hong Kong Polytechnic University, Hong Kong, China, 2000
148. Wang K.W., Chung C.Y., Tse C.T., and Tsang K.M., "Multimachine eigenvalue sensitivities of power system parameters", *IEEE Transactions on Power Systems*, vol. 15, no. 2, pp. 741-747, May 2000
149. Wang K.W., Chung C.Y., Tse C.T., and Tsang K.M., "Probabilistic eigenvalue sensitivity indices for robust PSS site selection", *IEE Proceedings-Generation, Transmission & Distribution*, vol. 148, no. 6, pp. 603-609, Nov. 2001

150. Wang K.W., Tse C.T., and Tsang K.M., "Algorithm for power system dynamic studies taking account the variation of load powers", *Electric Power Systems Research*, vol. 46, pp. 221-227, Aug. 1998
151. Wang L., Howell F., Kundur P., Chung C.Y., and Xu W., "A tool for small-signal security assessment of power systems", in *Proceedings of the International Conference on Power Industry Computer Applications*, Sydney, Australia, May 2001, pp. 246-252
152. Wang X.F. and Wang X.L., "Power system probabilistic load flow analysis", *The Journal of Xi'an Jiaotong University* (in Chinese), vol. 22, no. 3, pp. 87-97, 1988
153. Wolpert D.H. and Macready W.G., "No free lunch theorems for optimization", *IEEE Transactions on Evolutionary Computation*, vol. 1, no. 1, pp. 67-82, Apr. 1997
154. Wong K.P. and Li A., "Virtual population and acceleration techniques for evolutionary power flow calculation in power systems," invited paper in *Evolutionary Optimization*, Sarker R., Mohammadian M., and Yao X. (Eds.), Boston, Kluwer Academic Publishers, 2002, pp. 329-345.
155. Wu F.F. and Fu S., "China's future in electric energy", *IEEE Power and Energy Magazine*, vol. 3, no. 4, pp. 32-38, July 2005
156. Wu H.X., Tsakalis K.S., and Heydt G.T., "Evaluation of time delay effects to wide-area power system stabilizer design", *IEEE Transactions on Power Systems*, vol. 19, no. 4, pp. 1935-1941, Nov. 2004

157. Xiao Y., Song Y.H., Liu C.C, and Sun Y.Z., "Available transfer capability enhancement using FACTS devices", *IEEE Transactions on Power Systems*, vol. 18, no. 1, pp. 305-312, Feb. 2003
158. Xu L. and Ahmedzaid S., "Tuning of power system controllers using symbolic eigensensitivity analysis and linear-programming", *IEEE Transactions on Power Systems*, vol. 10, no. 1, pp. 314-322, Feb. 1995
159. Yang T.C., "Applying H_{∞} optimisation method to power system stabiliser design, Part 1: Single-machine infinite-bus systems, Part 2: Multimachine power systems", *Electrical Power & Energy Systems*, vol. 19, no. 1, pp. 29-43, 1997
160. Yang X. and Feliachi A., "Identification of optimal locations for decentralized controllers using residues", in *Proceedings of the Twenty-Second Southeastern Symposium on System Theory*, Mar. 1990, pp. 132-136
161. Yang X.T., *Theoretical Calculation and Analysis of Electric Network Losses*, Beijing: Chinese Hydro Resource and Electric Power Press, 1985
162. Yee S.K. and Milanovic J.V., "Nonlinear time-response optimisation method for tuning power system stabilisers", *IET Proceedings-Generation, Transmission & Distribution*, vol. 153, no. 3, pp. 269-275, May 2006
163. Yu Y.N. and Li Q.H., "Pole-placement power system stabilizers design of an unstable nine-machine system", *IEEE Transactions on Power Systems*, vol. 5, no. 2, pp. 353-358, May 1990

164. Yue M. and Schlueter R.A., " μ -synthesis power system stabilizer design using a bifurcation subsystem based methodology", *IEEE Transactions on Power Systems*, vol. 18, no. 4, pp. 1497-1506, Nov. 2003
165. Yue M. and Schlueter R.A., "Robust control designs for multiple bifurcations", *IEEE Transactions on Power Systems*, vol. 20, no. 1, pp. 301-311, Feb. 2005
166. Zanetta L.C., Jr. and Da Cruz Jose Jaime, "An incremental approach to the coordinated tuning of power systems stabilizers using mathematical programming", *IEEE Transactions on Power Systems*, vol. 20, no. 2, pp. 895-902, May 2005
167. Zein El-Din H.M. and Alden R.T.H., "Second order eigenvalue sensitivities applied to power system dynamics", *IEEE Transactions on Power Apparatus and Systems*, vol. PAS-96, no. 6, pp. 1928-1936, Nov. 1977
168. Zhang P. and Coonick A.H., "Coordinated synthesis of PSS parameters in multi-machine power systems using the method of inequalities applied to genetic algorithms", *IEEE Transactions on Power Systems*, vol. 15, no. 2, pp. 811-816, May 2000
169. Zhong J., Wang C., and Wang Y., "Chinese growing pains", *IEEE Power and Energy Magazine*, vol. 5, no. 4, pp. 33-40, July 2007
170. Zhou E., Malik O.P., and Hope G.S., "Design of stabilizer for a multimachine power system based on the sensitivity of PSS effect", *IEEE Transactions on Energy Conversion*, vol. 7, no. 3, pp. 606-613, Sept. 1992